ASSESSING AND MODIFYING BONE QUALITY

IN CHRONIC KIDNEY DISEASE

Christopher L. Newman

Submitted to the faculty of the University Graduate School
in partial fulfillment of the requirements
for the degree
Doctor of Philosophy
in the Department of Anatomy and Cell Biology
Indiana University

May 2015

Accepted by the Graduate Faculty, Indiana University, in partial fulfillment of the requirements for the degree of Doctor of Philosophy.

_____
Matthew R. Allen, Ph.D., Chair

_____
David B. Burr, Ph.D.

Doctoral Committee

_____
Sharon M. Moe, M.D.

March 09, 2015

_____
Alexander G. Robling, Ph.D.

_____
Joseph M. Wallace, Ph.D.

DEDICATION

For Alicia, Ian, and Alexis

Thank you for always reminding me of what truly matters.

ACKNOWLEDGEMENTS

I would like to thank the National Institutes of Health and the Indiana Clinical and Translational Sciences Institute for their funding of these experiments.

I would also like to thank the numerous members of the Allen, Moe, and Wallace labs for assistance with training and analysis. Specifically, I'd like to thank Drew Brown for his assistance with numerous components of these studies as well as passing on his knowledge for performing several techniques and how to interpret their results.

I also want to extend thanks to my committee for their valuable input throughout these studies. Specifically, I want to thank Dr. Allen for welcoming into his lab and encouraging me to continue this work and supporting me as I undertook it. You have been a great mentor and are the example I will seek to emulate with my own future students.

Most of all, I would to thank my family for their wonderful patience and support. I want to thank my children, Ian and Alexis, for the constant reminders to prioritize what is most important in my life. Finally, I want to thank my wife, Alicia, for all of her support and love throughout the years. Thank you for being a wonderful mother, a wonderful wife, and a wonderful friend.

Christopher L. Newman

ASSESSING AND MODIFYING BONE QUALITY IN CHRONIC KIDNEY DISEASE

Chronic kidney disease (CKD) results in an increased fracture risk, partially due to elevations in parathyroid hormone (PTH) that lead to substantial bone loss. On its own, bone loss does not explain bone fragility in CKD, suggesting that changes in skeletal tissue (bone quality) may also be present. Understanding the factors that lead to fracture in these patients will have a substantial impact on patient care and could lead to a better understanding of how to reduce their fracture risk. Due to their suppression of PTH, calcitriol and its analogues are the current standard of care for bone disease in CKD. Yet, surprisingly little is known of their effects on bone. Agents effective in treating osteoporosis are not recommended in advanced CKD due to the lack of data regarding their efficacy and safety in these patients. The goals of the current study were to determine (1) the impact of CKD on bone quality, (2) the ability of calcitriol to improve skeletal parameters, and (3) the efficacy of various pharmacological interventions (calcium, bisphosphonates, anti-sclerostin antibody, and raloxifene) on bone mass, quality, and mechanical properties in CKD bone disease. Using a slowly progressive rat model of CKD, renal and mineral metabolism, bone morphology, bone quality, and bone mechanics (at several length scales) were assessed. Primarily due to elevated PTH, mechanical testing and tissue-level assessments revealed compromised bone quantity (high cortical porosity and low trabecular volume) and quality (high

collagen cross-linking and low matrix bound water). Despite clinically relevant reductions in PTH, calcitriol treatment had no positive impact on skeletal properties. Most agents were only effective when PTH levels were normal. Raloxifene, however, led to greater whole bone and material toughness (the ability of bone to tolerate existing damage) despite modest PTH suppression. While the examination of bone quality in CKD is still in its infancy, these results indicate that enhancing bone quality with raloxifene may be an effective means to compensate for bone loss in CKD.

Matthew R. Allen, Ph.D., Chair

TABLE OF CONTENTS

CHAPTER 1

INTRODUCTION

Chronic kidney disease (CKD) is a major healthcare concern with widespread and detrimental impacts on both morbidity and mortality[1]. Nearly 1 in 8 individuals in the United States has some degree of kidney failure[2]. With the increasing prevalence of obesity, type 2 diabetes, and hypertension in the United States, these rates are projected to consistently increase because these factors are the most common causes of kidney failure[3].

CKD represents a fairly heterogeneous description of chronic renal damage from numerous causes. Nevertheless, once the kidneys have been irreparably damaged, the later stages of disease lead to similar outcomes regardless of the cause[4]. Even though only a small portion of patients will reach end stage disease and need dialysis or transplantation, CKD remains the most expensive chronic disease in the United States and has a significant impact on the lifespan and quality of life of those afflicted[5].

Unfortunately, there are currently no treatments to completely halt or reverse the progression of renal failure[6]. The primary goal of treatment is to slow the progression of disease by addressing the specific etiological factors (e.g., hypertension, diabetes, etc.) responsible for the damage[7]. When not addressed, CKD leads to abnormalities in endocrine function and mineral metabolism, which ultimately result in pathological dysfunction of cardiovascular, endocrine, and skeletal processes, a constellation now collectively known as CKD-mineral and bone disorder (CKD-MBD). Hence, the increasing rates of CKD and the absence

of a cure ensure that the prevalence of these manifestations will only increase in the coming years.

The pathogenesis of CKD-MBD leads to complex metabolic phenotypes.

Disturbances in bone and mineral metabolism are the hallmark of CKD-MBD[8-9]. Along with hyperphosphatemia, secondary hyperparathyroidism, and vascular calcification, patients exhibit an increased risk of fractures[10-19]. Given the complexities of normal mineral metabolism[20], CKD-MBD encapsulates the compensatory mechanisms (and their failure) that preserve calcium and phosphate homeostasis in the face of declining glomerular filtration[21] (**Figure 1**). These physiological and pathological adaptations play a significant role in fracture risk and mortality.

As kidney function begins to decline, there is an increased demand on the remaining nephrons to maintain mineral homeostasis and normal excretory functions[22-23]. Changes in phosphate excretion drive the metabolic derangements that characterize CKD-MBD. In response to increased phosphate load, osteocytes secrete fibroblast growth factor 23 (FGF23), which acts on tubular epithelial cells in the kidney to decrease phosphate reabsorption. In concert with FGF23, parathyroid hormone (PTH) levels also increase to compensate for these rises in phosphate (though simultaneous declines in vitamin D synthesis are also involved). While recent evidence indicates that FGF23 normally suppresses PTH

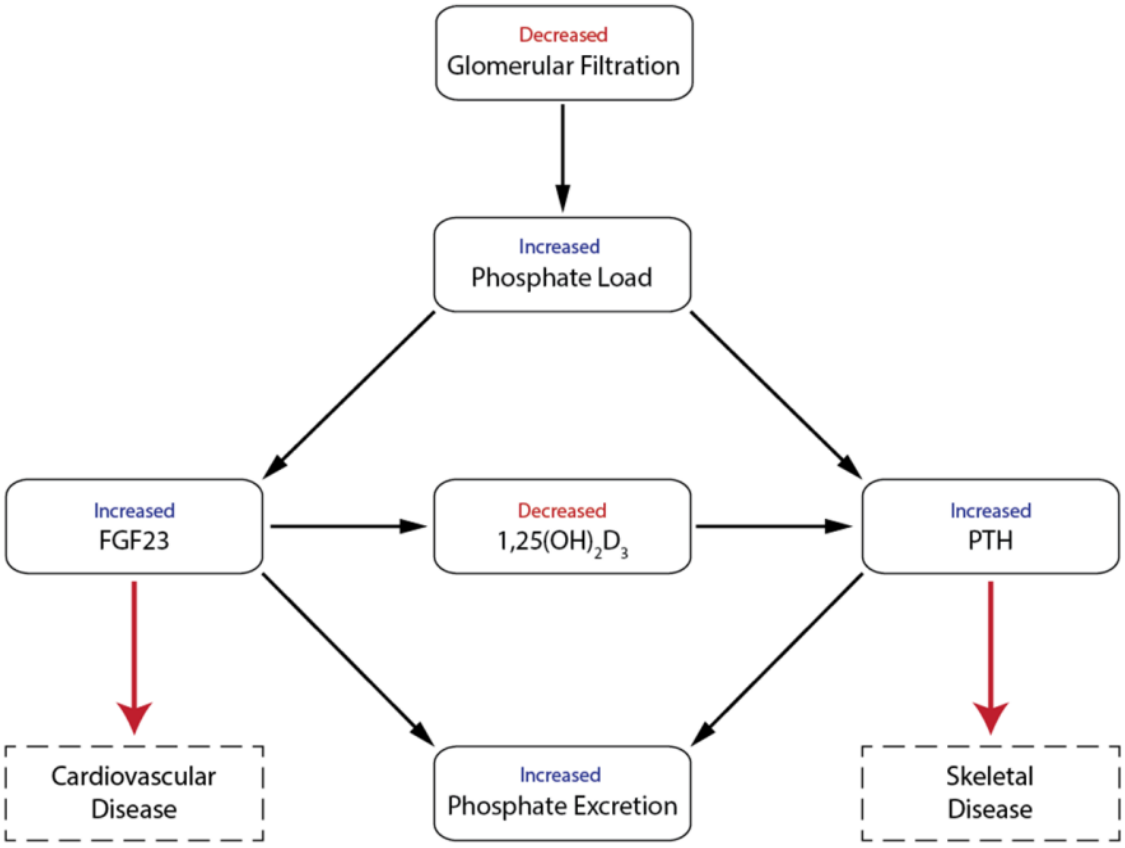

Figure 1. The adaptations of mineral metabolism that result from CKD.

activity[24-25], secondary hyperparathyroidism ensues nonetheless. Initially, these responses effectively maintain normal serum phosphate levels. Eventually though, this process fails, and serum phosphate begins to increase.

In skeletal tissue, concomitant increases in osteoclast differentiation and activity occur, which is what primarily leads to the bone deficits present in CKD-MBD[26]. Though several metabolic derangements may have some impact on osteoclast activity, high levels of PTH are most prominent[27]. Specifically, these levels are known to act through the PTH receptors present on osteoblasts and osteocytes to upregulate osteoclast formation and activation[28]. Though these changes in PTH are ultimately secondary to metabolic changes occurring during CKD, these patients begin to exhibit many of the same bone cell changes present in primary hyperparathyroidism[29]. While the circumstances specific to CKD are beginning to be elucidated, the metabolic complexity of CKD has led to great challenges in understanding and treating skeletal manifestations, resulting in an inability to substantially reduce fracture risk in this population.

Metabolic changes in CKD lead to significant skeletal alterations and, ultimately, fracture.

Patients with chronic kidney disease have more than double the risk of having a fracture compared to the general population[14-15]. Of even greater concern, mortality rates in CKD patients with hip fractures more than double those of non-CKD patients with hip fractures[18,30]. The presence of secondary hyperparathyroidism causes changes in bone metabolism that lead to the

preferential breakdown of cortical bone. Specifically, chronic elevations in PTH can lead to subperiosteal and intracortical erosion, resulting in drastic increases in cortical porosity[31] (**Figure 2**). The impact on cancellous bone is more variable. In cases of mild hyperparathyroidism, cancellous bone is usually unchanged or even increased[32]. But, imaging studies indicate that hyperparathyroidism can also detrimentally impact trabecular bone in CKD[33]. Nevertheless, cortical bone is thought to be prominently impacted and drive much of the increase in fracture risk. Specifically, CKD patients with a history of fracture have lower volumetric BMD and thinner cortices than those without fractures. These data may help explain why BMD estimates in the distal radius are the strongest predictors of fracture in these patients[31,34].

Fracture risk is affected by both bone mass and bone quality.

While bone mineral density (BMD) is a useful surrogate of fracture risk in the general population, its ability to predict fractures in CKD has been inconsistent, especially in patients on dialysis[35-42]. Even with recent indications that BMD does predict fracture in patients with CKD[34,43-45], bone mass is but one factor involved in fracture development. BMD does not assess the structural organization or material composition of bone (routinely referred to as bone quality)[46].

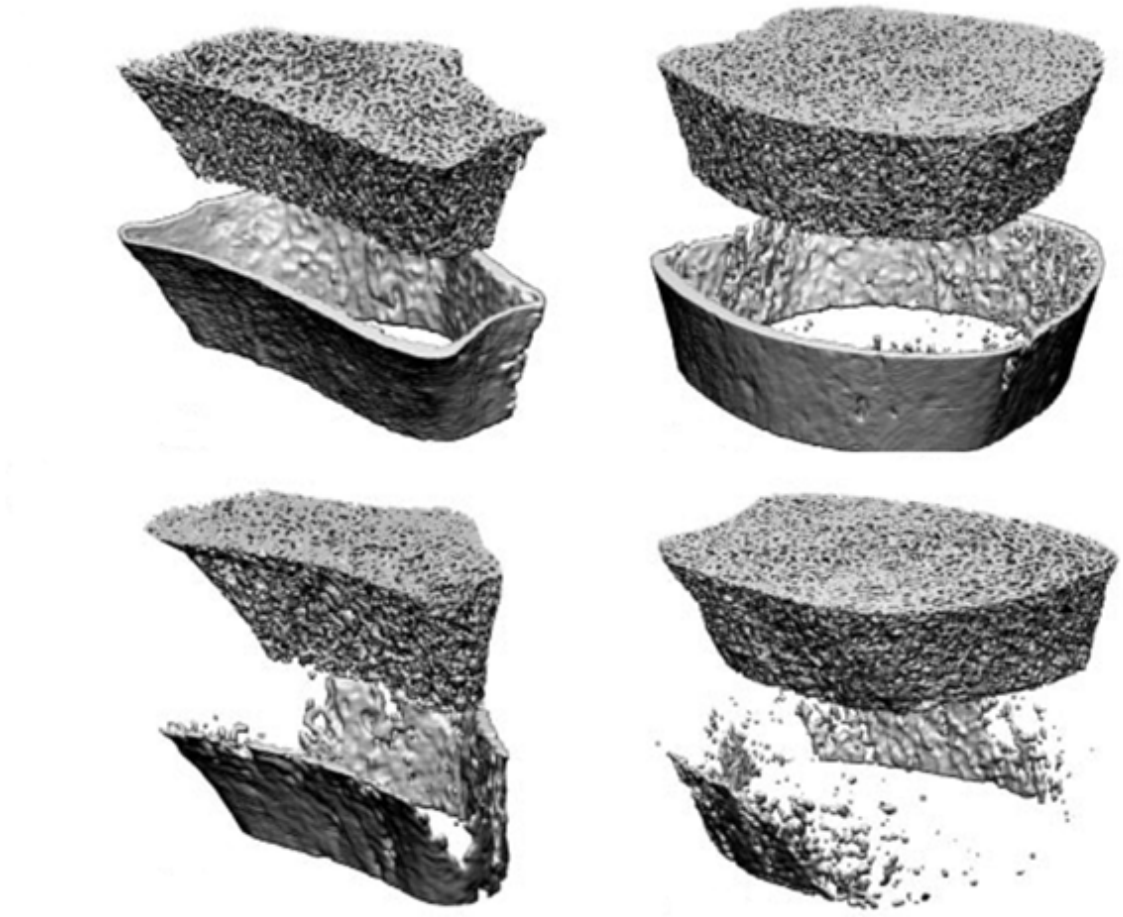

Figure 2. Tibiae (left) and radii (right) of an individual without CKD (top) and an individual with advanced CKD and severe cortical porosity (bottom)[31].

While environmental factors (activity, falls, etc.) play an important role in fracture, its occurrence is largely a reflection of the maximum load that can be borne by a bone (ultimate load) and the amount of energy it can dissipate (energy to failure). These structural properties are determined by the amount of skeletal tissue present, its three-dimensional orientation, and its material properties (**Figure 3**). Material properties are a product of tissue mineralization, the structure and composition of the organic matrix, tissue hydration, and the presence of existing microdamage. While standard engineering calculations derived from whole bone mechanical tests provide estimates of material properties[47], these derivations assume material homogeneity and are difficult to interpret in light of significant variations in composition.

While some direct bone quality data are available from patient biopsies[48], bone quality has not been extensively studied in CKD-MBD. A detailed assessment of material properties could provide insight into the tissue-level mechanisms responsible for fractures associated with CKD as well as reveal novel avenues of treatment. Unfortunately, assessing these multiscale mechanisms is either difficult or impossible in humans. Therefore, a thorough assessment of the hierarchical contributions to mechanical properties and their failure in light of kidney disease requires the use of animal models.

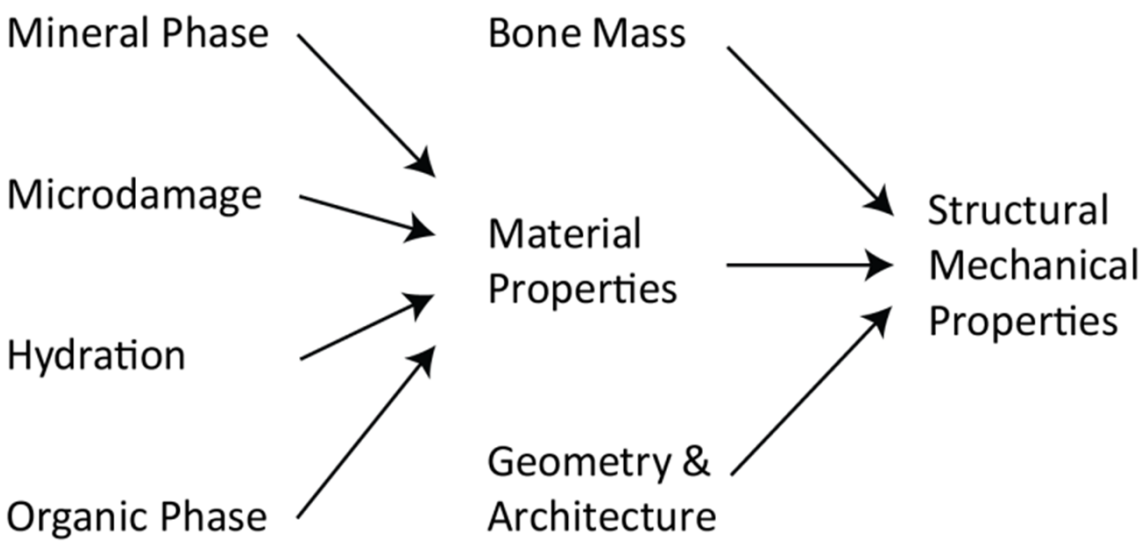

Figure 3. The hierarchical nature of the mechanical properties of bone.

Animal models present an opportunity to examine interventions against skeletal deterioration from CKD.

Because of the widespread impact of CKD on human health, numerous animal models have been developed to address the systemic repercussions of kidney disease. The most common approach is to induce end stage renal disease by surgical nephrectomies (with numerous variations), electrocautery, or the administration of adenine. These models represent an acute injury that leads to chronic renal failure. Given that the vast majority of patients with CKD have either hypertensive nephropathy or diabetic nephropathy[7], sudden trauma does not accurately represent the progression of disease in the majority of cases. While adenine does provide a slower progression (three to four weeks), animals exhibit severe weight loss not seen in other models[49]. The consequences of this weight loss on pertinent disease parameters are unclear. Despite the drawbacks of acute onset, these models still have important potential for examining the impact of CKD on mature skeletal tissue. Unfortunately, most of these data derive from experiments in which CKD is induced in skeletally immature animals with actively growing bones[50-51]. Not only do these animals exhibit rapid bone modeling not present in adult rodents, but there also is no way to distinguish the direct impact of kidney disease on bone from its impact on altered skeletal development.

Alternative models use genetic manipulation to induce kidney failure, primarily in the form of polycystic kidney disease[52]. For example, the *jck* mouse has a primary ciliary defect that leads to cystic kidney disease by four weeks of

age. Similarly, *pcy* mice exhibit ciliary disease leading to cysts by three weeks. The greatest challenge with most genetic models is the rapid onset of disease during early growth and development. As above, this makes it exceedingly difficult to determine if skeletal manifestations are a direct result of the disease or rather an indirect byproduct of disturbed skeletal development. While these are important models for pediatric CKD, their application to end stage disease in adults is limited.

The model utilized in the current studies (the Cy/+ rat) avoids many of the limitations intrinsic to other models. Unlike surgical models, these animals display a gradual onset of disease. And unlike most genetic models, they exhibit a slow enough progression that bone disease does not begin to occur until after skeletal maturity. The Cy/+ rat is characterized by autosomal dominant polycystic kidney disease (PKD)[53]. These animals have a mutation (R823W) in *Anks6*, a gene that codes for the protein SamCystin. Currently, the function of this protein is unknown, and the specific role of this mutation in the development of PKD is unclear. Aside from its expression in the kidney, little is known about its role in the cell[54]. But, unlike most other PKD-related proteins, SamCystin does not localize to the primary cilia of kidney cells[55]. While only recently has this gene been related to a known human disease (nephronophthisis)[56], its slow and gradual onset provides a helpful phenotypic animal model of human CKD[53]. It parallels the human condition through the gradual development of abnormal mineral homeostasis and vascular calcification of the great vessels, all of which typify CKD-MBD. Animals exhibit significant detriments in bone structural and

mechanical properties, with substantial cortical porosity arising in advanced disease (**Figure 4**). This cortical effect closely mimics the human condition[57]. The gradual progression of disease in the Cy/+ rat and the onset of mineral derangements after skeletal maturity make it the most promising rodent model available for examining the effects of chronic kidney disease on adult bone.

Clinical treatments focus on lowering PTH, but their effects on fracture risk and bone quality are unclear.

High levels of PTH have been implicated in cortical bone alterations and fracture risk in CKD patients[57], making PTH regulation a major goal of treatment[58-59]. For patients with early stage CKD, when PTH levels are still normal, most guidelines employ treatment recommendations for adults with osteoporosis[60-61]. Unfortunately, a lack of clinical data regarding patients with later stage disease has led to great difficulty in treating skeletal abnormalities in this population.

Current approaches have focused on minimizing phosphate intake and lowering PTH levels. Calcitriol and its various analogues (paricalcitol, doxercaliferol, etc.) effectively suppress PTH, though higher doses can lead to hypercalcemia[60,62-64]. Calcimimetics have also been shown to effectively decrease PTH[59]. Unfortunately, few studies have examined the skeletal effects of these therapies. Recent evidence indicates that cinacalcet does decrease fracture risk in advanced CKD patients[65]. Unfortunately, its failure to lower mortality rates and cardiovascular outcomes[66-67] and the cost

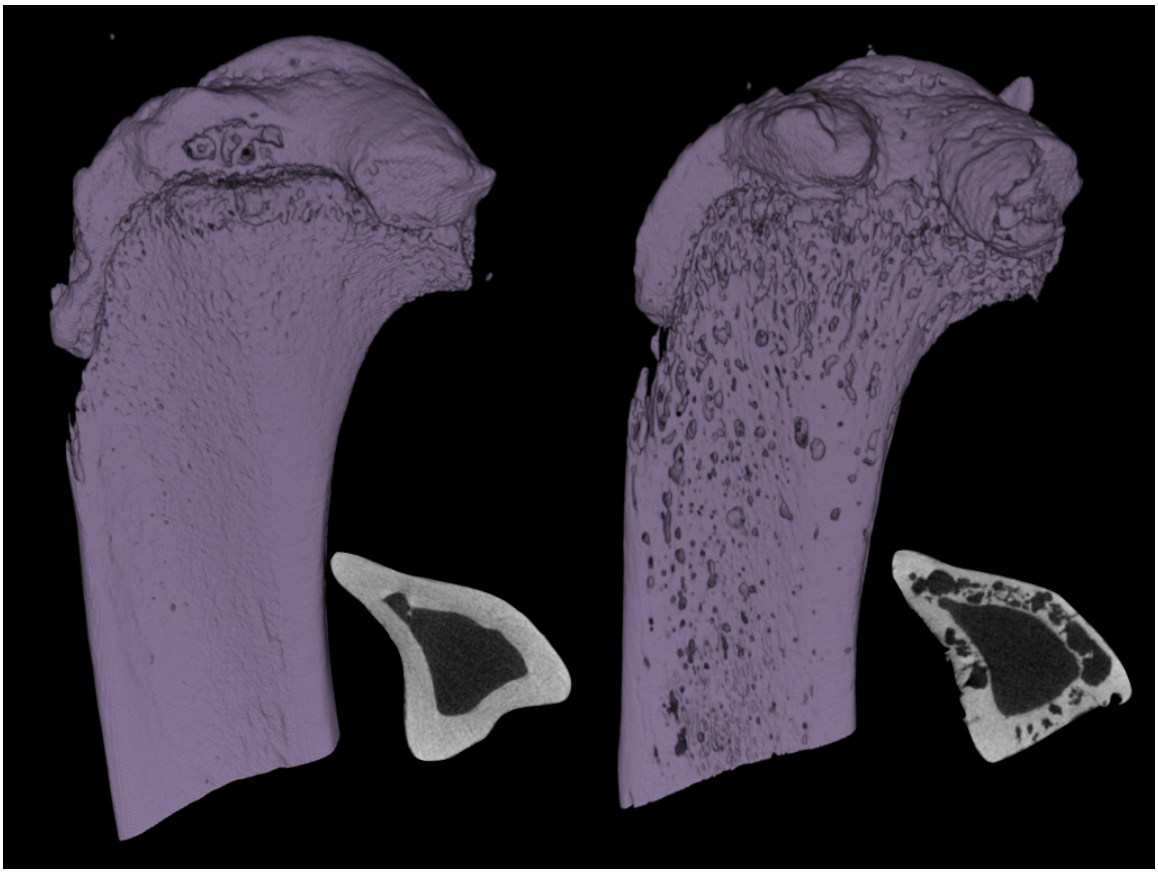

Figure 4. Tibiae of a normal rat without CKD (left) and a Cy/+ rat (right) with advanced CKD and severe cortical porosity.

effectiveness of less expensive vitamin D analogues[68] indicate that calcitriol and its analogues will remain the standard of care in this population.

Despite its prevalence in CKD patients, though, the impact of calcitriol on bone quality and fracture risk is currently unknown. While most osteoporosis clinical studies in non-CKD patients demonstrate that calcitriol reduces fracture risk through improvements in BMD[69-70], the extension of these benefits to patients with advanced kidney disease, where cortical bone is so adversely affected, is unclear[68]. In numerous rodent models of osteoporosis, vitamin D analogues have been shown to increase bone mass, improve whole bone mechanical properties, and decrease rates of bone remodeling[71-75]. However, whether these benefits extend to CKD in the presence of hyperparathyroidism is not clear. In addition, because these studies were limited to whole bone mechanical testing, how these analogues directly impact material properties remains to be seen.

The lack of data regarding traditional pharmacological agents has limited their application in late stage CKD patients.

The majority of patients with osteoporosis are treated with anti-resorptive agents that aim to prevent bone loss[76]. Though there are rare adverse events with these medications in patients with osteoporosis[77], they have largely been successful. As a result, the rate of fracture in patients with osteoporosis has been substantially reduced[78]. Unfortunately, the complex metabolic background of

patients with CKD has led to numerous concerns about the use of these osteoporosis agents in late stage CKD[60].

Bisphosphonate clinical trials that inadvertently included individuals with CKD showed similar benefits in CKD patients as those patients without kidney disease[79-80]. Unfortunately, these data did not include late stage CKD patients, where skeletal changes are more severe. Currently, CKD treatment guidelines do not recommend bisphosphonates due to concerns over their renal clearance and the impact of low bone turnover rates in these patients[60]. Because of the historical impact of aluminum toxicity on fracture risk in CKD patients[81] and the more concrete associations between low turnover bone disease and arterial calcifications[82-85], all forms of low bone turnover in CKD have become a significant concern[86]. These concerns have been exacerbated by the presence of low bone turnover in late stage CKD patients taking bisphosphonates[87]. Bisphosphonates clearly cause declines in bone turnover (this is precisely their mechanism of efficacy in osteoporosis). The link that has yet to be made is whether low bone turnover induced by bisphosphonate use is associated with fracture risk or vascular calcifications. Unfortunately, these concerns are ultimately theoretical as there are no data linking low bone turnover induced by bisphosphonates and an increased risk of fracture (or other negative effects) in CKD patients. The lack of data display a need for further preclinical studies using bisphosphonates to examine their safety and efficacy in CKD.

While bisphosphonate use in CKD is surrounded by a cloud of confusion, other osteoporosis treatments are even less clear[61] (**Table 1**). The recently

developed anabolic PTH analogue (teriparatide) has had a positive impact in patients with osteoporosis[88-89]. Unfortunately, as with bisphosphonates, there are theoretical concerns over administering PTH in the setting of secondary hyperparathyroidism, and again, the data are extremely limited. Teriparatide may have utility in patients with low turnover bone disease. Unfortunately, the lack of data significantly limits the conclusions that may be drawn in the setting of CKD.

More promising for CKD has been the recent development of a humanized anti-sclerostin antibody for the treatment of osteoporosis. Romosozumab has been employed successfully in women with postmenopausal osteoporosis[90] and is currently being examined in a randomized clinical trial. Given that sclerostin levels are elevated in the blood of patients with CKD[91] and the bones of patients and animals with CKD[92], the anabolic agent anti-sclerostin antibody may be efficacious in all forms of renal osteodystrophy independent of PTH and bone turnover. Because PTH suppresses sclerostin secretion from osteocytes[93], hyperparathyroidism may be partially explained by elevations in sclerostin levels. Hence, the early suppression of sclerostin using an anti-sclerostin antibody holds promise for controlling some of the earliest changes in CKD bone disease.

Name	FDA label year	Concerns for use in patients with CKD	Author's commentary
Alendronate	2013	Not recommended for CrCl <35 ml/min	Agree with the FDA recommendations
Risedronate	2013	Not recommended for CrCl <30 ml/min	Agree with the FDA recommendations
Ibandronate	2013	Not recommended for CrCl <30 ml/min	Agree with the FDA recommendations
Zoledronic acid	2013	Contraindicated with CrCl <35 ml/min or acute renal impairment	Agree with the FDA recommendations
Oestrogen	2011	None	Data limited in women with stage 4–5 CKD; use in younger women with amenorrhoea and BMD in the osteoporotic range or fracture
Raloxifene	2007	None	Pilot data in women on haemodialysis suggests beneficial effects; this agent is the best current choice in women with CKD who do not have coagulation problems
Teriparatide	2009	Use with caution in patients with recent urolithiasis	Preliminary data suggest a benefit in patients with CKD, low parathyroid hormone levels and BMD in the osteoporotic range
Calcitonin	2012	None	Probably safe, but concerns regarding cancer not resolved; effects on osteoporosis weaker than those of other drugs, and no data in patients with CKD
Denosumab	2013	Risk of hypocalcaemia in patients with CrCl <30 ml/min	Might be useful to treat hypercalcaemia but risky in patients with CKD and osteoporosis, owing to hypocalcaemia and suppressed bone formation

Table 1. Summary of approved agents for patients with CKD[61].

Raloxifene improves bone quality.

Raloxifene is a selective estrogen receptor modulator with mild anti-bone remodeling properties. Clinical trials have shown it to effectively reduce fracture risk in patients with osteoporosis despite modest improvements in BMD[95-96]. Preclinical studies have revealed that raloxifene improves mechanical properties in part through its effects on material properties[97-99]. This is in contrast to the more commonly used bisphosphonates. Bisphosphonates work primarily by increasing bone mass and improving bone strength (the ability of bone to resist damage)[100]. Raloxifene, on the other hand, works primarily by improving bone toughness (the ability of bone to tolerate damage before fracture occurs). In fact, this occurs in the absence of significant changes in bone mass[97-98]. In other words, raloxifene appears to improve bone quality. Specifically, both *ex vivo* and *in vivo* experiments demonstrate that increased bone matrix hydration is responsible for these improvements[101-102]. Recent studies have even indicated that these changes in hydration can be detected using clinical magnetic resonance methods[102], making raloxifene an appealing agent for examining the treatment of bone quality in patients with CKD.

Given its unique ability to positively affect bone quality, raloxifene could provide an important impact on fracture resistance in CKD. Furthermore, secondary analyses of a human clinical trial revealed beneficial renal outcomes in patients using raloxifene[103]. These results, which have been supported by animal models[104-105] and a clinical study in dialysis patients[106], led to the recommendation for further studies in patients with late stage kidney disease[60-61].

CHAPTER 2

CORTICAL BONE MECHANICAL PROPERTIES IN AN ANIMAL MODEL OF PROGRESSIVE CHRONIC KIDNEY DISEASE

Material in this chapter has been previously published:

PLoS One (2014) 9:e99262

Rationale

Based on previous studies in animals with CKD, whole bone mechanical testing indicates that structural mechanical properties are compromised by chronic kidney disease. Estimated material properties from these tests suggest that bone quality is also impacted. However, the specific tissue-level changes that are responsible have not been well defined. Hence, the purpose of this study was to directly examine these changes using mechanical, morphological, and compositional assessments at various length scales.

Introduction

Chronic kidney disease—mineral and bone disorder (CKD-MBD) is characterized by hyperphosphatemia, secondary hyperparathyroidism, and an increased risk of fractures[8-9,60]. Unlike osteoporosis, CKD-MBD appears to have a preferential impact on cortical bone, leading to reduced bone mass and increased porosity[31,33,38]. These effects likely underlie the increased fracture risk observed in patients with CKD[14-15,18].

Whole bone (structural) mechanical properties are dependent upon a number of variables[46,107]. While bone mass is a major determinant, both the distribution of bone and its material properties (inherent physical and chemical properties) also play crucial roles. Most biomechanical studies in rodent models of CKD have focused on structural mechanical properties, employing three-point bending or dynamic mechanical analysis (DMA)[51,92,108-112]. These studies indicate that the bending and viscoelastic properties of bone are compromised in animals

with CKD. Specifically, DMA indicates that diseased animals have lower storage modulus (a measure of stiffness) and tan delta (a measure of energy dissipation)[51,110], while three point bending studies indicate that ultimate load, stiffness, and energy to failure are lower in CKD animals[108].

While there is an increasing awareness of the importance of bone quality in CKD[48], few studies have explicitly examined material properties in animal models[50-51,110]. Material properties can be estimated from whole bone mechanical tests using standard engineering equations that account for whole bone structure and geometry. Because these estimates assume that skeletal tissue is homogeneous, isotropic, and linearly elastic, direct measures of material properties in bone would provide additional insight into how the disease is affecting fracture resistance. Therefore, the goal of the present study was to examine material-level changes in cortical bone at several length scales using a rat model with the progressive development of CKD. Specifically, we hypothesized that CKD adversely impacts cortical bone material properties as determined by material-level mechanical testing and assessments of bone composition and collagen morphology.

Materials and Methods

Animal Model

The current study utilized a slowly progressive animal model of CKD, the Cy/+ rat. Cy/+ rats are characterized by autosomal dominant polycystic kidney disease[53]. These animals have a mutation (R823W) in *Anks6*, a gene that codes

for the protein SamCystin. Currently, the function of this protein is unknown, and the specific role of this mutation in the development of polycystic kidney disease is unclear. Aside from its expression in the kidney, however, little is known about its role in the cell[52]. Unlike most other PKD-related proteins, though, SamCystin does not localize to the primary cilia of kidney cells[55]. While there is no known human disease associated with this gene, the spontaneous onset of disease provides a helpful phenotypic model of human CKD[52]. Unlike the more common surgical models[49], Cy/+ rats display a gradual onset of disease and, unlike most genetic models[54,113], they exhibit a slow enough progression that bone disease does not begin to occur until after skeletal maturity.

Skeletal tissue from animals in a previous study was utilized[108]. All animals were fed a casein diet (Purina AIN-76A; 0.7% Pi) to increase phosphorus availability in order to produce a more consistent kidney disease phenotype. Fresh frozen tibiae from 30-week-old male Cy/+ rats and their age-matched non-affected littermates were assessed mechanically, compositionally, and morphologically at several length scales. Fresh frozen femora were used for collagen cross-linking analyses. Blood was collected at the end of the experiment for biochemical analyses (previously reported in [108]). All procedures were conducted under the approval of Indiana University School of Medicine Institutional Animal Care and Use Committee protocol # 10479.

Reference Point Indentation

Tibiae were thawed to room temperature and soaked overnight in phosphate-buffered saline. The anteromedial surface of the proximal diaphysis of

the tibia was assessed using reference point indentation (RPI) (Biodent Hfc, Active Life Scientific, Santa Barbara, CA). The reference probe, which housed a BP2 test probe, was lowered vertically, normal to the surface, until it rested on the surface of the bone. In order to stabilize the unit, a reference force of ~13 N was applied before each measurement was initiated. Each test included a series of 10 cycles at 2 Hz to a force of 10 N. Bones were maintained in a hydrated state throughout the test. Five locations per sample, each ~2 mm apart, were indented. Raw data from the RPI analysis software (version 2.0) were imported into a customized MATLAB code (Mathworks) designed to provide cycle-by-cycle data for each test[114], from which first cycle unloading slope, indentation distance increase, first cycle energy dissipation, creep indentation distance, first cycle indentation distance, total indentation distance, and total energy dissipation were calculated for each test. All five tests from each animal were averaged to produce a single value for each variable.

Tissue Composition

Raman spectroscopy was performed using a LabRAM HR 800 Raman Spectrometer (HORIBA JobinYvon, Edison, NJ) connected to a BX41 microscope (Olympus, Tokyo, Japan). A 660 nm laser was focused on the bone surface using a 50X objective to a spot size of ~10 μm. Five locations were imaged ~1 mm apart on the anteromedial mid-diaphysis with five 20 second acquisitions at each location as previously published[115]. A five point linear baseline correction was applied in LabSpec 5 (HORIBA JobinYvon). Using OriginPro 8.6 (OriginLab, Northampton, MA), a single Gaussian peak was fit to

the PO_4^{3-}v1 peak, and the areas under the PO_4^{3-}v1, CO_3^{2-}v1, and Amide I peaks were calculated at each location. Type B carbonate substitution was found by the band area ratio of CO_3^{2-}v1/PO_4^{3-}v1. The degree of matrix mineralization was determined by the band area ratios of PO_4^{3-}v1/Amide I. Mineral maturity (crystallinity) was determined by the inverse of the full width at half maximum (FWHM) of the PO_4^{3-}v1 peak.

AFM Indentation

The anteromedial portion of the mid-diaphysis used above was polished with a 3 μm polycrystalline water-based diamond suspension in order to create a flat region for testing. Nanoindentation was performed using a BioScope Catalyst atomic force microscope (Bruker, Santa Barbara, CA), operating in peak force tapping mode using previously published methods[116]. Indentations were performed using a polycrystalline diamond probe (NaDia ND-DYC series; Advanced Diamond Technologies, Inc.) with a measured spring constant of 29.25 N/m. Four locations per sample were indented and, at each location (20 μm×20 μm grid), 49 indentations were performed. Samples were loaded to 200 nN with force-separation curves acquired from each indentation. Within each location, indentations were spaced about 2 μm apart in order to avoid interactions from neighboring indentations. In total, 196 indentations were performed for each sample. The indentation elastic modulus was calculated from 5% to 95% of the withdrawal curve using the classic Hertz model of contact between a rigid sphere and an elastic half space because the indentation depth is much smaller than the radius of curvature of the probe[116]. The indentation

elastic modulus was determined from the following equation: E = 3F(1-v∧2)/(4r∧(1/2) δ∧(3/2)) where E is the indentation elastic modulus, F is the indentation force, v is the Poisson's ratio of the sample (assumed to be 0.35), r is the tip radius (nominal radius of 50 nm, with the same probe used for all samples), and δ is the indentation depth. All of the individual indentations were averaged to produce a single value for each animal, though individual tests were used for distribution comparisons among the groups.

Collagen Morphology

Following AFM indentation, the polished surface was partially decalcified by soaking the bones in 0.5 M EDTA for 25 minutes followed by five minutes of sonication in a water bath. This process was repeated five times for each sample. For imaging, RTESPA probes were used (Bruker; radius nominally 8 nm, spring constant = 40 N/m). The scan size was set at 3.5 μm with 512×512 pixels and a scan rate of 0.5 lines/s. For measurements of collagen morphology, four locations were imaged per sample, and 10 to 15 fibrils were measured at each location. 40 to 50 fibrils per sample were averaged to produce a single value for each animal, though the individual tests were used for distribution comparisons. Using SPIP 5.1.10 (Image Metrology, Hørsholm, Denmark), D-periodic spacing was calculated using2D Fast Fourier Transformations (2D FFTs) as previously described[115].

Collagen Cross-Linking

Segments of bone (~3 mm in length) from the proximal femoral diaphysis were fully demineralized in 20% EDTA (0.68 M, pH 7.4). Approximately 10 mg of

demineralized bone were hydrolyzedin6 N HCl (~10 μL per 1 mg) at 110°C for 20 to 24 hours. After evaporating the acid using a SpeedVAC centrifuge with cold trap, each hydrolysate was resuspended in ultrapure water, split into two equal portions, and dried. Half the residue was resuspended in ultrapure water with an internal standard (5×10^{-6} g/L pyridoxine). The solution was filtered and diluted with 0.05% heptafluorobutyric acid in 10% acetonitrile, and 50 μL of each hydrolysate were assayed by a high performance liquid chromatography (HPLC) system (Beckman-Coulter System Gold 168) with a silica-based column (Waters Spherisorb). Standards with varying concentrations of pyridinoline (Pyd) (Quidel),deoxypyridinoline (Dpd) (Quidel), pentosidine (PE) (International Maillard Reaction Society), and a constant amount of pyridoxine were also assayed. Using a Waters 2475 fluorescence detector (excitation/emission of295/400 nm for Pyd and Dpd and 328/378 nm for PE), chromatograms were recorded to determine the amount of each crosslink. These amounts were then normalized by collagen content, which was determined from the other half of each hydrolysate by another HPLC assay[117]. Briefly, with α-amino-butyric acid (α-ABA) included as an internal standard, the amino acids were subjected to derivatization with phenyl isothiocyanate (PITC). Along with standards of varying concentrations of hydroxyproline (Sigma) and proline (Sigma) and a constant amount of α-ABA, the derivatized samples were resuspended in a buffer solution of 5% acetonitrile in 5 mM disodium phosphate. Upon injecting 50 μLof this sample, chromatograms were generated with a UV detector (Beckman-Coulter System Gold 168). The calculated mass of hydroxyproline was then multiplied by

7.5 (assuming 13–14% of type I collagen by mass) and divided by the molecular weight of collagen (30,000 Da)[118], thereby giving crosslink concentration as mol/mol of collagen.

Statistical Analysis

All analyses were performed using SPSS software. Comparisons between groups were made with Student's t-tests (assumptions validated by Shapiro-Wilk and Levene tests). When non-normal distributions or unequal variances were present, comparisons were made using Wilcoxon ranked-sum tests and unequal variance t-tests, respectively. Distributions included all measures from each individual, and comparisons were made using Kolmogorov-Smirnov tests.*A priori* α-levels were set at 0.05 to determine significance.

Results

Animal Model

Details about the phenotype of these animals have been previous published[108]. Briefly, measures of kidney function, including BUN (+116%) and the albumin-to-creatinine ratio (+301%), were significantly higher in Cy/+ animals compared to the normal controls. Similar to what is observed in humans with CKD, there were no differences between groups for phosphorus or calcium levels, but both serum PTH (+240%) and FGF23 (+195%) were drastically higher (**Figure 5**). Cy/+ animals had higher numbers of osteoclasts and higher levels of bone remodeling. Using three-point bending, they exhibited lower ultimate load (−28%), stiffness (−17%), and energy to fracture (−46%). Estimates of material

properties indicate that they had lower ultimate stress (−20%) and toughness (−47%)[108] (**Figure 6**).

Reference Point Indentation

Indentation distance increase (IDI) provides an assessment of the change in depth between the first cycle and the final cycle. Cy/+ animals had significantly higher IDI (+18%), indicating that the tissue is more prone to damage under the same applied load (**Figure 7**). The amount of energy dissipated during the first cycle was also significantly higher in animals with CKD (+8%). While the first cycle creep indentation distance (+18%) was higher in Cy/+ animals, there was no difference in microstructural stiffness (first cycle unloading slope) between the two groups. No differences were noted in first cycle indentation distance, total indentation distance, or total energy dissipation (**Table 2**).

AFM-based indentation

There was no difference in the indentation elastic modulus between the groups (**Figure 8**). However, when all indentations within each group were considered as a population, the distribution of elastic modulus values did differ between the two groups. Animals with CKD had a greater proportion of both high and low values of elastic modulus than their normal counterparts (**Figure 8**).

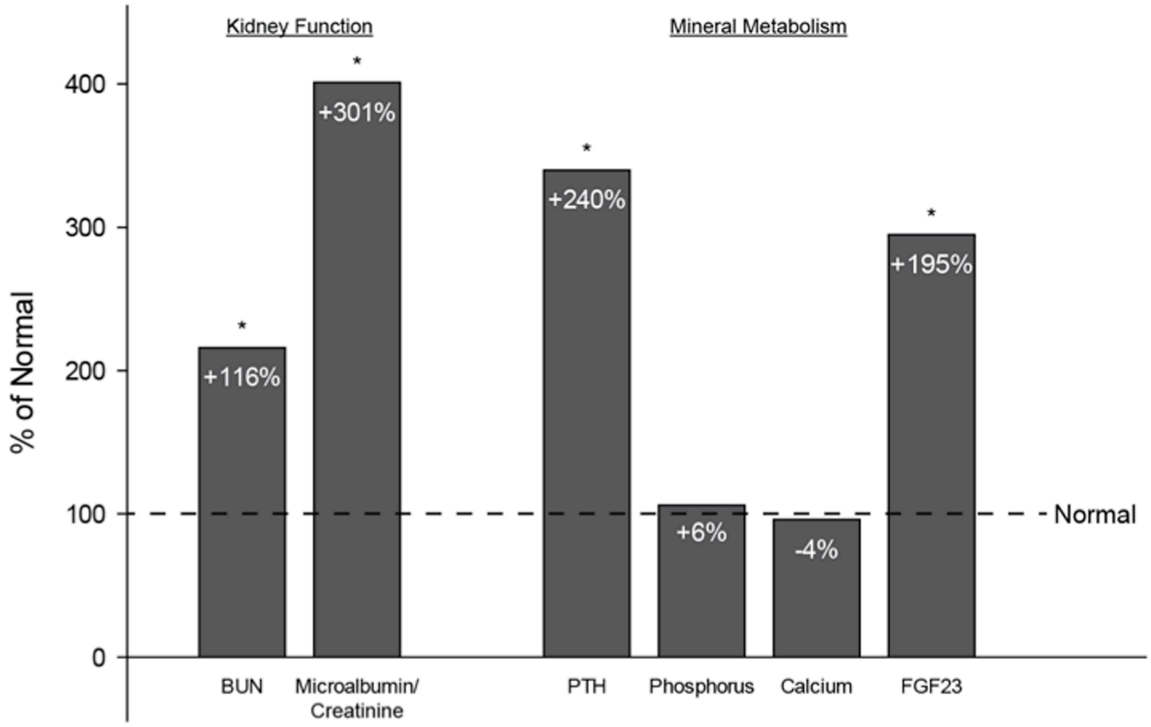

Figure 5. Biochemical assessment of kidney function and mineral metabolism. These previously published data[108] show abnormalities in kidney function and mineral metabolism resulting from hyperparathyroidism in the animals utilized in the current work. Data are presented as a percentage of non-affected normal animals with (*) representing statistical significance.

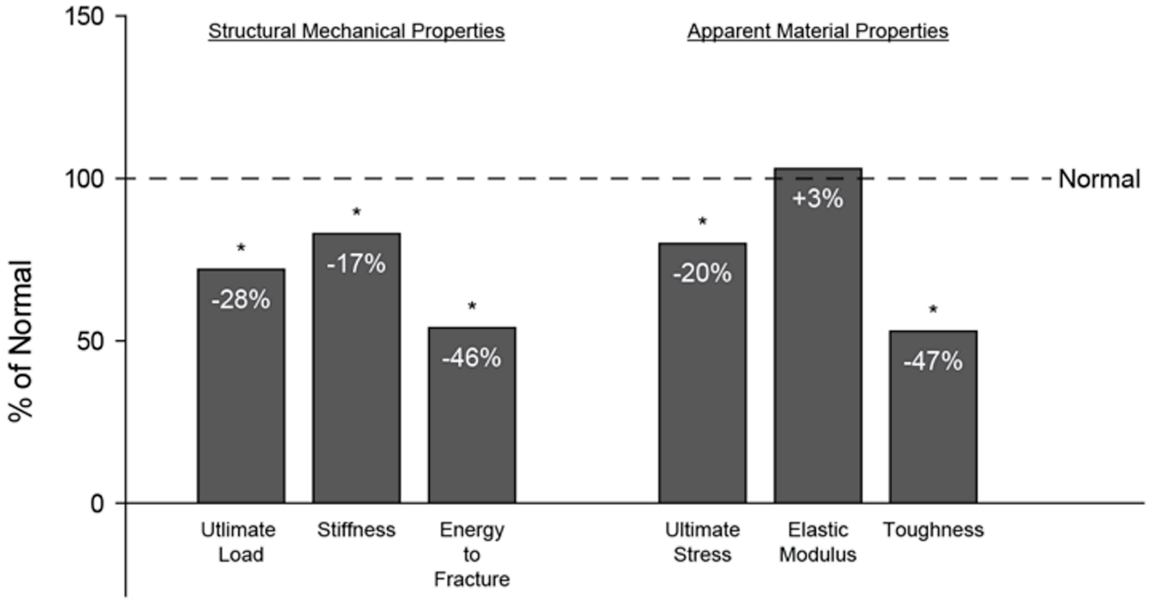

Figure 6. Structural mechanical properties and estimated material properties. These previously published data[108] show compromised whole bone mechanical properties from femoral 3-point bending and apparent material-level mechanical properties derived from standard beam bending equations in the animals utilized in the current work. Data are presented as a percentage of non-affected normal animals with (*) representing statistical significance.

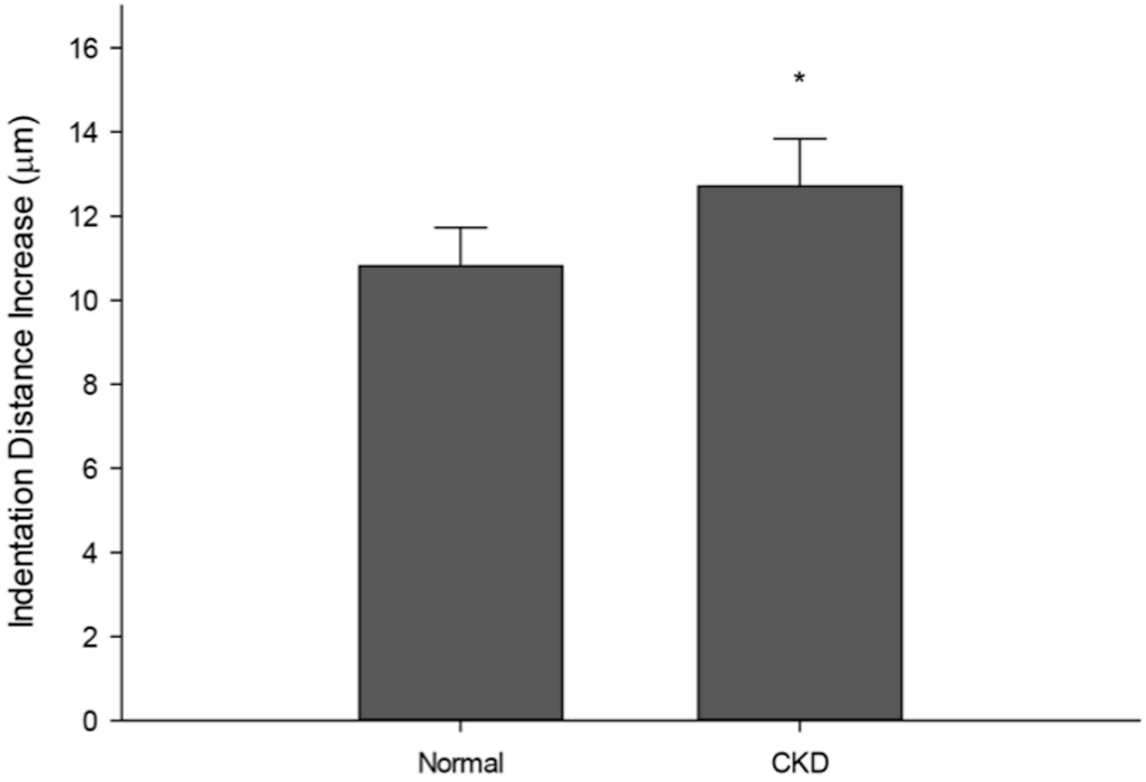

Figure 7**.** Microindentation reveals that CKD skeletal tissue is less able to resist damage.

Using reference point indentation (RPI), the indentation distance increase (IDI) was found to be significantly higher in CKD animals compared to normal. These data indicate that the mechanical integrity of the bone is less able to resist microscale damage formation and propagation. Data are presented as mean and standard deviation. *$p<0.05$ versus normal controls.

RPI	Normal (n = 6)	Cy/+ (n = 6)	p-values
First Cycle Indentation Distance (μm)	83.38±3.15	88.24±5.45	*0.088
First cycle Energy Dissipation (μJ)	275.53±14.00	297.94±19.35	***0.044**
First Cycle Unloading Slope (N/μm)	0.47±0.02	0.45±0.03	*0.113
First Cycle Creep Indentation Distance (μm)	6.08±0.43	7.17±0.95	***0.028**
Indentation Distance Increase (μm)	10.81±0.92	12.71±1.13	***0.009**
Total Indentation Distance (μm)	89.39±2.73	95.21±5.13	#0.080
Total Energy Dissipation (μJ)	663.06±43.53	712.30±89.19	*0.252
AFM	**Normal (n = 5)**	**Cy/+ (n = 4)**	**p-values**
Indentation Elastic Modulus (MPa)	962.99 345.98	996.73 588.99	0.920

Values are presented as mean ± standard deviation.
*equal variance t-test.
#Wilcoxon ranked-sum test.
p-values less than 0.05 are in bold.

Table 2. Mechanical properties from microindentation and nanoindentation.

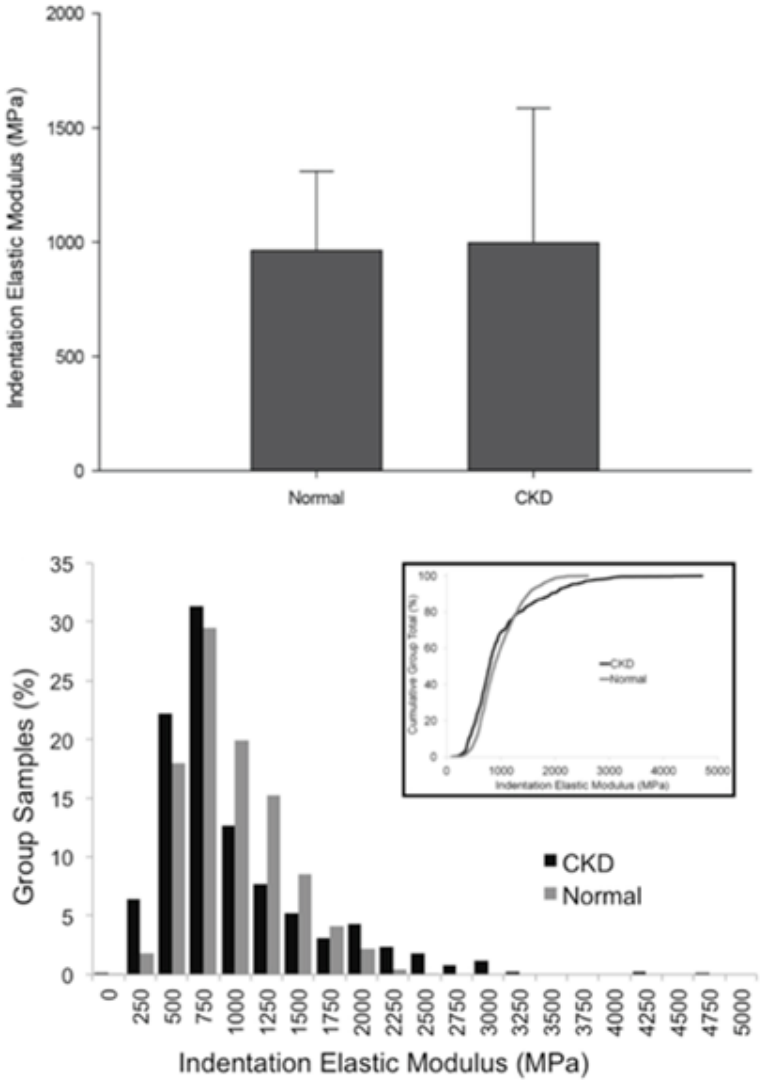

Figure 8**.** Nanoindenation reveals that CKD skeletal tissue has increased heterogeneity in the elastic modulus compared to normal bone. There was no significant difference in the average elastic modulus (A), but the distribution of elastic modulus values was significantly broader (B), with a greater proportion of both high and low values in CKD relative to normal ($p<0.0001$).

Tissue Composition

Raman spectroscopy revealed no differences between animals with CKD and their normal counterparts with regard to overall composition of the mineral and organic matrices (**Table 3**). Specifically, there were no differences between the groups in the phosphate-to-amide I ratio (the mineral-to-matrix ratio), mineral crystallinity, or the carbonate-to-phosphate ratio (a reflection of type B carbonate substitution).

Collagen Morphology and Cross-Linking

There were no mean differences in D-periodicity between the two groups (**Table 3**). There were also no differences in the distribution of D-periodicity when all fibrils were considered. In addition, both enzymatic and non-enzymatic cross-links as assessed by HPLC were similar between groups (**Table 3**).

Discussion

The mechanical integrity of skeletal tissue is determined by the amount of tissue present, its distribution, and its quality. Compromises in any of these factors can lead to an increased fracture risk. The notable loss of cortical bone mass associated with CKD is assumed to be primarily responsible for the increased fracture risk seen in patients[31]. The current study advances our understanding of bone fragility in CKD by showing that microscale and nanoscale mechanical properties are altered independently of changes in bone mass and porosity.

Raman	Normal (n = 6)	Cy/+ (n = 6)	p-values
Crystallinity (1/FWHM PO_4^{3-}ν1)	0.054±0.001	0.055±0.001	*0.4421
Carbonate Substitution (CO_3^{2-}ν1/PO_4^{3-}ν1)	0.618±0.037	0.608±0.019	#0.5375
Relative Mineralization (PO_4^{3-}ν1/Amide I)	2.539±0.253	2.699±0.317	*0.9372
AFM	**Normal (n = 6)**	**Cy/+ (n = 5)**	**p-values**
D-Periodicity (nm)	65.641±0.646	65.864±0.838	*0.631
HPLC	**Normal (n = 8)**	**Cy/+ (n = 6)**	**p-values**
Pyridinoline per Collagen (mol/mol)	0.60±0.17	0.54±0.10	**0.252
Deoxypyridinoline per Collagen (mol/mol)	0.37±0.07	0.37±0.04	**0.974
Pentosidine per Collagen (mol/mol)	878± 153	921±148	*0.523

Values are presented as mean ± standard deviation.
*equal variances t-test.
**unequal variances t-test.
#Wilcoxon ranked-sum test.

Table 3. Tissue composition and collagen morphology.

Our lab has previously documented reductions in both structural and estimated material properties in Cy/+ rats, animals with progressive CKD[108,119]. But, whole bone testing only provides indirect estimates of material properties, which is why we directly assessed microscale mechanical properties using reference point indentation (RPI). RPI data from the present study indicate that animals with CKD had higher IDI, higher first cycle creep indentation distance, and first cycle energy dissipation. Taken together, these results indicate that the tissue in animals with CKD is less resistant to indentation and more prone to damage. Indentation distance increase was nearly 20% higher in CKD animals compared to their normal counterparts. Similar differences in IDI have been previously reported in diabetic rats[120]. These data have two important implications. First, they show that CKD negatively affects skeletal tissue independently of bone mass, which means that estimates of bone mass alone likely underestimate the overall mechanical effects of CKD. These differences in bone quality may explain the conflicting data available on BMD and fracture risk in CKD patients[35-42]. Second, our data provide a basis for considering *in vivo* applications of RPI in the clinical setting of CKD. RPI has been used to successfully differentiate patients with and without hip fractures[121] as well as those with and without atypical femoral fractures[122]. A related indentation device has also been shown to discriminate patients with diabetes from their normal counterparts[123]. Assessment of tissue-level mechanical properties, combined with standard imaging modalities to measure bone mass, cortical geometry (especially porosity), and trabecular architecture, may prove to be an ideal

combination by which to assess the overall mechanical integrity of bones in patients with CKD.

The current study also employed a hierarchical approach by examining nanoscale mechanical properties with atomic force microscopy. AFM indentation provides a direct assessment of the nanoscale stiffness produced by the collagen and mineral composite. Consistent with measurements of microscale stiffness (first cycle unloading slope), these results show that the average indentation elastic modulus was not significantly different between the two groups. Yet, the distribution of elastic modulus values was different. Animals with CKD displayed a greater degree of heterogeneity in nanoscale elasticity. Because increased material heterogeneity is often considered advantageous[124], these results may reflect an adaptive response to declining integrity at larger length scales. Alternatively, extreme variations in nanoscale properties may lead to localized stress concentrations that result in damage accumulation from lower forces[125]. Although heterogeneity is likely necessary for normal mechanical integrity, extreme heterogeneity may be problematic from a mechanical standpoint[126]. Future studies should attempt to better understand the role of material heterogeneity in CKD in order to specify the contribution of microscale and nanoscale properties to whole bone mechanical properties.

While whole bone, microscale, and nanoscale mechanical differences are present in animals with CKD, tissue composition, collagen morphology, and collagen cross-linking fail to account for the differences. These data conflict with studies showing higher mineral-to-matrix ratios, lower mineral crystallinity,

increased advanced glycation end products (AGEs), and decreased gene expression of lysyl oxidase in alternative models of CKD[51,110,127]. One potential explanation for these disparate results is that these previous studies utilized younger animals that developed advanced CKD during skeletal growth. Teasing apart the interaction between growth and disease is difficult, which is why the present study employed the use of a model in which kidney disease occurs after skeletal maturity.

Previous studies have demonstrated that non-enzymatic cross-links (pentosidine, specifically) are increased in the circulation of patients with CKD[128-131]. These findings coincide with the accumulation of AGEs in soft tissues detected by fluorescence methods[132]. Because high levels in the circulation are associated with the deposition of AGEs in other tissues, this may be true of skeletal tissue as well. To date, this has only been confirmed in one small clinical study in patients on dialysis[133]. Currently, there are few data in animal models, and clinical trials examining predialysis patients are lacking. Using a low turnover 5/6 nephrectomy model, two studies have reported increased pentosidine using Raman spectroscopy[51,110]. While Raman spectroscopy has been utilized to detect AGEs in ocular tissue[134], its ability to detect changes in bone is unknown as HPLC is the standard method used to measure AGEs in skeletal tissue[133, 135-138]. Here, having employed HPLC, the hypothesized increases in AGE content were not observed. While increases may occur with more advanced disease in these animals, the relationship between circulating pentosidine and its accumulation in bone collagen in CKD remains unresolved.

At present, clinical data on bone quality in CKD are minimal. Aside from the aforementioned dialysis study[133], CKD patients with high bone turnover had reduced stiffness and a decreased mineral-to-matrix ratio as assessed on iliac crest biopsies[139]. As these data are from cancellous bone, though, direct comparison with the current work on cortical bone is difficult. Connecting these dots by examining cortical bone properties in patients (which is possible with iliac crest biopsies) and cancellous properties in rats will be an essential step in moving forward.

Limitations to the current study should also be recognized. First, because tissue from a previous study was used, the sample sizes used here were small. Hence, any applications to other animal models or patients should occur with a measure of caution. Second, the mechanical assessments were localized to the periosteal surface, which may not be fully representative of the entire cortex. As such, the assessed parameters may differ at other cortical sites. Finally, this study assessed material properties in 30-week-old animals. As the disease progresses, differences in composition and morphology may arise. Nevertheless, the advantage of using 30-week-old animals is that these animals are skeletally mature but do not yet exhibit the rampant increase in cortical porosity present at 35 weeks[119].

In conclusion, these data show that both microscale and nanoscale cortical bone material properties are altered in an animal model of CKD. The specific skeletal tissue alterations responsible for these mechanical differences remain unclear. Nevertheless, in addition to bone loss and cortical porosity,

defects in material-level mechanical properties may also contribute to the increased fracture risk associated with CKD.

CHAPTER 3

CHANGES IN SKELETAL COLLAGEN CROSSLINKS AND MATRIX HYDRATION IN HIGH AND LOW TURNOVER CHRONIC KIDNEY DISEASE

Material in this chapter has been previously published:

Osteoporosis International (2015) 26:977-985

Rationale

Given the difficulties explaining why microscale and nanoscale mechanical properties were impacted by CKD without obvious changes in tissue composition or morphology, samples from older rats were examined for changes in collagen cross-linking and bone matrix hydration. This was performed in order to assess the tissue properties of animals with more advanced disease to test the hypothesis that severe changes arise that are not apparent in the younger less disease-ridden animals.

Introduction

There are clear and consistent data showing that chronic kidney disease (CKD) is associated with an increased fracture risk compared to individuals without CKD[14,140-143]. More concerning is that individuals with CKD who experience a fracture are at greater risk of mortality compared to people without CKD who fracture[18,144]. There are numerous challenges to reducing fracture risk in CKD patients because of the complexity in the underlying bone disease. CKD is associated with significant metabolic derangements, including secondary hyperparathyroidism, yet some patients have low levels of parathyroid (PTH) for unclear reasons[140,145-146]. At the skeletal level, CKD appears to have a preferential impact on cortical bone, leading to increased porosity, and likely playing a major role in fracture[57,119,147-149]. Preclinical studies have documented CKD-associated reductions in biomechanical properties of whole bones, as well

as at the micro- and nanoscale levels of the hierarchical organization of bone[108-109,112,119,150]. Properties of the tissue, such as mineral content, have not shown clear differences between normal and diseased bone, leaving a cloud of uncertainty as to what properties of the tissue are responsible for this compromised mechanical phenotype associated with CKD[150].

Increased attention to “bone quality” (those aspects other than BMD that account for a bone’s resistance to fracture) has led to a greater understanding of various skeletal properties[46,139,150]. Collagen plays a vital role in bone with changes in collagen cross-links showing clear influence on bone mechanical properties[151-155]. CKD-induced collagen changes have been noted in serum and several soft tissues but data in bone are limited[110,127,133]. A less often discussed bone quality variable, bone hydration, also affects bone mechanical properties[156-158], but only recently has it become clear that in vivo modulation of hydration can play a role in a bone’s fracture resistance capacity[101,159-160].

While there is an increasing awareness of the importance of bone quality in CKD[48,139], few studies have explicitly examined material properties in animal models[108,110,112,119,150]. The goal of the present study was to examine two specific properties, collagen cross-links, and matrix hydration (bound and pore water) in a rat model with progressive development of CKD that can be manipulated to have either high- or low-turnover disease[53,119]. We hypothesized that CKD adversely affects both collagen cross-links and matrix hydration, and that these parameters would be most affected in high-turnover disease, and there would be relationships between these properties and bone mechanical outcomes.

Materials and methods

Animal model

The current study utilized a slowly progressive animal model of CKD, the Cy/+ rat, which has been described in detail several times[53,108,150,112,161,162]. Tissues analyzed in the current study were from select groups of animals that were part of a larger study[119]. Specifically, the animals were in one of three groups: Cy/+ animals that were untreated and thus had high-turnover bone disease, Cy/+ given calcium supplementation in their drinking water to suppress PTH starting at 25 weeks of age (low-turnover disease), or normal littermate controls (n = 8–10/gp). All animals were euthanized at 35 weeks of age and the femora (used to study both outcome measures) were saved and wrapped in saline-soaked gauze at −20 °C. Prior to the assays reported in this paper, the femora were tested in three-point bending[119]. Blood was also collected at the end of the experiment for biochemical analyses. Dynamic histomorphometry (detailing turnover rates), three-point bending, and biochemical assays have all been previously reported[119]. All procedures were conducted under the approval of Indiana University School of Medicine Institutional Animal Care and Use Committee protocol no. 10479.

Collagen cross-linking

Segments of the femoral diaphysis (~3 mm in length) were processed for collagen cross-links as previously described[150]. Briefly, following demineralized in 20 % EDTA (0.68 M, pH 7.4), demineralized bone was hydrolyzed. Each hydrolysate was resuspended in ultrapure water, split into two equal portions,

and dried. Half of the residue was resuspended in ultrapure water with an internal standard (5×10^{-6} g/L pyridoxine) and assayed by a high-performance liquid chromatography (HPLC) system (Beckman-Coulter System Gold 168). Standards with varying concentrations of pyridinoline (Pyd) (Quidel), deoxypyridinoline (Dpd) (Quidel), pentosidine (PE) (International Maillard Reaction Society), and a constant amount of pyridoxine were also assayed. Using a Waters 2475 fluorescence detector (excitation/emission of 295/400 nm for Pyd and Dpd and 328/378 nm for PE), chromatograms were recorded to determine the amount of each cross-link. These amounts were then normalized by collagen content (hydroxyproline), which was determined from the other half of each hydrolysate by another HPLC assay. The calculated mass of hydroxyproline was then multiplied by 7.5 (assuming 13–14 % of type I collagen by mass) and divided by the molecular weight of collagen (30,000 Da), thereby giving cross-link concentration as mole per mole of collagen. For each chromatogram, the area of the peak is calculated and divided by an internal standard. These values are then plotted onto a standard curve that plots the known masses of the standards to their given areas, providing an estimate of the mass of the given molecule in the unknowns (hydroxyproline, pyridinoline, deoxypyridinoline, and pentosidine).

^{1}H nuclear magnetic resonance spectroscopy

A ~5-mm cross-section of the femur mid-shaft was placed into a low proton, loop-gap-style radio-frequency (RF) coil[163] along with a reference microsphere of water ($T_2 \sim 2$ s). The nuclear magnetic resonance spectroscopy

(NMR) analysis to separate proton signals within the bone was then performed in a 4.7-T horizontal-bore magnet (Varian Medical Systems, Santa Clara, CA) using 90°/180° RF pulses of ~9/18-μs duration and collecting Carr-Purcell-Meiboom-Gill (CPMG) measurements with 10,000 echoes at 100-μs spacing. To generate the spectrum of transverse relaxation time constants (T_2), the echo magnitudes were fitted with multiple exponential decay functions[164]. Upon normalizing the integrated areas of bound water (T_2 = 100–800 μs) and pore water (T_2 = 800–600 ms) to the area of the reference (T_2 = 600 ms–10 s)[165], the volume of bound water and the volume of pore water were divided by the specimen volume (calculated from Archimedes' principle) to give bound water (bw) and pore water (pw) volume fractions.

Material-level biomechanical properties

Whole bone material properties, determined using three-point bending of the femora, have been previously reported[119]. Material-level properties were estimated using standard beam theory equations[156]. Bone diameters were measured at the mid-diaphysis using digital calipers, while cross-sectional moment of inertia was measured using micro-computed tomography.

Statistical analysis

All analyses were performed using SAS software. Comparisons among the groups were made using Student's *t*-tests as the focus of this work was to independently assess high/lower turnover conditions versus control. Pearson product moment correlation tests were used to assess the relationship between variables across all treatments with the exception of hydration for which

Spearman correlations were used, as the data were not normally distributed. A priori α levels were set at 0.05 to determine significance.

Results

High-turnover CKD model

Details about the phenotype of these animals with secondary hyperparathyroidism have been previous published[119]. Briefly, measures of kidney function and PTH were both significantly higher compared to normal (+200 and 2800 %, respectively), indicative of active disease. Trabecular bone turnover, measured by dynamic histomorphometry, was more than fourfold higher in compared normal; cortical porosity was more than doubled. Structural biomechanical properties, ultimate load, and stiffness, were both significantly lower than controls with no difference in energy to fracture, a biomechanical property that is not independent of bone structure[119].

All measured forms of collagen cross-links were significantly different compared to normal. The two mature enzymatic cross-links, Pyd and Dpd, were both significantly lower (−21 %; $p = 0.004$ and 0.02) compared to control (**Figure 9a**). There was no significant difference in the Pyd/Dpd ratio. PE, an advanced glycation product, was 71 % ($p = 0.001$) higher compared to normal (**Figure 9b**). Pore water volume fraction within the femoral cortex was higher (+46 %; $p = 0.024$), while matrix bound water volume fraction was significantly lower (−10 %; $p = 0.04$) compared to normal animals (**Figure 9c**).

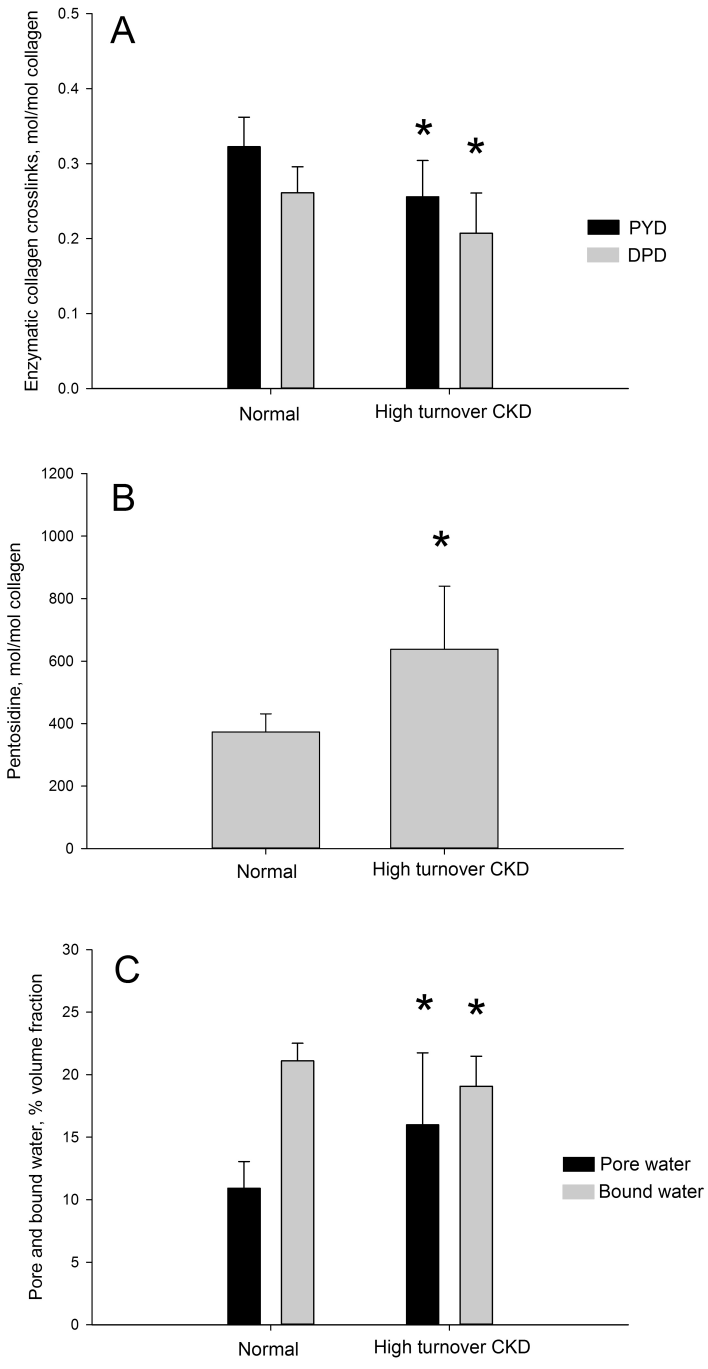

Figure 9. High-turnover CKD associated changes in skeletal collagen cross-linking and tissue hydration. (A) Enzymatic collagen cross-links (pyridinoline, Pyd

and deoxypyridinoline, Dpd) were significantly lower in CKD compared to normal littermates. (B) Pentosidine, an advanced glycation end product, was found in significantly higher concentrations in CKD bone compared to normal. (C) Pore water fraction was significantly higher and bound water fraction significantly lower in CKD animals compared to normal. *$p < 0.05$ compared to normal animals

Ultimate stress was significantly lower than normal animals (−22 %; $p = 0.001$) with no difference in modulus and a trend toward lower toughness (−21 %; $p = 0.11$) (**Table 4**).

Low-turnover CKD model

Details about the phenotype of these animals, where PTH is suppressed with the administration of calcium in the drinking water, have been previously published[119]. Briefly, measures of kidney function were significantly higher (+150 %), while PTH was significantly lower (−75 %) compared to normal. Trabecular bone turnover, cortical porosity, and structural properties were not different from controls.

Levels of Pyd in the bone matrix were not different from controls, while Dpd levels were significantly higher (+24 %;$p = 0.002$) compared to normal (**Figure 10a**). There was no significant difference in the Pyd/Dpd ratio. PE was 72 % higher ($p = 0.001$) compared to normal (**Figure 10b**). The NMR-derived pore water within the femoral cortex was lower (−60 %; $p = 0.001$), and bound water was significantly higher (7 %; $p = 0.04$) compared to normal animals (**Figure 10c**).

Toughness was significantly lower than normal animals (−27 %; $p = 0.005$) (Table 4). Ultimate stress and modulus were similar to normal animals.

	Normal	High turnover CKD	Low turnover CKD
Bone diameter, mm	3.7 ± 0.2	3.6 ± 0.2	3.7 ± 0.1
Porosity, %	0.1 ± 0.1	4.1 ± 5.4 *	0.5 ± 0.2 *
Cross-sectional moment of inertia, mm^4	10.1 ± 1.5	8.56 ± 0.9 *	11.1 ± 1.4
Ultimate stress, MPa	180 ± 17	140 ± 25 *	176 ± 27
Modulus, MPa	6777 ± 831	6609 ± 750	6701 ± 880
Toughness, MJ/m^3	5.3 ± 1.1	4.2 ± 1.8	3.9 ± 0.7 *

Values are presented as mean ± standard deviation.
* $p < 0.05$ versus normal controls.

Table 4. Femoral diaphysis morphology and calculated material-level biomechanical properties.

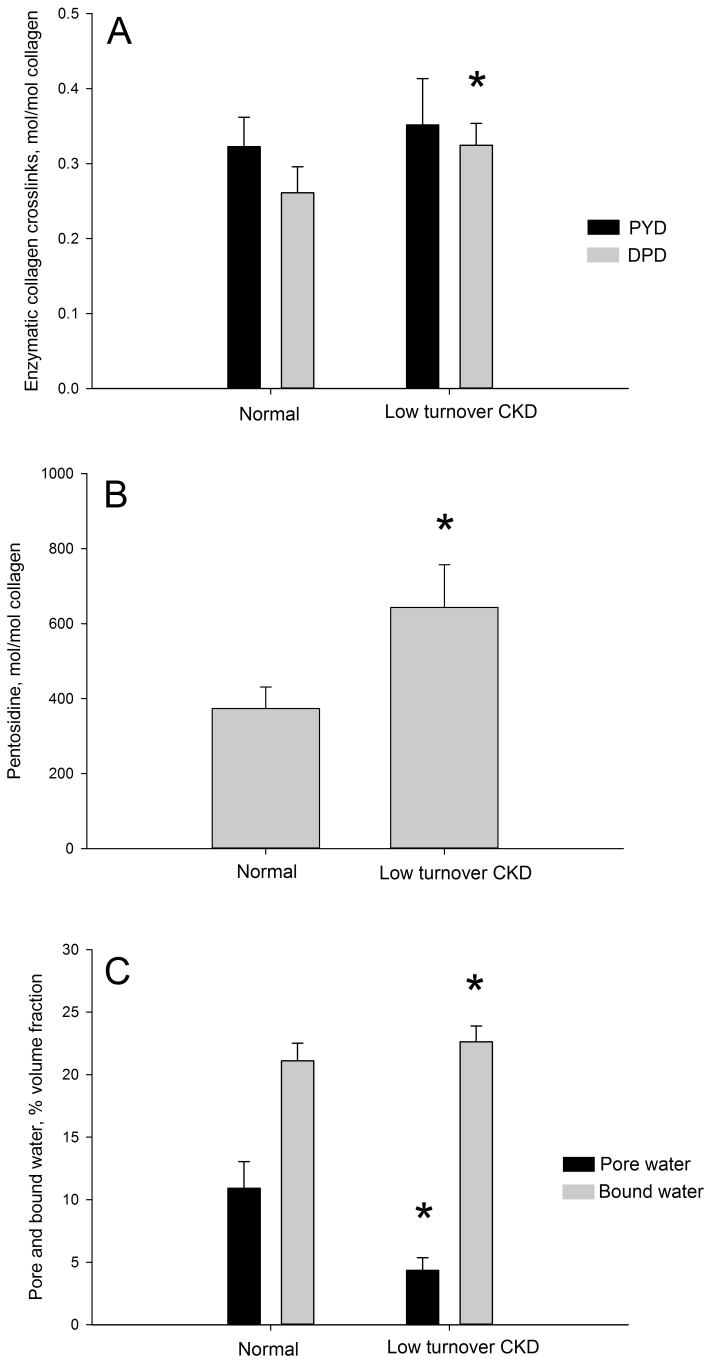

Figure 10. Low-turnover CKD associated changes in skeletal collagen cross-linking and tissue hydration. (A) The enzymatic collagen cross-link

(deoxypyridinoline, Dpd) was significantly higher than normal in low-turnover disease; pyridinoline, Pyd, was unaffected. (B) Pentosidine, an advanced glycation end product, was found in significantly higher concentrations in CKD bone compared to normal. (C) Pore water fraction was significantly lower and bound water fraction significantly higher in CKD animals compared to normal. *$p < 0.05$ compared to normal animals

Correlations

To examine relationships between outcome measures, correlations were assessed across the entire data set (controls, low-turnover CKD, and high-turnover CKD). Kidney function (assessed by BUN) was significantly correlated to PE ($R = 0.68$) (**Figure 11a**). PTH was significantly correlated to several outcomes including pore water ($R = 0.81$), bound water ($R = -0.70$), Pyd (−0.58), Dpd ($R = -0.72$), and PE ($R = 0.46$). PE levels were negatively correlated to ultimate stress and toughness ($R = -0.44$ and -0.57, respectively) (**Figure 11b**).

Discussion

It is becoming clear that the increased risk of skeletal fracture associated with chronic kidney disease is multifactorial and occurs due to changes in both bone quantity and quality[48,57,139,166]. We have previously documented in an animal of progressive kidney disease that compromised biomechanical properties can be quantified at the whole bone level as well as at the micro- and nanoscales[150]. These data illustrate that loss of bone mass, as has been repeatedly documented in both clinical and preclinical studies, is just one piece of the CKD fracture risk puzzle. Given the nanoscale changes in bone mechanical properties, our laboratory has focused on measuring properties of the tissue matrix that contribute to this level of mechanical integrity[150]. The results of the current work, in a preclinical animal model of progressive CKD, point to modification of both collagen cross-linking and bone hydration in

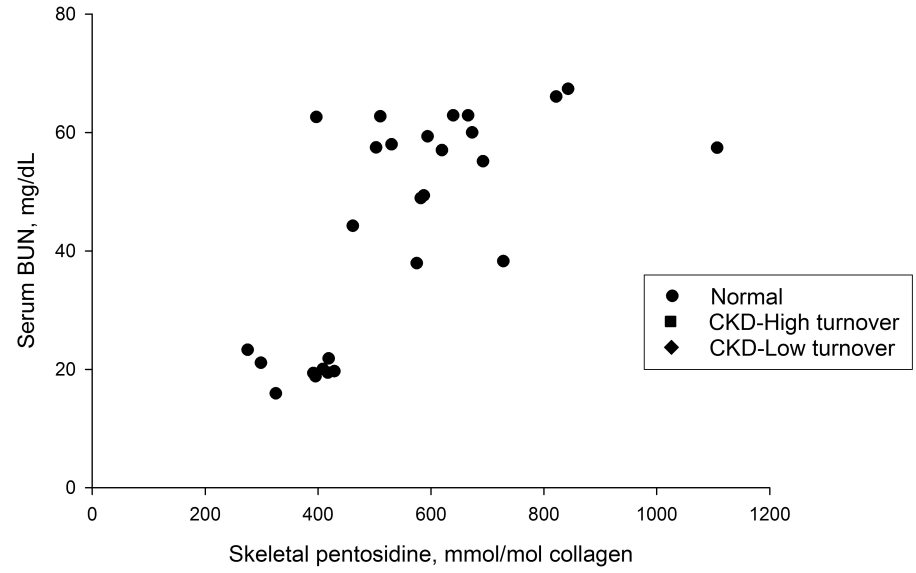

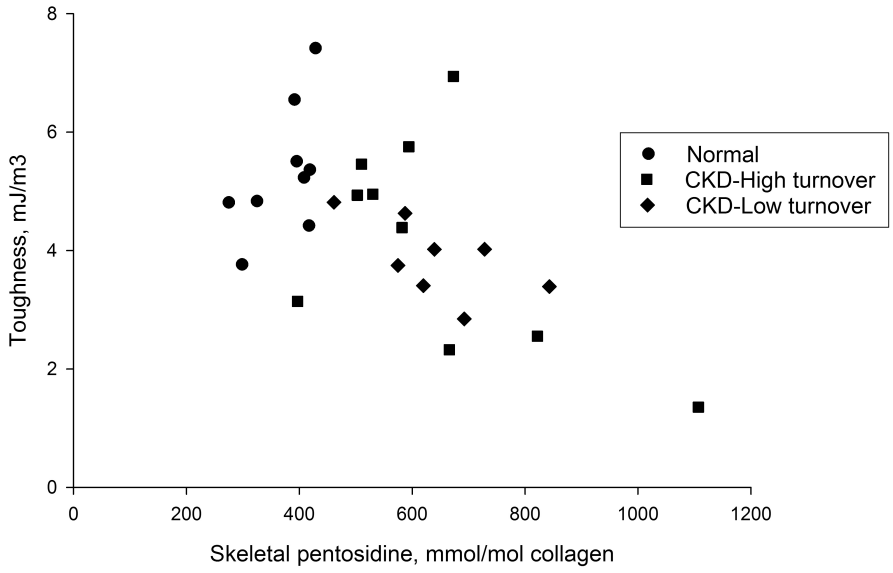

Figure 11. Correlations between skeletal pentosidine levels and kidney function (a) and mechanical properties (b). As both high- and low-turnover CKD models

were shown to have higher pentosidine levels compared to normal, we explored the relationship between kidney function and pentosidine. This relationship was statistically significant ($r = 0.68$, $p < 0.001$). Given the known role of pentosidine in modulation of mechanical properties, we also explored the relationship between pentosidine and bone toughness (b). This relationship was statistically significant ($r = -0.57$, $p = 0.002$)

late-stage CKD. The changes in cross-links confirm previous preclinical work in a different CKD model of high-turnover bone[110], while the hydration data results represent novel data and a potential variable that could be used for noninvasive clinical assessment of bone quality[159,167]. Collagen cross-links in bone are either enzymatically mediated (via lysyl oxidase) or nonenzymatically mediated (in the form of advanced glycation end products (AGEs) such as pentosidine)[151]. The predominant mature enzymatic cross-links pyridinoline and deoxypyridinoline (also known as hydroxylyslpyridinoline and lyslpyridinoline, respectively) have been shown to be associated with changes in bone mechanical properties[151]. Previous work by our lab in the same animal model as the current study showed no difference in Pyd or Dpd in CKD animals at 30 weeks[150]. We have documented that this animal model has rapid disease progression, in high-turnover states, between 30 and 35 weeks of age[108,119], leading us to hypothesize that major changes in collagen cross-links might manifest with progression to advanced disease. Although this turned out to be the case, the story is more complicated as the enzymatic cross-link changes were dependent of rate turnover; high-turnover groups had reduced enzymatic cross-links while low-turnover animals had higher than normal levels of Dpd.

The simplistic relationship between bone turnover and collagen cross-links is an inverse one. High bone turnover leads to lower levels of mature enzymatic cross-links because the mean tissue age is lower; while low-turnover bone typically has high levels. Yet this relationship model assumes that the process of collagen cross-links formation/maturation is not disrupted. Levels of lysyl

oxidase, the key enzyme involved in enzymatic cross-linking, are tissue-specific. Kidney levels of lysyl oxidase have been shown to be higher in CKD, and this is associated with increased fibrosis in renal tissue[168]. Serum measures of pyridinoline have been shown to be increased in patients with end-stage renal disease, and these levels were higher in patients with high turnover compared to those with low turnover[169]. Yet these serum measures do not provide insight into skeletal levels, as the latter are determined both the rate of formation/breakdown (i.e., bone turnover) and the rate of cross-link maturation (i.e., divalent to trivalent bonded). Skeletal levels of mature cross-links have been found to be lower in patients with high-turnover end-stage renal disease[133], while animal models of low turnover have shown reductions in bone lysyl oxidase levels[127]. Reduction in lysyl oxidase would reduce enzymatic cross-links—although neither the clinical nor preclinical study measured both enzyme and cross-links. Unfortunately, levels of lysyl oxidase were not assessed in the current work and thus definitive mechanisms underlying changes in mature cross-links cannot be ascertained.

Clinical studies have demonstrated that nonenzymatic cross-links (pentosidine, specifically) are increased in the circulation and soft tissue of patients with CKD[170]. Increased oxidative stress in CKD leads to increased production of AGE, and AGEs worsen oxidative stress, creating a vicious cycle that is independent of blood glucose levels[171]. Skeletal levels of AGEs have been shown to be elevated in a small clinical study in patients on dialysis[133]. Although we have recently shown that at 30 weeks of age there is no difference in skeletal AGEs in our progressive CKD model, the current results show that at 35 weeks

there is a striking difference (>70 % higher than normal). This suggests that, like the enzymatic cross-links, major changes occur between 30 and 35 weeks in this animal model. More interesting is that the levels of AGEs in the bone are independent of bone remodeling rate—both high- and low-turnover models had similarly higher AGE levels compared to controls (Figs. 1b and 2b). AGEs are typically linked to mean tissue age—since they accumulate in tissues over time when mean tissue age is higher AGEs are higher. It therefore follows that, in normal situations, bone with higher turnover rates will have lower AGEs compared to bone with lower turnover rates. This does not seem to hold true in the setting of CKD suggesting there is some intrinsic aspect of the disease that results in more AGE accumulation in bone independent of tissue age, perhaps due to ongoing AGE production in CKD[171] and reduced clearance by the kidney[172]. We hypothesize that elevations in oxidative stress may be underlying the accumulation of AGEs in this model. Thus, the severity of kidney disease may be more important than the level of bone turnover for determination of skeletal AGEs. The importance of the severity of kidney function is supported by a modest positive correlation between serum BUN and skeletal pentosidine ($R = 0.679$) in the current study (Fig. 11a).

The influence of hydration on bone mechanical properties has long been appreciated as it pertains to ex vivo mechanical testing[156-157]. More recently, data have emerged showing modulation of hydration can occur in vivo[101], suggesting that it could play a role in disease-related bone mechanical phenotypes. The results of the current study show that in high-turnover disease, pore water is

significantly higher, while in low-turnover disease, pore water is lower, than normal animals. Changes in pore water track closely to changes in cortical porosity, which is high in high-turnover animals and low in low-turnover animals at 35 weeks of age[119]. The changes in bound water, which have been shown to have predominant mechanical effect on bone[101], were unexpected and the mechanisms through which bound water is modulated in vivo remain unclear. Bound water tends to be inversely related to mineralization and at least at 30 weeks of age mineralization characteristics (determined by Raman spectroscopy) are not different from controls[150]. It is possible that mineral has changed by week 35 in these animals, yet unfortunately, tissue is not available for such analyses. Also, as intracortical porosity increases, there is more pore water but less matrix interactions with water molecules. This is confirmed in the current work by the positive correlation between pore water and porosity ($R = 0.69$).

Both AGE levels and bone hydration have been documented as having significant effects on bone mechanical properties. Increasing AGE levels either in vitro, or in vivo, are inversely related to bone toughness—the ability of the bone tissue to absorb energy before fracture[152,173]. Reductions in bone toughness reflect a bone that fractures more easily and in a more brittle fashion[174]. Conversely to AGEs, modulating bone hydration (specifically bound water) has been shown to have a positive relationship to bone toughness[101,175]. Estimation of material-level mechanical properties in the current study shows that both high- and low-turnover disease lower bone toughness relative to normal animals, with

only the lower turnover animals reaching statistical significance (**Table 4**). Interestingly, these two conditions had contrasting effects on pore and bound water, as well as enzymatically mediated cross-links. The only common feature of the two conditions was a significant increase in levels of AGEs (pentosidine). Skeletal pentosidine was negatively correlated to bone toughness ($r = -0.57$; Fig. 11b). While we cannot definitively conclude that the higher AGE levels are fully responsible for the biomechanical phenotype, the results of this work suggest it is an outcome that should be a primary focus in future studies.

In conclusion, using an animal model of progressive chronic kidney disease, we have shown that both collagen cross-linking and skeletal hydration are affected in late-stage renal disease. Although both of these variables are known to play roles in bone mechanical properties, the data suggest that accumulation on nonenzymatic collagen cross-links may be a key change that is responsible for altering mechanical properties associated with late-stage disease progression.

CHAPTER 4

CLINICALLY RELEVANT SUPPRESSION OF HYPERPARATHRYROIDISM WITH CALCITRIOL DOES NOT IMPROVE SKELETAL PROPERTIES IN AN ANIMAL MODEL OF CHRONIC KIDNEY DISEASE

Material in this chapter is being prepared for publication.

Rationale

Data from the previous studies indicate that in addition to significant bone loss, chronic kidney disease also has a direct effect on bone quality. Current treatment approaches primarily target the suppression of PTH with the goal of minimizing bone loss by slowing the activity of osteoclasts. While these agents (calcitriol and its analogues) improve BMD and reduce fractures in the general population, the extension of these benefits to patients with advanced kidney disease is unclear. Here, the impact of calcitriol on the skeleton is examined in the setting of 50% reduction in PTH levels, which is considered clinically efficacious in humans.

Introduction

Chronic kidney disease—mineral and bone disorder (CKD-MBD) represents a conglomeration of various metabolic and skeletal changes, such as hyperphosphatemia, secondary hyperparathyroidism, and an increased fracture risk[8-9,60]. Currently, the primary goal of therapy is the suppression of elevated levels of parathyroid hormone (PTH)[62]. Using calcitriol (and its analogues) and calcimimetics, clinicians target reductions of greater than 30% for serum PTH[167-177]. Unfortunately, the impact of these levels of suppression on vascular and skeletal outcomes is not clear due to a paucity of data[64-67].

While most osteoporosis clinical studies in non-CKD patients demonstrate that calcitriol reduces fracture risk through improvements in BMD[69-70], the extension of these benefits to patients with advanced kidney disease, where

cortical bone is so adversely affected, is unclear[62]. Previous studies in animal models of CKD have shown that suppression of PTH levels at or below normal levels with calcium has positive skeletal effects, essentially normalizing skeletal properties[108,119,178-179]. Unfortunately, this effectiveness comes at the cost of increased vascular calcification. These data are consistent with concerns raised about the use of calcium supplementation and calcium-based phosphate binders in late stage CKD patients[180-185].

In light of these data, a more thorough examination of the effects of calcitriol therapy on specific skeletal outcomes is necessary. Specifically, since current recommendations for PTH suppression still lead to PTH levels well above the normal range[60], how these levels of suppression affect bone parameters in CKD is not completely clear. Therefore, the current study sought to investigate how the clinically relevant suppression of PTH levels (~50%) in CKD would impact skeletal properties using an animal model of progressive chronic kidney disease.

Methods

Animal Model

Cy/+ rats are characterized by autosomal dominant polycystic kidney disease (PKD)[53]. Details of the model have been previously reported[108,119,178]. This model is characterized by the slow and gradual onset of CKD[53]. It parallels the human condition through the gradual development of abnormal mineral homeostasis and vascular calcification. Blood urea nitrogen (BUN) and creatinine are elevated by

20 weeks of age. Progressive hyperphospatemia, hyperparathyroidism, and skeletal abnormalities are present by 30 weeks.

Experimental Design

At 24 weeks, male Cy/+ rats were placed on a casein diet (Purina AIN-76A; 0.7% Pi, 0.6% Ca) to increase phosphorus availability. This diet has been shown to produce a more consistent kidney disease phenotype[53]. Starting at 25 weeks of age, Cy/+ rats were treated with vehicle (n=9) or calcitriol (n=11) (10 ng/kg 3x weekly; intraperitoneal) for 5 weeks. This treatment duration was chosen as it approximates an average bone remodeling cycle in skeletally mature rats (roughly six months in humans) and has been shown to be sufficient to detect treatment-induced skeletal changes in this model[108,119]. Calcitriol doses were chosen to achieve approximately 50% suppression of PTH levels in the Cy/+ rats. Non-affected male littermates served as controls (n=8). All rats were injected with calcein (10 mg/kg; subcutaneous) 14 and 4 days prior to sacrifice to label surfaces with active bone formation.

At 30 weeks of age, animals were anesthetized with isoflurane and underwent cardiac puncture for blood draw. The lumbar spine, tibiae, and femora were removed and stored at -20^{O}C for analysis. All procedures were approved by and carried out according to the rules and regulations of the Indiana University School of Medicine's Institutional Animal Care and Use Committee.

Biochemistry

Blood plasma at 30 weeks was analyzed for BUN, calcium, and phosphorus using colorimetric assays (Point Scientific, Canton, MI, or Sigma

kits). Intact PTH was determined by ELISA (Alpco, Salem, NH). FGF23 was assessed with a two-site assay (Immunotopics, San Clemente, CA)[11,53,112].

MicroCT

Using microCT (Skyscan 1172), trabecular architecture was determined from the metaphysis of the proximal tibia and the full length of the L4 vertebra. Cortical bone geometry was determined from the femoral midshaft. Cortical thickness was assessed at 75% of the height of the vertebra (from cranial to caudal) because this represents a region free of zygapophyseal attachment. All bones were wrapped in parafilm to prevent drying and scanned at a resolution of 12 μm in accordance with standard guidelines[186].

Histomorphometry

Static and dynamic histomorphometric measures were obtained from the proximal metaphysis of the tibia as well as the caudal metaphysis of the L3 vertebra. Histological processing followed previously used protocols from this lab[187-189]. Tissues were embedded in methyl methacrylate for undecalcified sections. Mid-transverse sections (4 μm) of cancellous bone from the proximal tibia and the caudal portion of the L3 vertebra were cut and left unstained for dynamic histomorphometry or stained with with tartrate-resistant acid phosphatase (TRAP) for osteoclast measurements (tibia only). For cancellous bone, a region of interest approximately 0.8 mm from the growth plate that was analyzed. Unstained sections were assessed for total bone surface, single-labeled surface, and double-labeled surface to calculate mineral apposition rate (MAR), percent mineralizing surface (MS/BS), and bone formation rate

(BFR/BS). TRAP-stained sections were assessed for bone surface, osteoclast number, and osteoclast surface to calculate the number of osteoclasts per unit bone surface (N.Oc/BS) and percent osteoclast surface (Oc.S/BS). All histomorphometric nomenclature follows standard usage[190].

Whole Bone Mechanics

Structural mechanical properties of the left femur were determined by four-point bending. The anterior surface was placed on two lower supports located +/- 9 mm from the mid-diaphysis (18 mm span length) with an upper span length of 6 mm. Specimens were loaded to failure at a rate of 2 mm/min. Structural mechanical properties were obtained directly from the force-displacement curves, while apparent material properties were derived from the force-displacement curves, cross-sectional moments of inertia (I_{ml}), and the distances from the centroid to the tensile surface using standard beam-bending equations for four-point bending[47].

Structural mechanical properties of the L4 vertebra were determined by uniaxial compression. Vertebra height was assessed from microCT images. Prior to mechanical testing, the vertebral arch and endplates were removed to create parallel surfaces for compression testing. Specimens were loaded at a rate of 0.5 mm/min. Structural mechanical properties were obtained directly from the force-displacement curves, while apparent material properties were derived from the force-displacement curves, pre-test sample heights, and the average bone area of five microCT slices (10%, 30%, 50%, 70%, and 90% slices of the pre-test sample height) using equations for uniaxial compression[191-192].

Tissue Composition

The anteromedial portion of the tibial mid-diaphysis was polished with a 0.05 μm alumina suspension in order to create a flat region for spectroscopy and indentation testing. Composition was assessed using a LabRAM HR 800 Raman Spectrometer (HORIBA JobinYvon, Edison, NJ). A 660 nm laser was focused on the bone surface using a 50X objective to a spot size of ~10 μm. Three locations were imaged ~3 mm apart with five 20 second acquisitions at each location as previously published[115]. A five-point linear baseline correction was applied in LabSpec 5 (HORIBA JobinYvon). Using OriginPro 8.6 (OriginLab, Northampton, MA), a single Gaussian peak was fit to the $PO_4^{3-}\nu1$ peak, and the areas under the $PO_4^{3-}\nu1$, $CO_3^{2-}\nu1$, and Amide I peaks were calculated at each location. Type B carbonate substitution was found by the band area ratio of $CO_3^{2-}\nu1/PO_4^{3-}\nu1$. The degree of matrix mineralization was determined by the band area ratio of $PO_4^{3-}\nu1$/Amide I. Mineral maturity (crystallinity) was determined by the inverse of the full width at half maximum (FWHM) of the $PO_4^{3-}\nu1$ peak.

Nanoindentation

After Raman spectroscopy, nanoindentation was performed on the same tibial samples using a Hysitron TI950 TriboIndenter. Samples were partially submerged in ultrapure water with the surface remaining uncovered for optical imaging of the surface to determine indentation locations but then fully submerged during testing. Locations were imaged using *in situ* scanning probe imaging. Then, 6 indentations were performed on a 10 μm x 20 μm grid, avoiding interactions from neighboring indentations. A previously calibrated fluid cell

Berkovich diamond probe was used for the indentations. Machine calibrations were performed at the beginning of each day of testing. Tests were conducted in load control with a 10s loading period, a 10s hold at 3000 μN, and a 10 s unloading period. From the resulting load-displacement profiles, the indentation elastic modulus and hardness were calculated according to the following equations:

$$E_r = \frac{\sqrt{\pi}}{2\sqrt{A(h_c)}} \cdot S$$

$$H = \frac{P_{max}}{A(h_c)}$$

where E_r is the reduced indentation elastic modulus of the sample, A is contact area, h_c is the contact displacement, S is the stiffness of the sample determined from 40-95% of the unloading slope, H is the hardness of the sample, and P_{max} is the peak force. All of the individual indentations (n=6 per location) were averaged to produce a single value for each location, and each of these locations was averaged to produce a single value for each sample.

Statistics

Comparisons among groups were assessed by one-way ANOVA with Fisher's LSD post-hoc tests. *A priori* α-levels were set at 0.05 to determine significance.

Results

Mineral Metabolism

Animals with CKD had higher serum levels of BUN compared to normal littermates. Serum calcium was normal, while phosphorus, FGF23, and PTH levels were all significantly higher than their normal counterparts (**Table 5**). Animals treated with calcitriol had BUN, calcium, and phosphorus values similar to their untreated CKD counterparts. PTH levels in calcitriol animals were significantly lower than untreated CKD animals (-61%) but still higher than normal controls (+381%). Likewise, FGF23 values in calcitriol-treated animals were lower than the vehicle-treated animals (-25%) but higher than normal controls (+176%).

MicroCT

Vehicle-treated CKD animals had lower trabecular bone volume than normal animals at the proximal tibia. A similar pattern was observed in the vertebra. In both cases, animals treated with calcitriol displayed no differences compared to their CKD-vehicle counterparts (**Figure 12** and **Table 6**). All other trabecular parameters were similar between calcitriol animals and the untreated CKD animals.

Cortical bone of the femoral midshaft and lumbar vertebra was also negatively affected by CKD. CKD animals had lower cortical area, cortical thickness, and bending moments of inertia compared to normal controls (**Table 6**). Animals treated with calcitriol displayed cortical values similar to CKD-vehicle animals. Calcitriol did not correct CKD-induced changes in cortical area,

Biochemistry	Normal	CKD (Vehicle)	CKD (Calcitriol)
BUN (mg/dL)	14.62 ± 1.95	48.32 ± 8.20 *	43.01 ± 7.07 *
Calcium (mg/dL)	9.979 ± 0.987	11.610 ± 2.323	10.240 ± 1.872
Phosphorus (mg/dL)	4.527 ± 0.579	6.682 ± 2.408 *	7.776 ± 1.170 *
PTH (pg/mL)	181.97 ± 105.05	2194.39 ± 1811.01 *	875.12 ± 432.51 *#
FGF23 (pg/mL)	698.36 ± 93.03	2556.83 ± 1401.96	1924.78 ± 748.81 *#

* vs. Normal
# vs. CKD (Vehicle)

Table 5. Biochemistry

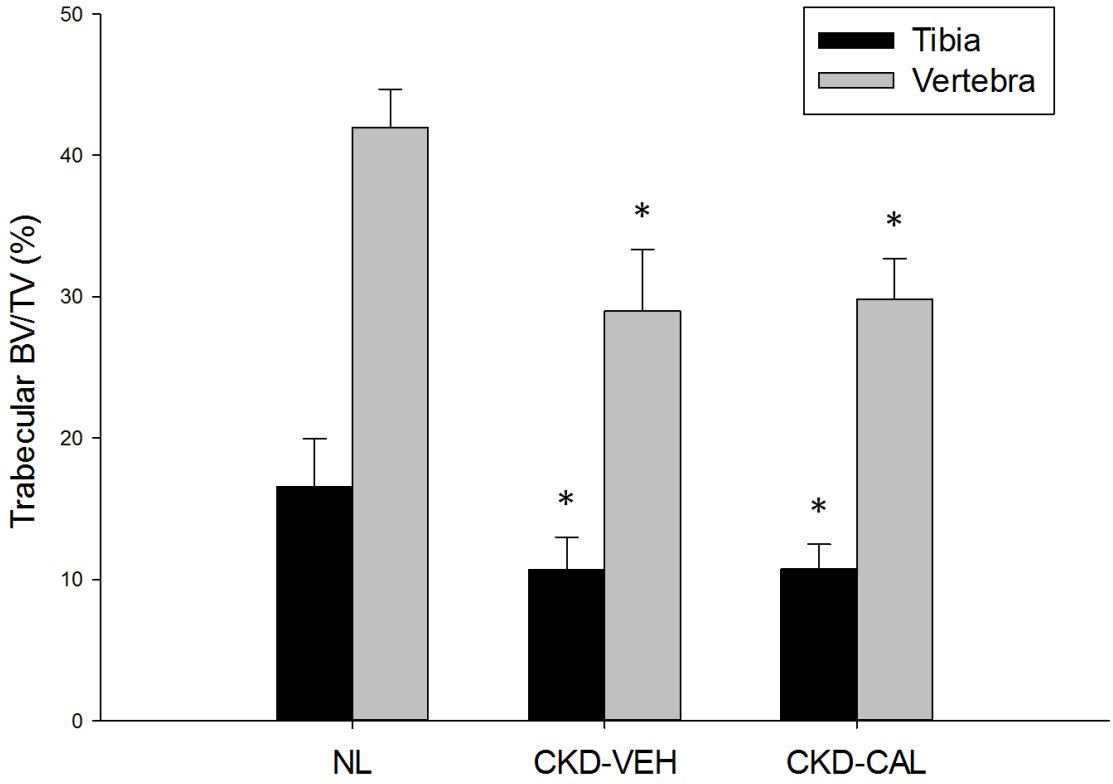

Figure 12. Cancellous bone structure in the proximal tibia and lumbar vertebra as determined by microCT. *, $p<0.05$ compared to NL

Proximal Tibia	Normal	CKD (Vehicle)	CKD (Calcitriol)
BV/TV (%)	17.04 ± 3.34	11.26 ± 1.51 *	10.70 ± 1.77 *
Tb.Th (mm)	0.106 ± 0.010	0.108 ± 0.004	0.101 ± 0.005 *
Tb.N (1/mm)	1.611 ± 0.253	1.052 ± 0.150 *	1.057 ± 0.163 *
Tb.Sp (mm)	0.369 ± 0.044	0.604 ± 0.114 *	0.523 ± 0.084 *
Femoral Diaphysis			
Ct.Th (mm)	0.876 ± 0.037	0.748 ± 0.056 *	0.769 ± 0.045 *
Ct.Ar (mm^2)	8.767 ± 0.631	7.324 ± 0.358 *	7.647 ± 0.378 *
I_{ap} (mm^4)	15.00 ± 2.59	12.40 ± 0.58 *	13.19 ± 0.89 *
I_{ml} (mm^4)	10.23 ± 1.56	7.50 ± 0.59 *	8.30 ± 0.99 *
Ct.Po (%)	0.681 ± 0.348	0.750 ± 0.357	0.769 ± 0.377
Lumbar Vertebra			
BV/TV (%)	41.88 ± 2.92	30.01 ± 3.98 *	29.83 ± 2.88 *
Tb.Th (mm)	0.119 ± 0.004	0.110 ± 0.007 *	0.105 ± 0.008 *
Tb.N (1/mm)	3.581 ± 0.258	2.726 ± 0.324 *	2.823 ± 0.220 *
Tb.Sp (mm)	0.213 ± 0.021	0.280 ± 0.031 *	0.275 ±0.018 *
Ct.Th (mm)	0.236 ± 0.033	0.170 ± 0.012 *	0.191 ± 0.035 *

* vs. Normal
# vs. CKD (Vehicle)

Table 6. MicroCT

thickness, porosity, or polar moment of inertia of the femur or cortical thickness of the vertebra (**Table 6**).

Histology

Vehicle-treated CKD animals had higher trabecular bone formation rates in the tibia and vertebra as well as higher osteoclast number and percent osteoclast surface than their normal counterparts (**Figure 13** and **Table 7**). Calcitriol animals displayed similar values to CKD-vehicle animals with regard to mineral apposition rate, osteoclast number, and percent osteoclast surface. While animals with calcitriol had a slightly higher proportion of mineralizing surfaces than CKD-vehicle animals (in the tibia only), bone formation rates at both sites were similar between these groups.

Whole Bone Mechanics

Animals with CKD had lower femoral ultimate force, stiffness, and energy to fracture compared to normal animals (**Figure 14** and **Table 8**). Estimated material properties revealed a significantly lower modulus of toughness in CKD animals (**Figure 14**) with no differences in the ultimate stress or elastic modulus (**Table 8**). Animals treated with calcitriol displayed no treatment effects compared to vehicle-treated CKD. They were similar with regard to ultimate force, stiffness, and energy to fracture (**Figure 14**). Calcitriol treatment also had no effect on estimated material properties (**Table 8**).

Vertebral compression tests, which assess both trabecular and cortical bone, revealed that CKD animals had lower ultimate force and energy to ultimate force but no differences in stiffness compared to normal animals (**Figure 14**).

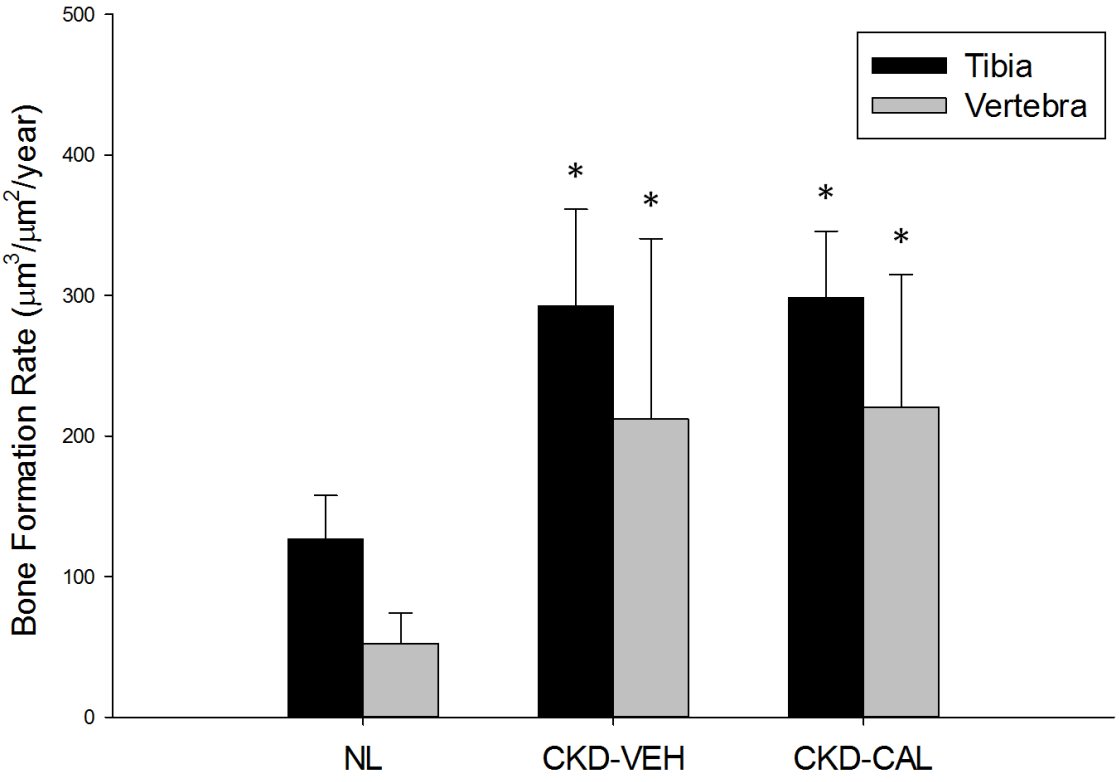

Figure 13. Bone formation rates in the proximal tibia and caudal lumbar vertebra as determined by dynamic histomorphometry. *, $p<0.05$ compared to NL

Tibia	Normal	CKD (Vehicle)	CKD (Calcitriol)
MAR (μm/day)	1.305 ± 0.185	2.470 ± 0.569 *	2.285 ± 0.343 *
MS/BS (%)	26.56 ± 5.14	33.32 ± 4.11	35.86 ± 3.26*#
BFR ($\mu m^3/\mu m^2$/year)	126.65 ± 31.02	299.62 ± 74.35 *	298.51 ± 47.41 *
Oc.S/BS (%)	7.157 ± 1.250	15.739 ± 3.332 *	13.538 ± 2.790 *
N.Oc/BS (1/mm)	1.966 ± 0.412	4.125 ± 0.785 *	3.604 ± 0.590 *
Vertebra			
MAR (μm/day)	1.057 ± 0.339	1.983 ± 0.876 *	1.87 ± 0.52 *
MS/BS (%)	13.62 ± 3.98	27.81 ± 5.73 *	31.39 ± 4.58 *
BFR ($\mu m^3/\mu m^2$/year)	52.14 ± 21.76	211.94 ± 128.49 *	220.61 ± 94.32 *

* vs. Normal
# vs. CKD (Vehicle)

Table 7. Histomorphometry

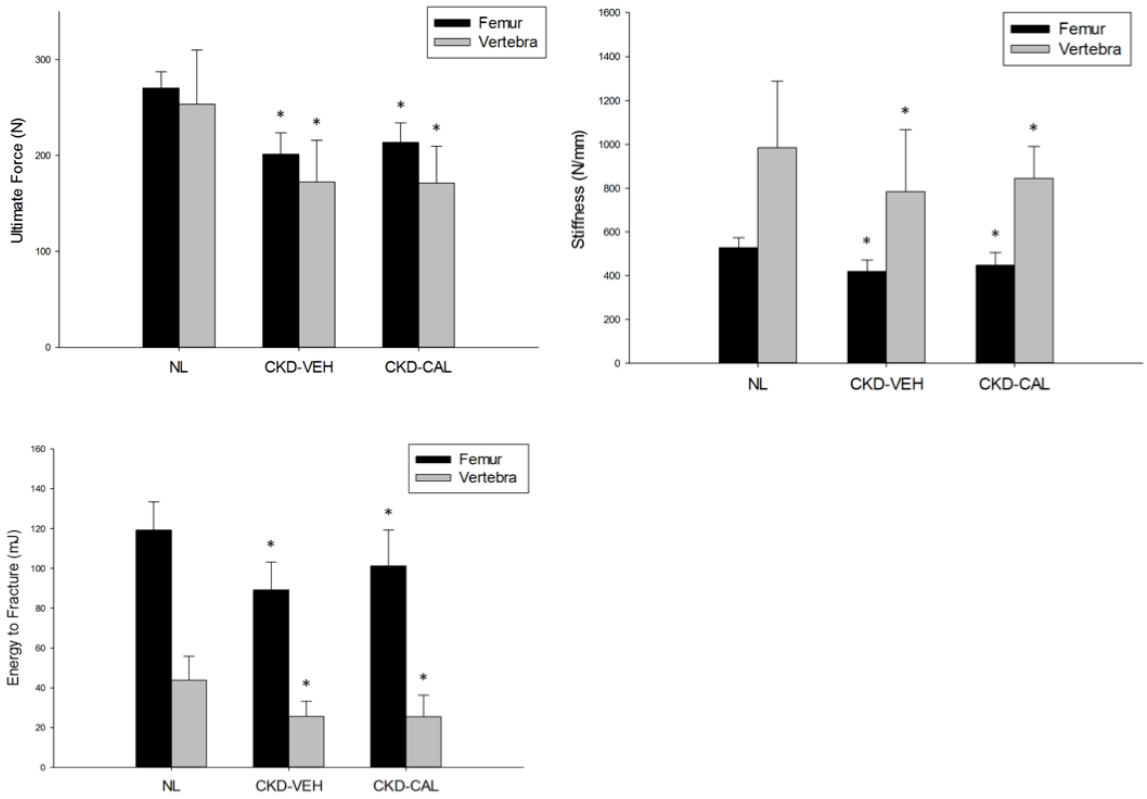

Figure 14. Whole bone mechanical properties of the femur as determined by four-point bending: (a) ultimate load, (b) stiffness, and (c) energy to fracture. *, $p<0.05$ compared to NL

Femur	Normal	CKD (Vehicle)	CKD (Calcitriol)
Ultimate Force (N)	272.08 ± 17.75	204.81 ± 23.20 *	214.00 ± 20.04 *
Stiffness (N/mm)	531.67 ± 47.41	412.96 ± 56.28 *	446.99 ± 58.57 *
Energy to Fracture (mJ)	119.16 ± 15.33	91.65 ± 14.13 *	101.305 ± 17.98 *
Ultimate Stress (MPa)	153.81 ± 15.68	143.94 ± 17.93	136.49 ± 9.60
Elastic Modulus (MPa)	4.649 ± 0.633	5.144 ± 0.971	4.830 ± 0.696
Toughness (MPa)	4.336 ± 0.382	3.652 ± 0.545 *	3.815 ± 0.518 *
Vertebra			
Ultimate Force (N)	256.89 ± 60.01	187.06 ± 48.03 *	171.31 ± 38.19 *
Stiffness (N/mm)	952.09 ± 314.20	866.74 ± 260.33	845.67 ± 144.32
Energy (mJ)	46.27 ± 10.60	28.05 ± 8.93 *	25.38 ± 10.88 *
Ultimate Stress (MPa)	42.49 ± 10.00	38.74 ± 9.16	35.33 ± 10.88
Elastic Modulus (MPa)	954.37 ± 334.35	1174.00 ± 447.08	1131.84 ± 170.17
Toughness (MPa)	1.310 ± 0.470	0.924 ± 0.347	0.819 ± 0.386

* vs. Normal
# vs. CKD (Vehicle)

Table 8. Whole Bone Mechanics

Estimated material properties were similar among all three groups. As above, vertebrae from calcitriol animals were no different than their untreated CKD counterparts.

Bone Quality

Animals with CKD were found to have no differences in indentation properties determined using nanoindentation compared to normal controls. Calcitriol animals showed no effect on these properties either (**Table 9**). Tissue composition assessed by Raman spectroscopy revealed no differences in any of the compositional parameters among the groups.

Discussion

The goal of this study was to assess the impact of clinically relevant levels of PTH suppression on CKD-induced bone disease. Using calcitriol, the current standard of care in patients with secondary hyperparathyroidism, PTH levels were suppressed by 60% in animals with CKD. Despite this reduction, no skeletal benefits were observed. This is likely due in part to the failure of calcitriol to suppress bone formation rates and osteoclast formation, which remained significantly higher than normal in both long bone and vertebral cancellous bone. While there is value in examining the efficacy of larger doses, these data raise important questions regarding how much PTH suppression is needed to produce skeletal benefits in the setting of CKD.

Raman Spectroscopy	Normal	CKD (Vehicle)	CKD (Calcitriol)
Crystallinity (1/FWHM PO_4^{3-}ν1)	0.0529 ± 0.0003	0.0534 ± 0.0008	0.0534 ± 0.0004
Carbonate Substitution (CO_3^{2-} ν1/ PO_4^{3-}ν1)	0.247 ± 0.008	0.242 ± 0.013	0.238 ± 0.013
Relative Mineralization (PO_4^{3-} ν1/Amide I)	2.598 ± 0.341	2.403 ± 0.442	2.759 ± 0.299
Nanoindentation			
Elastic Modulus (GPa)	11.066 ± 2.766	9.666 ± 1.021	9.987 ± 2.610
Hardness (MPa)	202.62 ± 22.86	192.68 ± 47.35	209.426 ± 43.65

* vs. Normal
# vs. CKD (Vehicle)

Table 9. Bone Quality

Numerous studies have examined the effectiveness of calcitriol and its analogues for patients with CKD using biochemical outcomes[61,64]. These studies indicate that patients receiving vitamin D supplementation exhibit effective restoration of $1,25[OH]_2D_3$ serum levels and suppression of PTH levels roughly 25-50% of pre-treatment levels[193-194]. Few studies have examined the impact of these treatments on bone outcomes, however. Calcitriol treatment suppressed high bone turnover in pediatric patients and was associated with normal PTH values[195]. Clinical strategies generally do not successfully (nor even seek to) attain these levels of suppression. In adult populations, decreases in static osteoblast and osteoclast measures were observed in patients taking alfacalcidol, but no changes were observed by dynamic measures[196]. Similar results have been observed with calcitriol. Both osteoblast and osteoclast static measures were lowered, but there were no changes in dynamic measures[197]. In the current study, dynamic measures were consistent with those studies, but osteoclast number and percent surface remained at the level of untreated CKD animals. Unfortunately, neither of these previous studies revealed clear relationships between bone remodeling and PTH suppression. Despite these data, there have been no fracture trials using calcitriol in CKD. More extensive bone analyses of calcitriol and its analogues have been conducted in patients with osteoporosis[69-70]. While fracture reduction is clear in that population, similar effects in CKD patients have not been examined.

Despite the lack of data in humans, there are several studies examining the impact of vitamin D analogues in animals. Using adult nephrectomized rats,

some studies have shown suppression of PTH, while others have not[111,198-200]. Even in the studies with PTH suppression, only one showed positive bone outcomes[111]. In that study, levels of PTH suppression similar to the current study were observed in 5/6 nephrectomized rats. Femoral neck bone mineral density and mechanical properties were higher than CKD animals and equivalent to normal animals. Interestingly, in their analysis of the femoral diaphysis (a site also assessed in the current study), no benefits were observed in bone mineral density or mechanical properties. Hence, while variations in these models may explain some of the skeletal differences, one possible explanation is that calcitriol has a preferential effect at certain skeletal sites. Although the femoral neck is a clinically relevant site, why it would be positively affected when the proximal tibia, femoral diaphysis, and lumbar vertebra in the current study were not is unclear.

Calcitriol is generally thought to increase FGF23 levels[201-204]. In the current study, though, animals treated with calcitriol had lower levels of FGF23. Several studies have failed to show a clear relationship between FGF23 levels and calcitriol[205-206]. Because serum $1,25[OH]_2D_3$ levels were not obtained from these animals, determining the cause of lower FGF23 levels will require further studies in this model. Furthermore, because the anticipated bone effects were less than expected, these results may represent a dosage effect.

The current study demonstrated that calcitriol treatment, while efficacious in terms of PTH suppression in animals with CKD, did little to curb the detrimental effects of CKD on the skeleton. This was demonstrated by its lack of effect on biochemical and histomorphometric measures. Animals treated with

calcitriol also showed no effect with regard to bone structural properties, whole bone mechanical properties, or bone quality despite a greater than 50% reduction in PTH levels. This indicates that a greater degree of PTH suppression may be required for efficacy in skeletal properties to occur in the setting of CKD.

CHAPTER 5

A COMPARISON OF CALCIUM TO ZOLEDRONIC ACID FOR IMPROVEMENT OF CORTICAL BONE IN AN ANIMAL MODEL OF CKD

Material in this chapter has been previously published:

Journal of Bone and Mineral Research (2014) 29:902-910

Rationale

The role of pharmacological interventions routinely used in the treatment of metabolic bone diseases, such as osteoporosis, has been understudied in the setting of CKD-MBD. While the current clinical strategy is to lower PTH levels in an effort to reduce bone resorption, the previous study indicates clinical levels of suppression may not translate into skeletal benefits. To better understand basic treatment approaches in CKD, this study compared calcium (to lower PTH and bone resorption) and zoledronic acid, one of the most common and effective anti-resorptive therapies employed in osteoporosis.

Introduction

Chronic kidney disease–mineral and bone disorder (CKD-MBD) is a disorder of abnormal biochemistries, bone fragility, and arterial calcification in patients with advanced CKD[140]. Patients with CKD have increased risk of bone fracture compared to the general population[17]. The increased fracture risk is due to a combination of abnormal bone quantity and quality[31,207].

The pathophysiology of bone loss associated with CKD-MBD is different than postmenopausal osteoporosis, suggesting that extrapolation of data from trials of treatments in postmenopausal or corticosteroid-induced osteoporosis may not be appropriate. Secondary analyses of randomized controlled trials of bisphosphonates in postmenopausal women subsequently identified to have kidney disease demonstrated reduced fracture risk and improved bone mineral density without adverse consequences[79-80]. However, these patients had neither

advanced kidney disease nor elevated parathyroid hormone (PTH) levels. These differences provided the rationale for global clinical practice guidelines to recommend against treating patients with CKD stage 3b-5 with bisphosphonates without a bone biopsy[60]. We have previously used our slowly progressive animal model of CKD-MBD to test different doses of the bisphosphonate zoledronic acid on bone mass, turnover, and biomechanical properties in animals with hyperparathyroidism and moderate renal disease[108]. In the present study, we extend these findings to compare the skeletal (both cortical and cancellous) and vascular effects of zoledronic acid with and without calcium in the setting of high and low PTH levels in CKD animals with more advanced renal disease.

Subjects and Methods

Animal model and experimental design

Male Cy/+ rats, Han:SPRD rats with autosomal dominant polycystic kidney disease, and their nonaffected (normal) littermates were used for this study. Male heterozygous rats (Cy/ +) develop characteristics of CKD (azotemia) around 10 weeks of age that progresses to terminal uremia by about 40 weeks. This animal model spontaneously develops all three manifestations of CKD-MBD: biochemical abnormalities, extraskeletal calcification, and abnormal bone[53,112].

At 25 weeks of age, animals were assigned to treatment groups. In the CKD (Cy/ +) animals, this age represents approximately 30% to 40% of the kidney function of the normal littermates. This was chosen to simulate late stage 3b CKD, a stage at which there is elevated PTH, yet normal calcium and

phosphorus levels, and a stage at which clinical practice guidelines do not recommend treatment with bisphosphonates[60]. The CKD treatment groups (*n* = 10 per group) were given: (1) a single subcutaneous (SQ) dose of vehicle as control (CTL) and normal deionized drinking water; (2) a single SQ dose of zoledronic acid (ZOL) (20 μg/kg body weight) and normal deionized drinking water; (3) no injection but administered 3% calcium gluconate (3% Ca) in the drinking water; or (4) zoledronic acid plus 3% Ca in the drinking water (Ca + ZOL). The calcium gluconate group was used to simulate calcium administration as a phosphate binder. In addition, we studied age-matched normal (NL) littermate animals (*n* = 10) to determine if treatments normalized bone manifestations or extraskeletal calcification. All animals were fed a casein diet (Purina AIN-76A, Purina Animal Nutrition, Shreevport, LA, USA); 0.53% Ca and 0.56% P) during the experiment, which has been shown to produce a more consistent kidney disease in this model[53]. Two weeks prior to the end of the study, all animals were given an intraperitoneal injection of calcein (1% concentration, 0.1 mL/100 g body weight); a second injection was given 10 days later. At 35 weeks of age all animals were euthanized by an overdose of sodium pentobarbital. All procedures were reviewed and approved by the Indiana University School of Medicine Institutional Animal Care and Use Committee.

Tissue collection and analysis

At euthanasia at 35 weeks, blood and urine were collected by cardiac and bladder puncture, respectively. The heart and aorta arch were excised and weighed. Left ventricular mass index (LVMI) was determined by dividing total

heart weight by body weight. To quantify aorta and heart calcification, proximal segments of the ascending aorta and a segment of the inferior apex of the left ventricle of the heart were snap frozen and the degree of calcification was determined biochemically as described[208]. Left tibias were placed in 10% neutral buffered formalin for 48 hours and then changed to 70% ethanol for imaging followed by histological processing.

Serum and urine biochemical measurements

Blood plasma was analyzed for blood urea nitrogen (BUN), calcium, phosphorus, and creatinine using colorimetric assays (Point Scientific, Canton, MI, USA; or Sigma kits; Sigma, St. Louis, MO, USA). Intact PTH was determined by ELISA (Alpco, Salem, NH, USA). FGF23 was assessed with a two-site assay (Immunotopics, San Clemente, CA, USA). Urine was analyzed for creatinine, calcium, and phosphorus using colorimetric methods[112].

Computed tomography

Morphological parameters of the proximal tibia were assessed using high-resolution micro–computed tomography (μCT) (Skyscan 1172). Bones were wrapped in parafilm to prevent drying during scanning. Scans were obtained using an X-ray source, set at 60 kV and 167 μA over an angular range of 180 degrees (rotational steps of 0.70 degrees) with a 12-μm pixel size. Projection images were reconstructed using standard Skyscan software (NRecon). A 1-mm region of interest of the proximal tibia (located ~0.5 mm distal to the growth plate) was analyzed by segmenting the trabecular bone from the cortical shell and calculating trabecular bone volume per total volume (BV/TV) in accordance with

recommended guidelines[186]. On the most distal slice of the 1-mm region of interest, the cortical shell was manually isolated from the trabecular bone by tracing the periosteal and endocortical edges. Porosity of the cortical shell was calculated as total bone area within the cortex divided by total area of bone plus void space within the cortex.

Bone histomorphometry

Tibias were embedded in methylmethacrylate for sectioning as described[108,209]. The proximal tibial metaphysis was thin sectioned (4 μm) and mounted unstained using nonfluorescent medium. Sections were analyzed using a microscope interfaced with a semiautomatic analysis system (Bioquant OSTEO 7.20.10; Bioquant Image Analysis Co.). Two of 10 CKD vehicle-treated animals, and 2 of 9 CKD calcium-treated animals did not have double labels in the proximal tibia section region of interest. In these animals, tibia midshafts were sectioned and also found to contain no double label. This suggests these animals were not properly administered both labels (likely due to injection directly into bladder) and thus these animals were excluded from the histological analysis, according to published recommendations[210]. For trabecular bone analyses, a region of interest of approximately 8 mm^2 within the secondary spongiosa (~0.5 mm distal to the growth plate) was defined, and then measures of single-label and double-label perimeter (sL.Pm, dL.Pm), total bone perimeter (B.Pm), and interlabel width (Ir.L.Wi) were conducted. From these primary measurements, derived parameters were calculated as: mineralizing surface (MS/BS = [1/2sL.Pm + dL.Pm]/B.Pm; %), mineral apposition rate

(MAR = Ir.L.Wi/days between labels; μm/d), and bone formation rate (BFR/BS = MAR × MS/BS × 3.65; $\mu m^3/\mu m^2$/year). All parameters were measured and calculated in accordance with ASBMR recommended standards[211].

Bone mechanics

Femurs were tested via three-point bending using standard methods as described for the rat[108]. Femurs were thawed to room temperature, hydrated in 0.9% saline, and placed on the bottom support of a servohydraulic test system (Test Resources). All bones were loaded to failure in an anterior-posterior direction using a displacement rate of 2 mm/min with force versus displacement data collected at 10 Hz. Structural mechanical properties, ultimate load, stiffness, and energy to failure were determined from the load-deformation curves using standard definitions.

Statistics

All analyses were run using SigmaStat software. The five groups were compared using a one-way ANOVA with Fisher's post hoc analyses for within group comparisons. Correlations were examined by the Pearson product-moment algorithm. A priori α-levels were set at 0.05. Data are presented as means and standard errors.

Results

Biochemical outcomes

At 35 weeks, there was no difference in the plasma BUN in the CKD animal treatment groups, but values for all CKD animals were higher than normal

animals as expected (CKD BUN 59.6 ± 1.5 versus NL BUN 19.9 ± 0.63 mg/dL). The total body weight was not different between any of the five groups. There were overall differences in the other blood results (**Figure 15**). In the CKD rats, treatment with calcium, both alone and in combination with zoledronic acid, led to an increase in plasma calcium ($p < 0.001$) and FGF23 ($p < 0.005$) levels and a decrease in PTH ($p < 0.001$) and phosphorus ($p < 0.05$) levels compared to CKD-CTL. In contrast, treatment with zoledronic acid alone had no significant effect on these biochemical measures. The effect of the combination of zoledronic acid with calcium was not different than calcium alone for any of these plasma biochemistry results. The plasma calcium level was negatively correlated with PTH ($r = -0.53$, $p < 0.001$) and positively correlated with FGF23 ($r = 0.44$, $p < 0.002$). The plasma phosphorus level was more strongly related to the PTH ($r = 0.79$, $p < 0.001$) than FGF23 ($r = 0.33$, $p < 0.003$). The urine calcium/creatinine ratio was significantly increased in both calcium treatment groups (Vehicle = 0.27 ± 0.09; Zol = 0.27 ± 0.12; Ca = 0.70 ± 0.22; Zol + Ca = 0.50 ± 0.20 mg/mg, $p < 0.0001$). The urine phosphorus/creatinine ratio was decreased in both calcium treatment groups (Vehicle = 1.33 ± 0.56; Zol = 1.75 ± 0.44; Ca = 1.08 ± 0.49; Ca + Zol = 0.79 ± 0.35 mg/mg, overall $p = 0.002$). The albumin/creatinine ratio was not different among the groups.

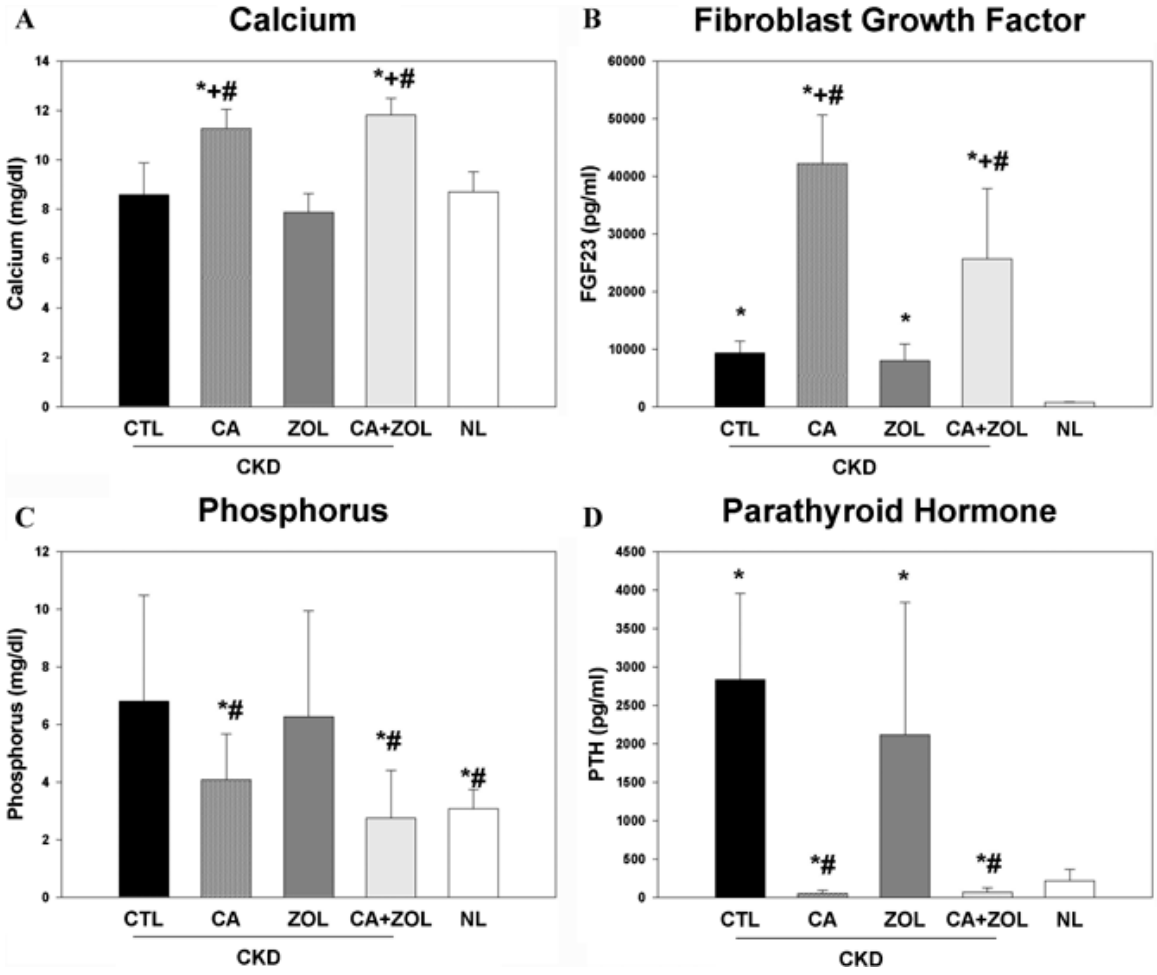

Figure 15. Biochemical changes in response to therapies. CKD animals were treated beginning at 25 weeks of age with control vehicle (CTL), calcium in drinking water daily for 10 weeks (Ca), zoledronic acid 20 µg/kg given subcutaneously once at 25 weeks (ZOL), or the combination of Ca + ZOL. The results were compared to normal animals (NL) treated with vehicle. Blood was drawn at 35 weeks of age. The results demonstrate that treatment with calcium, with or without zoledronic acid, led to increased calcium levels (*A*), increased fibroblast growth factor 23 (*B*), decreased parathyroid hormone levels to those in NL (*C*), and decreased phosphorus levels (*D*). *different than NL; +different than

CKD-CTL; #different than CKD + ZOL; all $p < 0.05$. Graphs are mean ± SEM, $n = 8$ to 10 per group. CKD = chronic kidney disease; CTL = control; ZOL = zoledronic acid; NL = normal animals.

Cardiovascular outcomes

At 35 weeks, the CKD animals had increased left ventricular mass index (LVMI) compared to normal animals ($p < 0.001$) that was unaffected by treatments (CKD + CTL = 3.8 ± 0.19, CKD + Ca = 3.9 ± 1.2, CKD + ZOL = 4.0 ± 0.4, CKD + Ca + ZOL = 4.0 ± 0.4, NL +Vehicle 3.2 ± 0.06, overall $p = 0.035$). However, treatment with calcium increased aortic arch calcium content, and this adverse effect was mitigated by zoledronic acid (**Figure 16**). The aorta arch calcium content was significantly (all $p < 0.01$) correlated with LVMI ($r = 0.48$), BUN ($r = 0.47$), calcium ($r = 0.43$), and FGF23 ($r = 0.51$) but not phosphorus or PTH. In contrast to our previous studies in this model[208], there was no difference in the heart calcification between any of the groups.

Bone outcomes

By μCT, there was no difference in the trabecular bone volume between CKD and NL animals. ZOL, calcium, and calcium + ZOL treatment significantly increased percent bone volume ($p < 0.0001$) in CKD rats but there was no difference among these three treatment groups (**Figure 17a**). The bone volume was strongly correlated with trabecular number ($r = 0.77$, $p < 0.001$). The trabecular bone volume was positively correlated with the calcium ($r = 0.53$) and FGF23 ($r = 0.42$), negatively correlated with PTH ($r = -0.47$; all $p < 0.01$), but not correlated with phosphorus. Cortical porosity was increased in CKD animals compared to normal animals, with significant reduction in animals treated with calcium and calcium plus ZOL; the ZOL treatment showed a nonsignificant reduction ($p = 0.13$; **Figure 17b**). Corresponding 3D reconstruction of the μCT

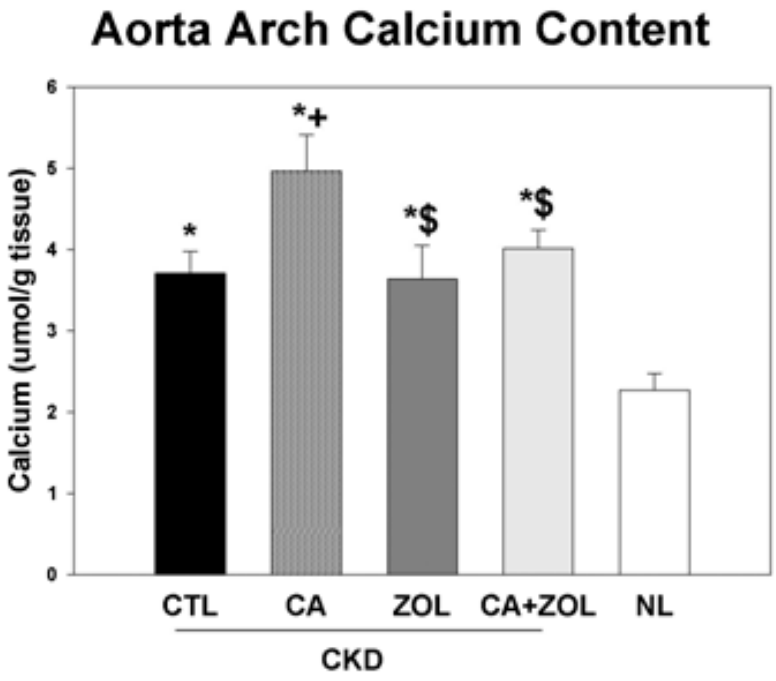

Figure 16. Aorta arch calcification in response to therapies. CKD animals were treated beginning at 25 weeks of age with control vehicle (CTL), calcium in drinking water daily for 10 weeks (Ca), zoledronic acid 20 µg/kg given subcutaneously once at 25 weeks (ZOL), or the combination of Ca + ZOL. The results were compared to normal animals (NL) treated with vehicle. The aorta calcium content was determined biochemically. The results demonstrated that CKD animals given any treatment had increased aorta calcification compared to NL animals, and that the treatment with calcium increased calcification further among the CKD animals. The coadministration of calcium with zoledronic acid led to a reduction of the calcium induced arterial calcification compared to calcium alone. *different than NL; +different than CKD-CTL; $different than CKD + Ca; all $p < 0.05$. Graphs are mean ± SEM, $n = 8$ to 10 per group.

CKD = chronic kidney disease; CTL = control; ZOL = zoledronic acid; NL = normal animals.

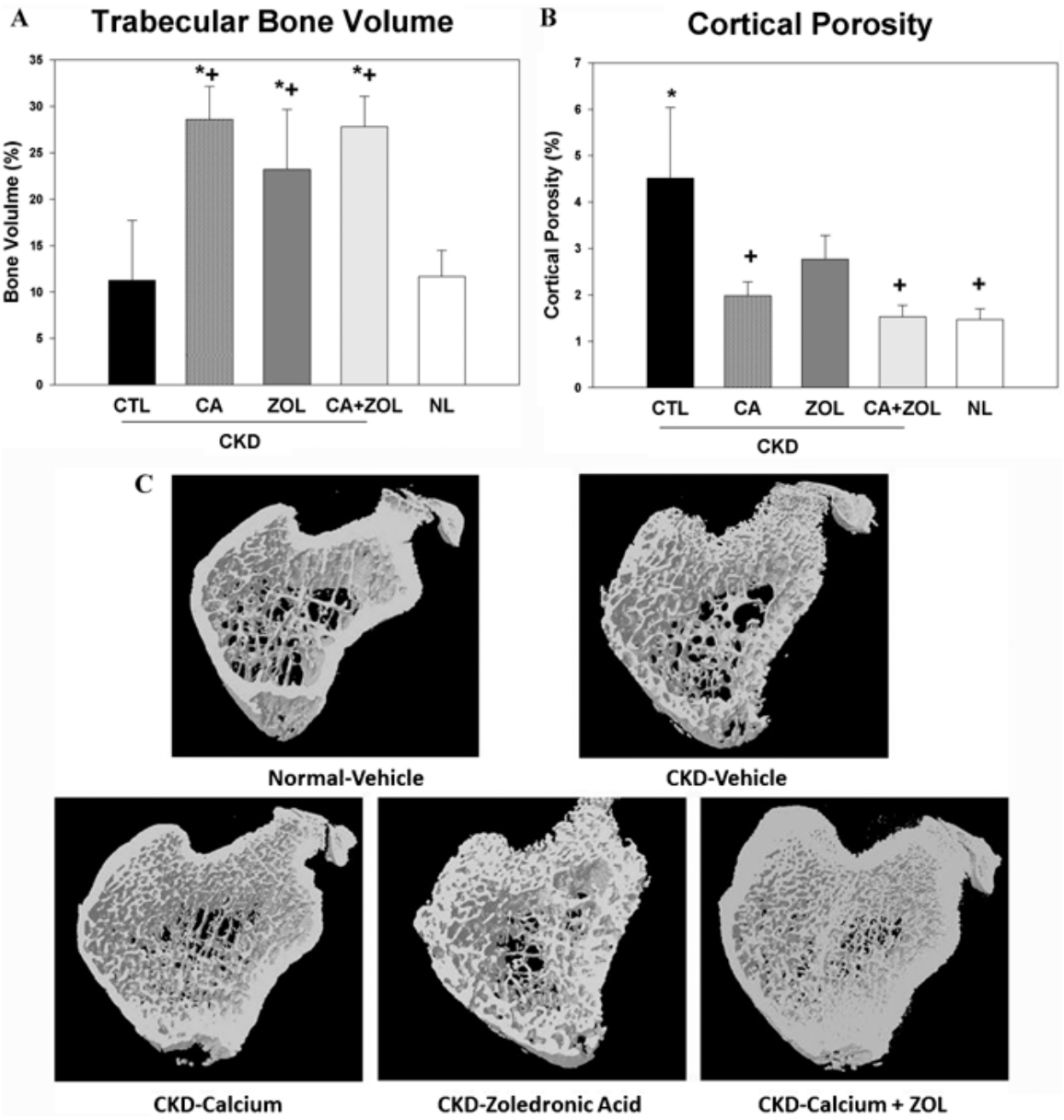

Figure 17. Trabecular bone volume and cortical porosity in response to therapies. CKD animals were treated beginning at 25 weeks of age with control vehicle (CTL), calcium in drinking water daily for 10 weeks (Ca), zoledronic acid 20 μg/kg given subcutaneously once at 25 weeks (ZOL), or the combination of Ca + ZOL. The results were compared to normal animals (NL) treated with vehicle. At euthanasia at 35 weeks, the tibias were assessed by μCT for trabecular bone

volume (*A*) and cortical porosity (*B*). The results demonstrate that there was no difference in trabecular bone volume between CKD and NL animals treated with vehicle. However, all of the treatments led to higher bone volume in the CKD animals compared to CKD-vehicle. In contrast, the cortical porosity was increased in vehicle-treated CKD animals compared to NL animals. Treatment with calcium, or calcium plus zoledronic acid, but not ZOL alone, reduced cortical porosity to NL levels. The 3D reconstructions (*C*) provide visualization of these trabecular and cortical effects across groups. *different than NL; +different than CKD-CTL; all $p < 0.05$. Graphs are mean ± SEM, $n = 7$ to 10 per group.
CKD = chronic kidney disease; CTL = control; ZOL = zoledronic acid; NL = normal animals.

images are shown in **Figure 17c**. The magnitude of cortical porosity was strongly associated with phosphorus ($r = 0.80$) and PTH ($r = 0.70$, both $p < 0.001$), but not associated with FGF23, calcium, or bone volume.

Dynamic bone histomorphometry demonstrated that the MAR was increased in the CKD animals compared to normal, and decreased by all treatments in the CKD animals to levels similar to that observed in NL animals (**Figure 18a**). Similar results were observed for mineralizing surface (MS/BS; **Figure 18b**) and BFR (**Figure 18c**). PTH and phosphorus were positively associated with all three histomorphometric indices with the strongest relationship with MAR ($r = 0.61$ for PTH and $r = 0.42$ for phosphorus, both $p < 0.01$). The calcium level was negatively correlated only with BFR ($r = -0.35$, $p = 0.03$) and MS/BS ($r = -0.53$, $p < 0.001$).

Ultimate load and stiffness of the femoral diaphysis were both significantly lower in untreated CKD animals compared to NL (**Table 10** and **Figure 19**). CKD animals treated with ZOL had properties similar to untreated CKD (and lower than NL-VEH), while those treated with calcium, or the combination of ZOL and calcium had mechanical properties significantly higher than CKD and similar to NL.

Relationship of bone to cardiovascular outcomes

The aortic arch calcification was correlated with trabecular bone volume ($r = 0.43$, $p = 0.005$) and cortical porosity ($r = 0.34$, $p = 0.03$), but not with any of the three histomorphometry measures.

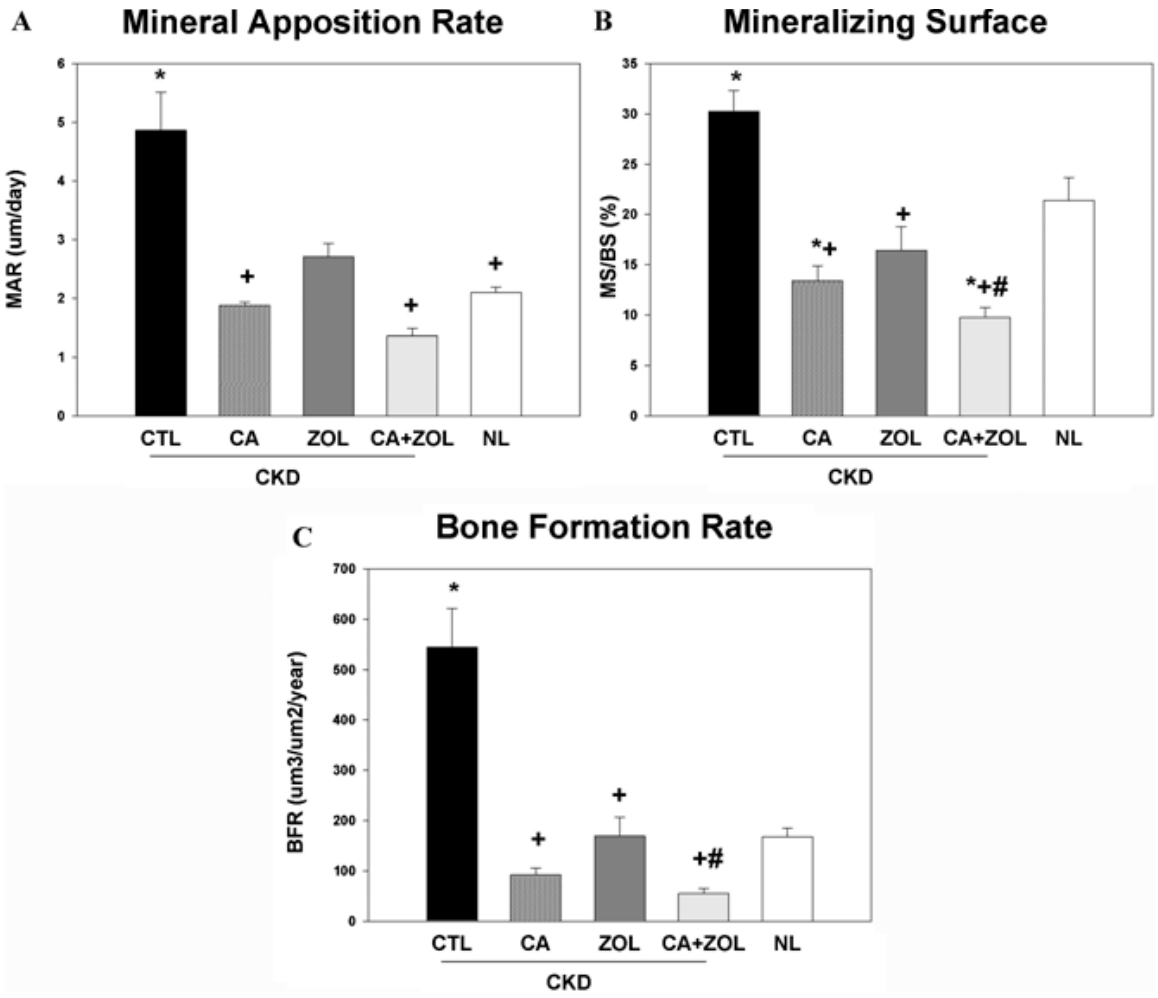

Figure 18. Bone histomorphometry in response to therapies. CKD animals were treated beginning at 25 weeks of age with control vehicle (CTL), calcium in drinking water daily for 10 weeks (Ca), zoledronic acid 20 µg/kg given subcutaneously once at 25 weeks (ZOL), or the combination of Ca + ZOL. The results were compared to normal animals (NL) treated with vehicle. At euthanasia at 35 weeks, the tibias were processed for bone histomorphometry. The results for MAR (*A*), MS/BS (*B*), and BFR (*C*). The results demonstrate that there was higher MAR, BFR, and MS/BS in the CKD animals treated with vehicle compared to NL animals. Treatment with calcium or zoledronic acid reduced all

parameters to levels similar in the NL animals with additive reduction in the calcium plus zoledronic acid group. *different than NL; +different than CKD-CTL; #different than CKD + ZOL; all $p < 0.05$. Graphs are mean ± SEM, n = 7 to 10 per group. CKD = chronic kidney disease; CTL = control; ZOL = zoledronic acid; NL = normal animals; MAR = mineral apposition rate; MS/BS = mineralizing surface as a percentage of bone surface; BFR = bone formation rate.

	CKD-CTL ($n = 10$)	CKD-Ca ($n = 9$)	CKD-ZOL ($n = 9$)	CKD-Ca + ZOL ($n = 6$)	NL ($n = 10$)
Ultimate load, N	$142 \pm 31^{*}$	$222 \pm 11^{+\#}$	$160 \pm 42^{*}$	$219 \pm 18^{+\#}$	$206 + 20$
Stiffness, N/mm	$395 \pm 55^{*}$	$512 \pm 20^{+\#}$	$378 \pm 90^{*}$	$473 \pm 32^{+\#}$	$473 + 32$
Energy to failure, mJ	72 ± 31	83 ± 12	80 ± 37	85 ± 18	85 ± 18

Values are mean ± SD.
CKD = chronic kidney disease; CTL = control; ZOL = zoledronic acid; NL = normal.
$^{*}p < 0.05$ versus NL.
$^{+}p < 0.05$ versus CKD-CTL.
$^{\#}p < 0.05$ versus CKD-ZOL.

Table 10. Mechanical properties of the femoral diaphysis.

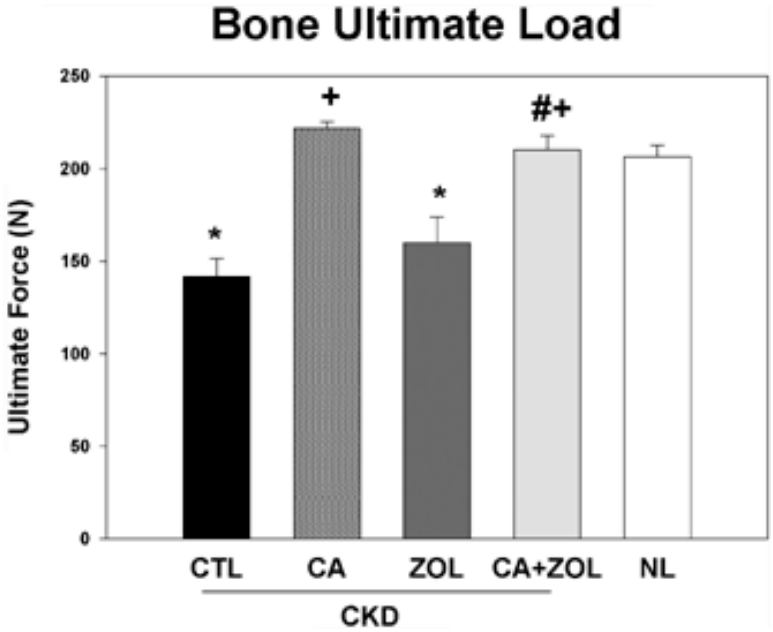

Figure 19. Bone biomechanics in response to therapies. CKD animals were treated beginning at 25 weeks of age with control vehicle (CTL), calcium in drinking water daily for 10 weeks (Ca), zoledronic acid 20 µg/kg given subcutaneously once at 25 weeks (ZOL), or the combination of Ca + ZOL. The results were compared to normal animals (NL) treated with vehicle. At euthanasia at 35 weeks, the femurs were tested via three-point bending. The results demonstrate that the CKD animals had reduced ultimate load (fracture predisposition) than normal animals and this was improved by calcium treatment with or without zoledronic acid. *different than NL; +different than CKD-CTL; #different than CKD + ZOL; all $p < 0.05$. Graphs are mean ± SEM, $n = 7$ to 10 per group. CKD = chronic kidney disease; CTL = control; ZOL = zoledronic acid; NL = normal animals.

Discussion

Multiple studies have documented increased fractures in patients with CKD as a result of a combination of abnormal bone volume and bone quality[38,141]. Although secondary analyses support the use of bisphosphonates in postmenopausal women with moderate to advanced kidney disease, these studies did not enroll individuals with elevated PTH levels[79-80]. Clinical practice guidelines recommend lowering PTH as a primary treatment approach in CKD[60]. There is no evidence that bisphosphonates directly reduce PTH; however, their potent bone resorption inhibition could effectively offset the osteoclast-medicated effects of high PTH.

We have previously shown efficacy of zoledronic acid in improving trabecular bone volume in animals with earlier stages of CKD and mild hyperparathyroidism[108]. In the present study we tested the hypothesis that zoledronic acid would be efficacious in animals with more advanced CKD, severe hyperparathyroidism, and even when combined with oral calcium supplementation. The latter has been shown to induce low bone turnover in patients on dialysis[212]. Our results demonstrate that individually, zoledronic acid and calcium each improved trabecular bone volume and reduced bone formation rate and the mineralizing surface to a similar magnitude, but only the calcium treatment improved cortical porosity and cortical biomechanical properties. In addition, only the calcium treatment induced hypercalcemia and increased arterial calcification, although hypercalcemia was not a prerequisite for aortic calcification. These results demonstrate that lowering PTH is more effective at

improving cortical bone porosity and biomechanical integrity; however, doing so with calcium may adversely impact arterial calcification risk. The elevations in plasma calcium levels may have a played a role in inducing aorta calcification, and it is possible that lower doses of calcium would not results in this adverse effect. In our previous study in this animal model we demonstrated that the administration of calcium at similar doses to the current study led to aorta calcification. This occurred even if the calcium was given together with a calcimimetic that resulting in normal plasma calcium levels resulting in increased calcium load but normal calcium levels[208]. These results would imply that it is the calcium load, not the level itself that contributes to calcification. However, dose finding studies would be required to fully assess the importance of elevated calcium levels versus calcium load or decreased bone formation.

The concern over the use of bisphosphonates in CKD has been the potential induction of low-turnover bone disease[60]. In the present study, zoledronic acid did not suppress BFR any more than calcium alone. In humans, zoledronic acid has been shown to improve bone mineral density and reduce bone fractures in both primary and secondary prevention trials in patients with postmenopausal osteoporosis[213-215]. In contrast, in postmenopausal osteoporosis the efficacy of calcium alone on fracture prevention is minimal to uncertain[216] and its adverse effects have recently come under scrutiny[217]. We cannot definitively determine if the efficacy of calcium on bone in the present study was due to calcium itself, or suppression of PTH, but based on the strong correlation of PTH, but not calcium, with cortical porosity it is most likely PTH-mediated. Interestingly,

the effects of zoledronic acid on improving trabecular bone volume in the present study was less than compared to our previous study[108] when the drug was given at an earlier time point with less severe hyperparathyroidism and over a 5-week duration. One possible explanation is that the severe hyperparathyroidism induced such a profound increase in bone resorption that the zoledronic acid bound to bone was actually resorbed out of bone with the “first pass” effect of the osteoclasts, leaving little drug bound for continued effect because the drug was only dosed one time. This dosing schedule was used to mimic the dosing to osteoporosis patients, in whom a single dose is given once per year—about two remodeling cycles in humans. Ten weeks in a rat is also equivalent to about two remodeling cycles. If true that a single dose was inefficient to control osteoclasts over this duration, this could be overcome by using a less potent bisphosphonate, such as alendronate or risedronate, normally administered on a more regular basis (daily/weekly). Current clinical practice guidelines recommend dose reduction of bisphosphonates in the setting of CKD[60]. Our data suggests that the pharmacokinetics could be altered in the setting of significant secondary hyperparathyroidism requiring increased dosing frequency although perhaps a lower dose could still be given. Thus, further studies are needed to evaluate pharmacokinetics of bisphosphonates in CKD, and further studies should determine if the efficacy and adverse effects of zoledronic acid are different when given to CKD animals and humans with and without hyperparathyroidism. It should also be emphasized that changes in bone volume may not reflect an improvement in biomechanical properties/strength. Zoledronic acid did not

improve cortical measures of strength, but similar measures to test strength of trabecular bone are not available.

In our CKD animals, the hyperparathyroidism produced profound changes in cortical bone porosity and biomechanical properties that were corrected with the administration of calcium. Cortical bone is more adversely affected than trabecular bone in hyperparathyroidism[218-219]. However, traditional assessment of renal osteodystrophy by bone biopsy in CKD patients has been with trabecular bone. Our results suggest that the apparent disconnect between PTH and bone turnover assessed by histology in cross-sectional studies[220] may be partly due to the use of trabecular bone. Supporting this is that in patients with CKD, the distal radius DXA, which is nearly entirely cortical bone, is more predictive of fractures than other sites[166]. These data, and our results in the present study, support current clinical practice guidelines that emphasize treating hyperparathyroidism as first line initial therapy in patients with CKD stages 3-5D[60]. However, in a recent study of nearly 4000 hemodialysis patients, the largest fracture assessment study to date in CKD, there was no effect of the calcimimetic cinacalcet on fractures despite improved PTH[66]. However, this study only evaluated clinical (reported) fractures and thus may have underestimated true fracture prevalence and efficacy of lowering PTH. Thus more studies specifically designed to compare the treatment of hyperparathyroidism versus antiresorptive agents on fracture prevention in CKD are required.

Previous studies have demonstrated that bisphosphonates reduce arterial calcification in CKD animal models. Tamura and colleagues[221] found that

etidronate decreased arterial calcification in 5/6th nephrectomy rats also given calcitriol. Price and colleagues[222] found similar efficacy in the adenine model of CKD treated with alendronate or ibandronate. Lomashvili and colleagues[223] found that pamidronate reduced arterial calcification in 5/6th nephrectomy animals treated with high phosphate diet, but also found suppression of bone turnover and concluded the drug may be efficacious but not safe, although there was no comparison of the degree of bone turnover to normal animals. Bisphosphonates work by suppression of remodeling and therefore induce lower bone formation rates are expected. In our previous study, the level of BFR suppression was no different in CKD animals treated with zoledronic acid compared to normal animals treated with zoledronic acid[108]. In the current study, the turnover was equally suppressed with zoledronic acid compared to calcium given in the drinking water (to act as a phosphate binder, a treatment used worldwide).

A major concern about inducing suppressed bone turnover is the association of such suppression with arterial calcification in patients with CKD and in dialysis patients[212,224-225]. This has been hypothesized to be due to the inability of bone to take up excess calcium in the setting of low bone formation rates[226], predisposing to extra skeletal deposition. In the present study we found that despite similar suppression of BFR with zoledronic acid and calcium, only the calcium induced arterial calcification and suppression of PTH and zoledronic acid appears to ameliorate this effect but had no efficacy by itself. Thus, positive calcium balance that occurs in CKD[227] may be a critical factor involved in the

development of arterial calcification. The calcium treatment also increased FGF23, as has been noted in animals[228]. In other studies of human and animal arteries, FGF23 appeared to be protective against arterial calcification, but only when klotho was present[229]. We have previously shown in our animal model that klotho expression in the kidney is markedly decreased as early as 20 weeks[230] and thus, assuming similar suppression in arteries, this potential positive effect of FGF23 may have been negated with advanced kidney disease. The mechanism by which calcium stimulates FGF23 is likely direct on the osteocytes, because calcium altered FGF23 secretion in rats who had undergone a parathyroidectomy and then were infused with calcium or given a high calcium diet[228]. This increase in FGF23 may have adverse cardiac consequences in rodents[224,230], and higher FGF23 levels have been found to predict progression of left ventricular hypertrophy (LVH) in patients with CKD 3-4[230]. In the current study, we did not observe differences in LVH in animals with the various treatments, but the duration of therapy was relatively short.

In humans with end-stage renal disease (ESRD), there are only small studies examining the role of bisphosphonates in the prevention of arterial calcification. In small cohort or observational studies from Japan, etidronate reduced arterial calcification[231-233]. In contrast, in a randomized controlled trial of 50 patients, Toussaint and colleagues[234] found that alendronate had no effect on arterial calcification. These differences may be explained by the increased mineral dissolution properties of etidronate compared to alendronate and other

nitrogen-containing bisphosphonates, although a number of other explanations such as dosing and disease stage are also plausible.

In summary, we found similar efficacy of calcium and a single dose of zoledronic acid on improving trabecular bone volume in animals with advanced CKD and severe hyperparathyroidism. However, only the calcium treatment improved cortical porosity and lowered PTH. Unfortunately, calcium also induced arterial calcification, whereas zoledronic acid did not, despite similar suppression of bone remodeling. These results suggest that suppression of bone remodeling with bisphosphonates may not have the same adverse consequences as suppression of bone remodeling with calcium. It is important to caution on the extrapolation of changes in bone remodeling or bone volume in animal studies to human disease. However, the data supports the conduct of a study in CKD patients, directly testing whether suppression of PTH with non-calcium-containing agents (eg, calcimimetics) is more effective than antiresorptive agents for fracture prevention.

CHAPTER 6

ANTI-SCLEROSTIN ANTIBODY TREATMENT IN A RAT MODEL OF PROGRESSIVE RENAL OSTEODYSTROPHY

Material in this chapter has been previously published:

Journal of Bone and Mineral Research (2015) 30:539-549

Rationale

Building upon the previous study, the goal of this study was to further examine potential therapies in the treatment of CKD-MBD by assessing the utility of anabolic therapy using anti-sclerostin antibody. As before, calcium was used to lower PTH. However, in this case, it was employed to create a low turnover condition. So, in both high and low bone turnover settings, anabolic (anti-sclerostin antibody) and anti-resorptive (zoledronic acid) therapies were assessed.

Introduction

Chronic Kidney Disease affects over 20 million Americans and many of these individuals are older and at risk for fragility fractures[60]. CKD-Mineral Bone Disorder is a systemic disease in patients with estimated glomerular filtration rates (eGFR) < 60 ml/min (CKD stage 3-5) that manifests as abnormal biochemistries, renal osteodystrophy, and extraskeletal calcification[140,235].

The potential contribution of renal osteodystrophy, versus osteoporosis, in the pathogenesis of fragility fractures in patients with impaired kidney function has led to confusion on the treatment of bone loss. In human trials, secondary analyses of individuals with CKD stage 3-5 have found a beneficial effect of bisphosphonates, raloxifene, and denosumab in post-menopausal women with reduced fractures and improved bone mineral density without adverse consequences[79-80,236-237]. However, these individuals were enrolled into the studies based on normal kidney function and parathyroid hormone levels and

only subsequently identified to have CKD in post hoc analyses. With normal PTH levels, one can argue that the change in GFR is related to age-based decline in kidney function rather than intrinsic disease and therefore not representative of CKD-MBD.

The role of PTH in renal osteodystrophy has been the focus of therapies for many years. Low and high levels of PTH have been correlated with low and high bone formation rates, and lowering elevated PTH with calcitriol and its analogs or cinacalcet is currently the primary therapy for renal osteodystrophy. Clinical practice guidelines recommend correction of elevated PTH prior to any consideration for other bone/anti-osteoporotic treatment in patients with bone loss[60]. The concern over the use of anti-resorptives has stemmed from reports that these agents may 'over suppress' PTH and cause adynamic bone disease[60], which may be associated with bone fractures and extra-skeletal calcification. Unfortunately, PTH, despite being a major contributor to the pathogenesis of renal osteodystrophy, lacks ideal discriminatory ability for the differentiation of low and high turnover and thus misclassification is common[238]. Therefore, treatments that are efficacious in improving or ameliorating bone loss regardless of the PTH are needed.

In addition to elevated PTH, patients with CKD also have elevated FGF23 and sclerostin levels. PTH stimulates FGF23 secretion from osteocytes via a sclerostin mediated pathway[239-240] and suppresses sclerostin secretion from osteocytes[93]. Sclerostin levels are increased in CKD compared to normal individuals with osteoporosis, and levels are inversely associated with PTH

levels[94]. Sclerostin, the protein product of the gene SOST, binds to LRP5/6 on the osteocyte to competitively inhibit the binding of Wnt ligands. Normally, Wnt binding to LRP5/6 leads to stabilization of β-catenin (canonical pathway), and regulation of normal bone accrual via osteoblast differentiation. In the presence of sclerostin, the β-catenin is degraded and mesenchymal stem cell differentiation to mature bone cells is inhibited (reviewed in [241]). In animal models, sclerostin deletion enhances bone accrual[242-246] and in early human trials[247] treatment with an antibody to sclerostin is anabolic. Given that sclerostin levels are elevated in blood of patients with CKD[91] and bone of patients and animals with CKD[92] the anabolic agent anti-sclerostin antibody may be efficacious in all forms of renal osteodystrophy independent of PTH and bone turnover. To test this hypothesis we used a slowly progressive model of CKD-MBD, manipulating the PTH to low and high levels. We then compared treatment with anti-sclerostin Ab, zoledronic acid, or no treatment on biochemical, vascular calcification, and bone outcomes.

Materials and Methods

Animal model and experimental design

We tested the hypothesis that anti-sclerostin antibody is efficacious in preventing bone loss in animals with both high PTH and low PTH, the latter induced by calcium in the drinking water. We have previously shown that these two extremes of PTH lead to high and low activation frequencies and bone formation rates, respectively[108,248]. Briefly, male Cy/+ rats, Han:SPRD rats with

autosomal dominant polycystic kidney disease, and normal age matched Han:SPRD rats (NL) were used for this study. Male heterozygous rats (Cy/+) develop characteristics of CKD (azotemia) around 10 weeks of age which progresses gradually. By 35 weeks, as we have previously reported[53,112,119], untreated CKD animals at 35 weeks of age have biochemical abnormalities that parallel advanced CKD in humans: in the CKD animals versus NL littermates, the BUN was 49.3 ± 8.3 vs 22.0 + 4.7 mg/dl, the PTH was 1560 ± 859 vs 132 ± 67 pg/ml; the phosphorus was 8.4 ± 1.8 vs. 3.6 + 0.6 mg/dl; and the calcium was 8.99 ± 2.0 vs. 10.3 ± 0.5 mg/dl.

For the current study, animals were placed on a standard casein diet (Purina AIN-76A; 0.53% Ca and 0.56% P) at 24 weeks of age which has been shown to produce a more consistent disease in this model[53]. At 25 weeks of age, with an estimated kidney function of 35% of normal, animals were randomly assigned to 3% calcium in the drinking water or normal water to suppress or maintain the hyperparathyroid state (**Figure 20**). The additional calcium intake based on average water consumption is 1.98 ± 0.57 g/day. At 30 weeks of age with estimated kidney function at 20% of normal, animals in both the low and high PTH groups were randomly assigned to anti- sclerostin Ab (Scl-Ab; 100 mg/kg given by tail vein IV q week for 5 total doses; Novartis Institutes for BioMedical Research, Novartis Pharma AG), zoledronic acid (ZOL; 20 μg/kg body weight given subcutaneously once at week 30, a dose previously shown to suppress bone remodeling in this model[95]), or no treatment (CTL) for 5 weeks. In addition, we studied age-matched normal (NL) littermate animals as a positive

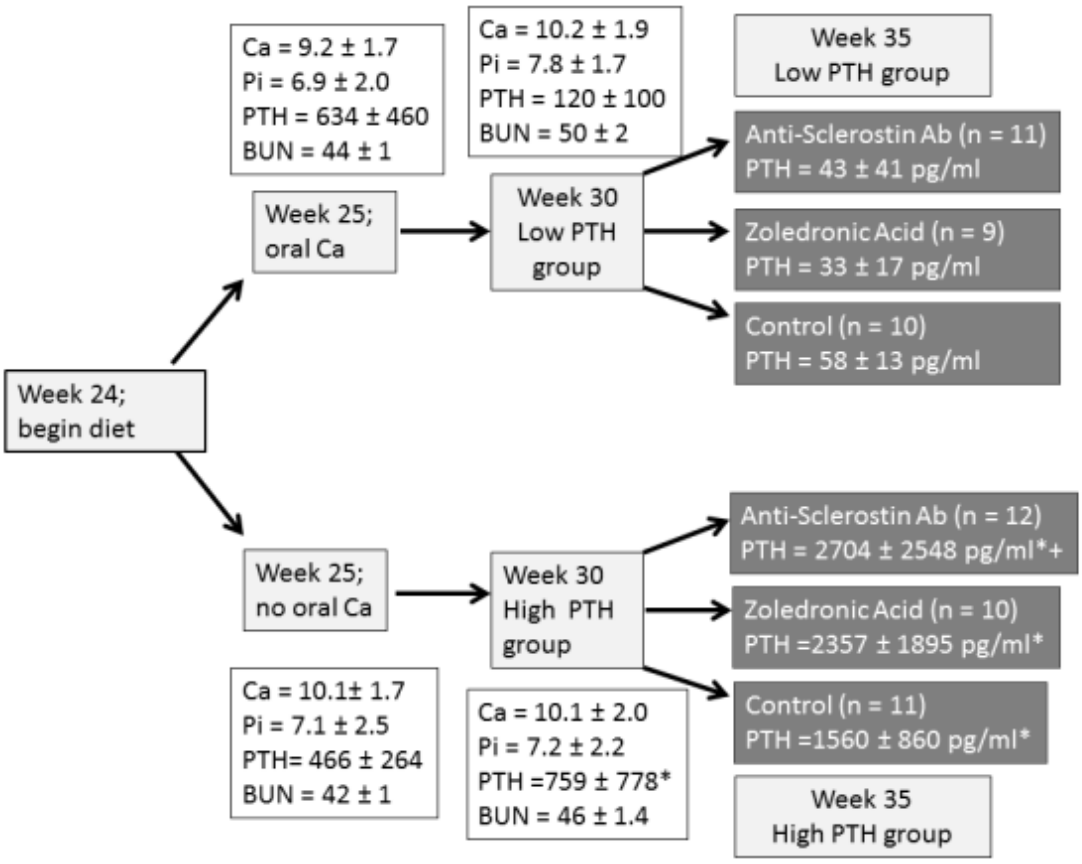

Figure 20. Schematic of study design: CKD animals were fed a casein based diet beginning at 24 weeks, then given drinking water with or without 3% calcium beginning at 25 weeks. Drug administration began at 30 weeks of age, and sacrifice was at 35 weeks. Data are mean ± SD. * = $p < 0.05$ for comparison between animals given calcium or no calcium, + = $p < 0.05$ for anti-sclerostin Ab versus control. Final n for each group is included in the boxes.

control for the anti-sclerostin Ab. Each group had a final n of 9 to 12 animals (**Figure 20**); 1 animal died suddenly in each of three groups: the CKD group treated with zoledronic acid, the CKD group treated with calcium and anti-sclerostin Ab, and the CKD group treated without calcium and anti-sclerostin Ab. This is consistent with our previous studies. In addition, two animals had to be sacrificed early in the anti-sclerostin treatment groups due to saphenous vein inflammation resulting from pharmacokinetic blood sampling. These animals were not included in the final analyses. At 35 weeks of age all animals were euthanized by an overdose of sodium pentobarbital. All procedures were reviewed and approved by the Indiana University School of Medicine Institutional Animal Care and Use Committee.

Tissues collection and analysis

At sacrifice at 35 weeks, blood was collected by cardiac puncture. Left tibiae were placed in 10% neutral buffered formalin for 48 hours and then changed to 70% ethanol for imaging followed by histological processing. Right femora were wrapped in saline-soaked gauze and frozen for later biomechanical analyses and CT evaluation. Left ventricular mass index (LVMI) was determined by dividing total heart weight by body weight. To quantify aorta and heart calcification, proximal segments of the ascending aorta were snap frozen and the degree of calcification determined biochemically as previously described[108,119].

Serum and urine biochemical measurements

Pharmacokinetics analyses of the Scl-Ab were performed by measuring levels of the antisclerostin Ab in serum of eight CKD rats after the first and last

dose at 6 and 24 hours post injection using a custom made immunoassay (Novartis Pharma AG). Blood plasma was analyzed for BUN, calcium, phosphorus, and creatinine using colorimetric assays (Point Scientific, Canton, MI, USA, or Sigma kits). Intact PTH was determined by ELISA (Alpco, Salem, NH, USA). FGF23 was assessed with a two-site assay (Immunotopics, San Clemente, CA, USA). Dickkopf-related protein family-1 (Dkk-1) and Sclerostin levels were measured by ELISA (Enzo Life Sciences, Farmingdale NY; R&D systems, Minneapolis, MN, respectively).

Computed tomography (CT)

Morphological parameters of the proximal tibia and femoral mid-diaphysis were assessed using high-resolution microCT (Skyscan 1172) as previously described[119]. Scans were obtained using a 60kV x-ray source (167 μA), an angular range of 180 degrees (rotational steps of 0.70 degrees with 2 frame averaging) with a 12-μm pixel size and 0.5mm Al filter. Projection images were reconstructed using standard Skyscan software (NRecon). A 1mm region of interest of the proximal tibia (located ~ 0.5 mm distal to the growth plate) was analyzed by manually segmenting the trabecular bone from the cortical shell and calculating trabecular bone volume normalized to total volume (BV/TV) in accordance with recommended guidelines[186]. The most distal slice of the region of interest was analyzed for cortical porosity. Scans of the femoral diaphysis were conducted with similar scan settings to assess geometry (bone area, perimeter, cross-sectional moment of inertia) for normalization of mechanical

properties. Measures were made in accordance with recommended guidelines[249].

Biomechanics

Femoral diaphysis mechanical properties were assessed in 4-point bending studies on an electromechanical test system (Test Resources). Bones were thawed, hydrated in saline, and then placed posterior surface down on bottom supports (span = 18 mm). The upper supports (span = 6 mm) were brought down in contact with the specimen's anterior surface, and then testing was conducted at a displacement rate of 2 mm/min. Force versus displacement data was collected at 10 Hz and structural parameters were determined from curves using a customized MATLAB program. Material properties were estimated using standard equations[250].

Bone Histomorphometry

Proximal tibiae were embedded in methylmethacrylate for sectioning as previously described[108,209]. The proximal tibial metaphysis was thin sectioned (4 μm) and mounted unstained using non-fluorescent medium. Sections were analyzed using a microscope interfaced with a semiautomatic analysis system (Bioquant OSTEO 7.20.10, Bioquant Image Analysis Co.). For trabecular bone analyses, a region of interest of ~ 8 mm2 within the secondary spongiosa (~ 0.5 mm distal to the growth plate) was outlined, and then measures of single- and double-label perimeter (sL.Pm, dL.Pm), total bone perimeter (B.Pm) and interlabel width (Ir.L.Wi) were conducted. From these primary measurements, derived parameters were calculated as: mineralizing surface (MS/BS = [1/2sL.Pm

+ dL.Pm]/B.Pm; %), mineral apposition rate (MAR =Ir.l.W/days between labels; μm/day), and bone formation rate (BFR/BS = MAR x MS/BS x 3.65; m3/μm2/yr). All parameters were measured and calculated in accordance with ASBMR recommended standards[211].

Real time RT-PCR analysis of SOST expression

Total RNA was isolated from tibiae using miRNeasy Mini kit (Qiagen, Valencia, CA) after flushing out the bone marrow. The SOST expression in bone was determined by real time PCR using 1 ug of total RNA in TaqMan Reverse Transcription reagent (Applied Biosystems, Foster City, CA). Target-specific PCR primer for SOST was obtained from Applied Biosystems.

Real-time PCR amplification was performed using TaqMan Gene Expression Assays (TaqMan MGP probes, FAM dye-labeled) using Applied Biosystems ViiA-7 RealTime PCR system (Applied Biosystems). The cycle number at which the amplification plot crosses the threshold was calculated (CT), and the ΔΔCT method was used to analyze the relative changes in gene expression using β-actin as a housekeeping gene.

Western blot analysis of β-catenin activation in bone tissue

To determine the effect of sclerostin antibody treated animals on β-catenin signaling in bone tissue, proteins were isolated from tibiae by homogenizing the tissue with RIPA buffer using the Bullet Blender (Next Advance, Inc, Averill Park, NY) according to manufacturer's instructions. The β-catenin activation was determined by Western blot as we previously described[251] using phosphorylated β-catenin antibody. Briefly, the blots were incubated with antibody against

pSer33/37 β-catenin (1:1000, Cell Signaling Technology, Danvers, MA) overnight at 4oC followed by incubating with peroxidase conjugated secondary antibody (1:5000 dilution), and immunodetection with the Enhanced Chemiluminescence Prime Western blot Detection Reagent (Amersham, Piscataway, NJ). The band intensity was analyzed by ChemiDocMP Imaging System (Imaging Lab 4.0, Bio-Rad, Richmond, CA).

Statistics

All analyses were run using SigmaStat software. The two CKD groups (high and low PTH) at week 30, prior to drug treatment and the normal animals with and without Scl-Ab were compared by t-test. The six CKD groups at 35 weeks were analyzed by two-way ANOVA after log transformation for non-normally distributed data. The two groups compared were PTH status (low vs. high), and drug effect (Scl-Ab, Zol, CTL) in order to test the efficacy of treatments in the setting of low and high PTH. Fisher's Post hoc tests were done for within group comparisons for the different drugs if the overall drug effect was significant. When there was a significant interaction between PTH group and drug treatment we made statements regarding the relative effect of the drug in the setting of high PTH versus low PTH. Correlations were done by Pearson Product after log transformation if appropriate. A priori α-levels were set at 0.05. Data are presented as means and standard deviation.

Results

Biochemical outcomes

As detailed in **Figure 20**, at 25 weeks of age, the CKD animals had established secondary hyperparathyroidism. After 5 weeks on oral calcium, the PTH was suppressed to 120 ± 100 pg/ml in the calcium treated group compared to 759 ± 778 in the high PTH ($p < 0.05$). At 35 weeks, the calcium treated animals (low PTH groups) had a further decline in PTH compared to week 30, whereas the non-calcium (high PTH groups) animals had a further rise in PTH (overall $p < 0.001$; **Figure 20**). There was no difference of drug treatment on PTH with the exception of a slightly more elevated PTH in the high PTH group treated with anti-sclerostin Ab compared to control ($p = 0.03$). At 35 weeks, there was no difference in the level of BUN among CKD groups, indicating no adverse effect on kidney function (data not shown). **Figure 21** shows the high PTH (left set of bars) compared to low PTH groups (right set of bars) at 35 weeks for calcium, phosphorus, FGF23, and Dkk-1. The high vs. low PTH groups were different for calcium ($p = 0.016$), phosphorus ($p = 0.034$), and FGF23 ($p< 0.001$), but the drug effect was not significant for any of these and there was no interaction between PTH group and drug treatment by 2 way ANOVA.

As expected, serum levels of Dkk-1 and sclerostin were both elevated in CKD compared to NL animals ($p = 0.04$, $p < 0.001$). In the CKD animals, Dkk-1 levels were unaffected by PTH group ($p = 0.52$), but were affected by drug treatment (overall $p = 0.004$; ZOL different than SclAb and CTL, both $p < 0.03$; **Figure 21**). There was a weak correlation between Dkk-1 and FGF23

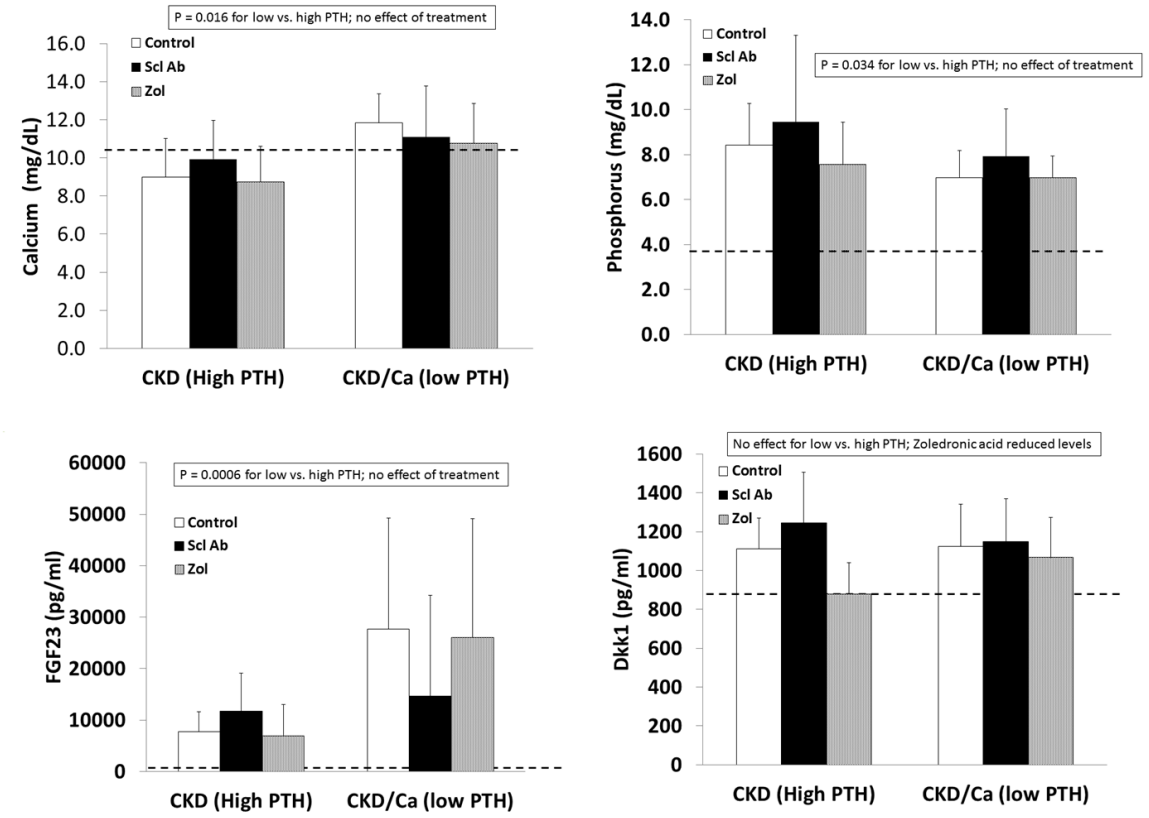

Figure 21. Biochemical results: At 35 weeks, the CKD animals had blood assessed for calcium (A), phosphorus (B), FGF23 (C), and dkk-1 (D) levels. The animals with high PTH (left) were compared to those treated with calcium and with low PTH (right) by two way ANOVA examining effect of PTH and treatment. For calcium ($p = 0.016$), and FGF23 ($p = 0.0003$) there was a difference between the high and low PTH (large bar across top), but no effect of treatments (groups of 3 bars). For phosphorus, there was a significant effect of both PTH ($p < 0.001$), and a significant effect of treatment ($p < 0.001$) due to significant effects of zoledronic acid to increase phosphorus levels compared to both sclerostin Ab treated and control treated animals (both $p < 0.001$). In contrast, for dkk-1, there

was no effect by PTH group, but the treatment effect was significant ($p = 0.004$), with zoledronic acid lowering the dkk-1 compared to both control ($p = 0.03$)

(r = 0.32, p = 0.01) and calcium (r = 0.25, p = 0.047), a modest correlation with kidney function (BUN; r = 0.51, p < 0.001), but no significant correlation with PTH. The sclerostin levels were inconsistent in the groups treated with the anti-sclerostin Ab due to probable crossreactivity with the antigen-antibody complex and the assay in both the CKD and the NL animals and thus only the other groups were evaluated. The sclerostin levels in the high PTH group were 458 ± 122, high PTH with zol= 563 ± 339, low PTH 249 ± 122, and low PTH with zol = 260 ± 102 (p = 0.005). There was a strong positive correlation of the log sclerostin vs log PTH (r = 0.73, p < 0.001; **Figure 22**). Given the assay limitations, we measured SOST gene expression in the bone by real time PCR to determine if anti-sclerostin Ab had any effect on SOST gene expression. The results showed an increase in SOST expression with the administration of the anti-sclerostin Ab, but only in the calcium treated low PTH animals (**Figure 22**).

Cardiovascular outcomes

As previously reported, the left ventricular mass index was greater in untreated CKD animals (3.59 ± 0.12) compared to NL animals (2.99 ± 0.24) (p < 0.001). Within the CKD groups there was no difference by PTH or by drug treatment by two way ANOVA (p = 0.26). Similarly, there was a difference between the aorta arch calcification between untreated CKD and NL animals (p = 0.01) but within the CKD animals no effect on calcification by PTH (p = 0.15) or treatments (p = 0.26) by 2 way ANOVA (**Figure 23**). There was a trend towards reduction in calcification by both zoledronic acid and anti-sclerostin Ab in the low

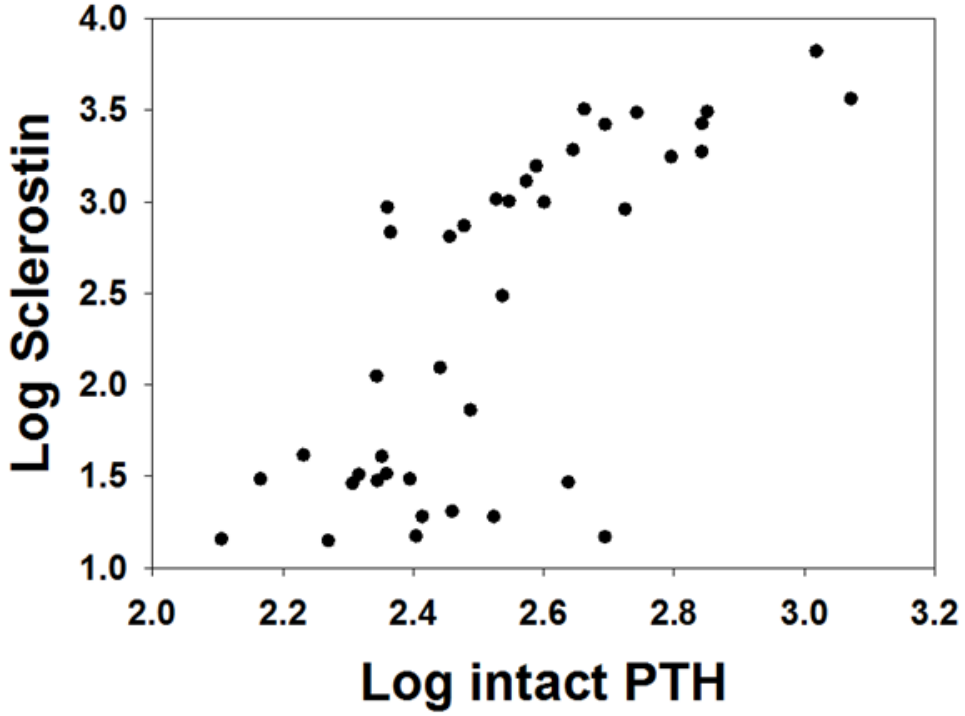
Log Sclerostin
4.0
3.5
3.0
2.5
2.0
1.5
1.0
2.0
2.2
2.4
2.6
2.8
3.0
3.2
Log intact PTH

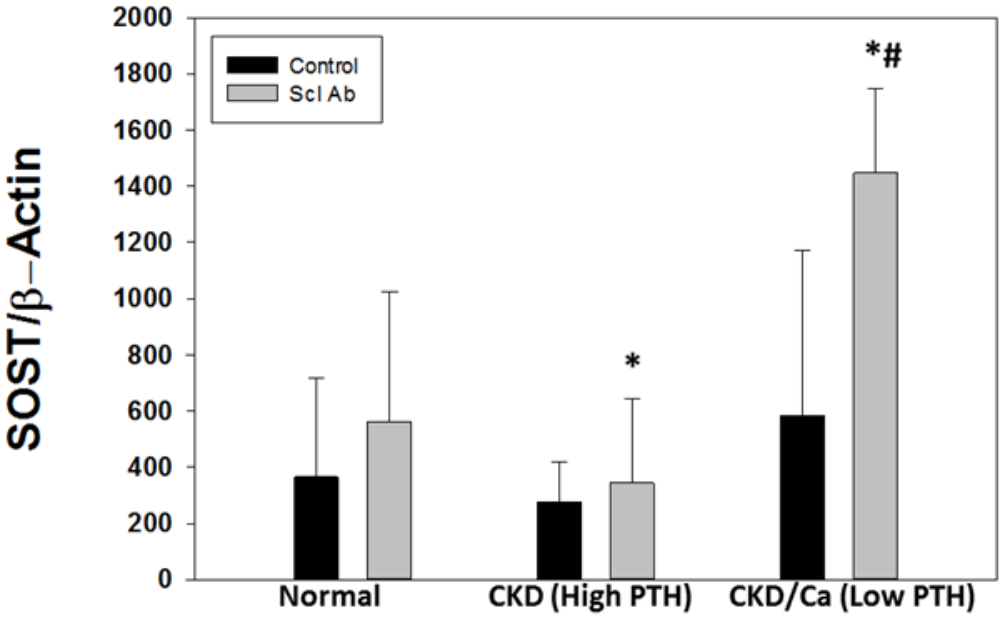
SOST/β–Actin
2000
1800
1600
1400
1200
1000
800
600
400
200
0
Control
Scl Ab
*
*#
Normal
CKD (High PTH)
CKD/Ca (Low PTH)

Figure 22. Sclerostin levels and SOST expression: Figure 22A shows the relationship between the sclerostin and PTH levels ($r = 0.73$, $p < 0.001$) for the CKD animals. Those animals treated with anti-sclerostin Ab are not included due to interference with the assay. Figure 22B shows the expression of total bone SOST with and without treatment with anti-sclerostin Ab. There was an increase with Ab treatment in only the low PTH animals (* $p < 0.001$). The expression level of SOST in the low PTH animals was significantly greater than in the high PTH animals (#, $p < 0.001$). Data are mean ± SD.

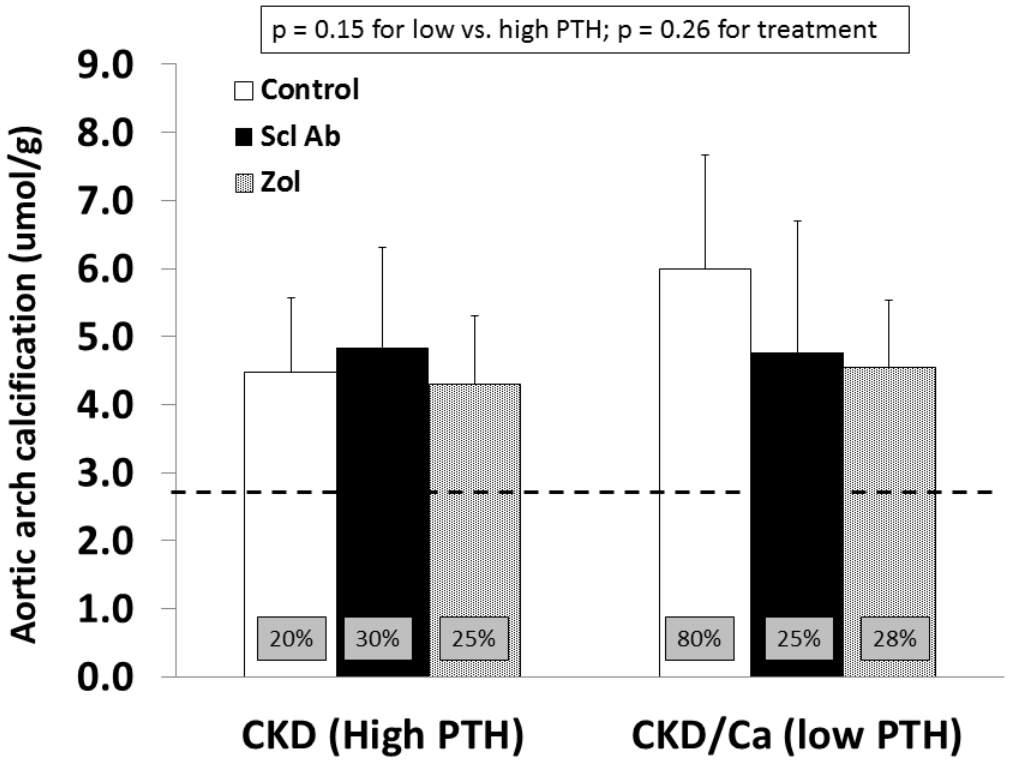

Figure 23. Aorta arch calcification: At 35 weeks, the aorta arch was dissected free and analyzed for calcium content after HCl extraction, normalizing for tissue weight. By 2-way ANOVA there was no significant difference between the groups, although there was a trend towards increased calcification in the calcium treated control animals; an effect that appeared attenuated by both drug treatments. The bar graphs represent the mean ± SD. The box insets in each bar indicate the percentage of animals in each group with significant calcification (defined as > 5.26 umol/g which is the normal littermate average value of mean + 2SD). The dashed line represents the mean value from the normal littermate animals.

PTH group. Eighty percent of animals in the low PTH control group had significant calcification (defined as > 5.26 umol/g which is the normal littermate average value of mean + 2SD), compared to 20-30% of animals in the other groups (boxes in bars in **Figure 24**).

Bone outcomes

As we have previously reported[119], the trabecular BV/TV of the untreated CKD animals was not different from the normal animals (9.1 ± 4.1 vs. 10.2 ± 4.2%, respectively) but the cortical porosity was greater (CKD: 2.37 ± 1.74 vs NL: 0.97 ± 0.39, $p = 0.02$). In the CKD animals at 35 weeks, there was an effect of both PTH ($p < 0.0001$) and drug treatment ($p = 0.03$) on trabecular BV/TV (**Figure 24**). The within drug treatment group difference was significant for only Anti-sclerostin Ab vs. CTL ($p = 0.008$). There was also a significant PTH group*Drug treatment interaction ($p = 0.04$) in that the anti-sclerostin Antibody treatment increased BV/TV in the low but not high PTH group. Similar results were demonstrated for femoral mid-diaphysis cortical bone area and cross-sectional moment of inertia (**Table 11**). In contrast, proximal tibia cortical porosity as well as all mechanical and geometrical parameters of the femoral mid-diaphysis showed significant PTH effects ($p < 0.001$ for all) but only a trend towards an effect of drug treatment ($p = 0.9$) (**Figure 24** and **Table 11**). The periosteal perimeter was not different, but the endocortical perimeter was greater in the high PTH group compared to the low PTH group ($p < 0.001$) with no effect of treatment due to the wide variability (**Figure 24**). As a positive control, NL

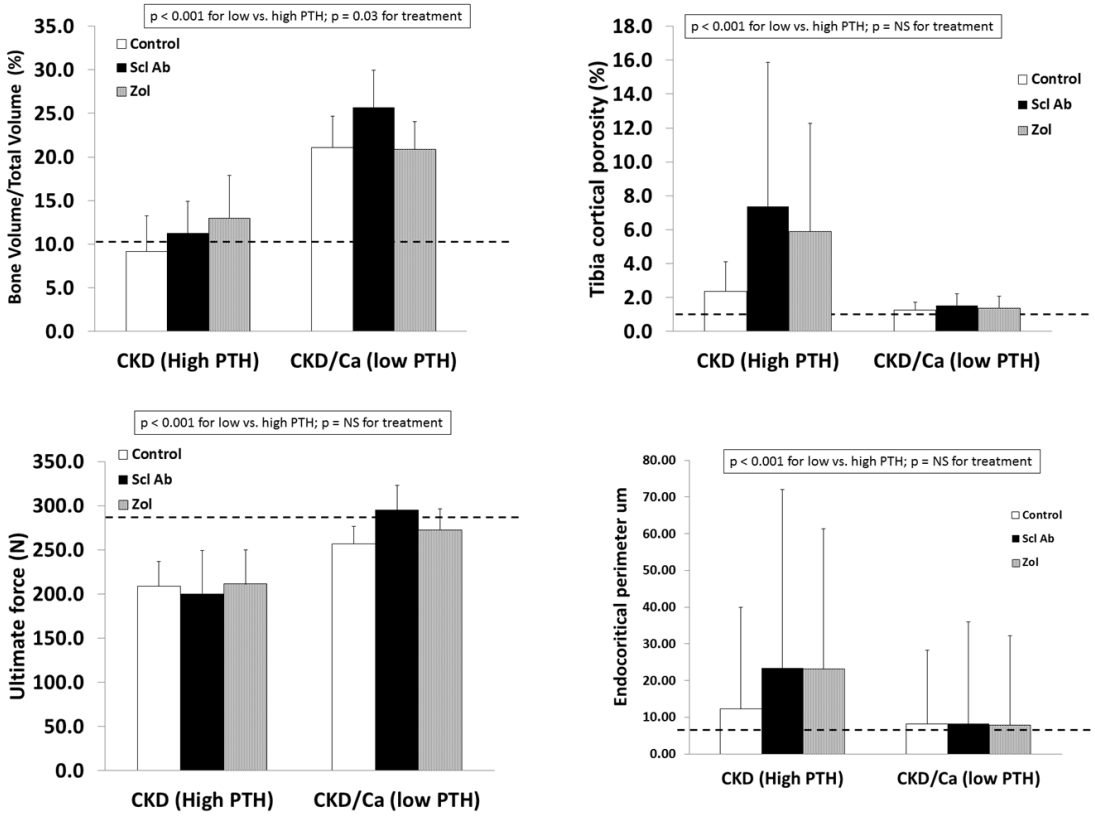

Figure 24. Bone Results: At 35 weeks, bone from the CKD animals was assessed by microCT for proximal tibial trabecular bone volume, cortical porosity, femur ultimate force and for femur cortical bone endocortical. The animals with high PTH (left) were compared to those treated with calcium and with low PTH (right) by two way ANOVA examining effect of PTH and treatment. For bone volume, porosity, and ultimate force (all $p < 0.001$) there was a difference between the high and low PTH. There was a positive effect of treatment on bone volume with the sclerostin Ab increasing the volume more than control ($p = 0.008$). There was no effect of treatment for cortical porosity or ultimate force. The dashed line represents the mean value from the normal littermate animals.

	Proximal tibia		Femoral mid-diaphysis									
	BV/TV (%)	**Cortical Porosity (%)**	**Ultimate Force (N)**	**Stiffness (N/mm)**	**Energy to failure (mJ)**	**Ultimate Stress (MPa)**	**Modulus (MPa)**	**Toughness (MPa)**	**Cortical thickness (mm)**	**Cortical bone area (mm^2)**	**Cortical porosity (%)**	**CSMI (mm^4)**
CKD High PTH												
CTL	10.2 ± 1.9	2.4 ± 1.7	208.9 ± 27.7	456.7 ± 64.6	93.8 ± 18.5	100 ± 16	3686 ± 546	2.7 ± 0.6	0.58 ± 0.10	7.4 ± 0.4	2.8 ± 2.9	22.4 ± 1.8
Scl-Ab	11.3 ± 3.7	7.4 ± 8.5	200.5 ± 48.7	471.9 ± 99.0	83.8 ± 35.4	92 ± 28	3527 ± 916	2.3 ± 1.1	0.49 ± 0.19	8.1 ± 0.4	7.2 ± 5.8	23.9 ± 2.2
Zol	13.0 ± 4.9	5.9 ± 6.4	211.2 ± 38.3	428.8 ± 59.7	96.6 ± 30.0	104 ± 25	3570 ± 683	2.8 ± 0.9	0.54 ± 0.18	7.8 ± 0.6	6.2 ± 7.0	21.9 ± 2.7
CKD Low PTH												
CTL	21.1 ± 3.6	1.3 ± 0.5	256.7 ± 20.2	561.6 ± 47.5	112.6 ± 15.2	115 ± 9	4306 ± 419	2.9 ± 0.5	0.80 ± 0.07	8.8 ± 0.7	4.5 ± 8.3	23.6 ± 2.5

Scl-Ab	25.6 ± 4.3*	1.5 ± 0.7	295.1 ± 27.8	593.9 ± 31.1	126.6 ± 29.7	127 ± 19	4224 ± 555	3.3 ± 0.9	0.80 ± 0.05	9.0 ± 0.7	0.77 ± 0.48	25.7 ± 3.1
Zol	20.9 ± 3.2	1.4 ± 0.7	272.3 ± 24.3	567.6 ± 43.9	111.9 ± 23.5	124 ± 11	4349 ± 667	3.0 ± 0.7	0.82 ± 0.06	8.9 ± 0.8	0.71 ± 0.57	23.9 ± 3.7
Normal animals												
CTL	10.2 ± 1.9	1.0 ± 0.4	268.0 + 21.0	562.4 ± 37.5	131.1 ± 29.1	116 ± 16	3767 ± 320	3.6 ± 1.0	0.73 ± 0.05	8.6 ± 0.3	1.8 ± 0.6	26.4 ± 2.4
Scl-Ab	16.0 ± 1.9*	1.2 ± 0.6	339.5 ± 31.3^{+}	663.5 ± 101.9*	169.7 ± 29.5*	114 ± 12	3254 ± 443*	3.9 ± 0.9	0.79 ± 0.03 *	10.3 ± 0.6^{+}	1.3 ± 0.3	36.8 ± 3.5^{+}

Table 11. Bone CT and Biochemical Results

CTL= control or no treatment; Scl-Ab = treatment with anti-sclerostin Ab; Zol = treatment with zoledronic acid; CSMI = cross sectional moment of inertia. Data presented as mean and standard deviation.

The CKD animals were compared by two-way ANOVA evaluating the effect of PTH and treatment. There were significant differences ($p < 0.01$) by PTH group for all bone parameters. There was a significant effect of drug treatment in that treatment with sclerostin Ab was different than control for trabecular bone volume ($p = 0.03$), cortical bone area ($P = 0.05$), and CSMI ($p = 0.043$) with no differences among treatments for the other parameters. Data are mean ± SD.

The Normal animals with and without treatment with anti-sclerostin Ab were compared by t-test. * = $p < 0.05$, $^{+}$ = $p < 0.01$.

animals given similar doses of Scl-Ab, demonstrated a robust increase in trabecular BV/TV ($p < 0.001$). There was also an increase in biomechanical properties and cortical geometry (**Table 11**). The anti-sclerostin Ab treatment of NL animals had no effect on any of biochemistries. Thus, in the NL rats, there was the expected benefit of the anti-sclerostin antibody.

As we have previously reported, the high PTH group is a high bone remodeling model of CKD, with untreated animals having BFRs of nearly three times NL controls. There were significantly higher dynamic bone formation properties of the proximal tibia trabecular bone in the high PTH animals (**Table 12**) compared to the low PTH animals. In both high and low PTH cohorts those animals treated with anti-sclerostin antibody had higher remodeling rates compared to animals treated with zoledronic acid.

To understand the differential effects of anti-sclerostin Ab on bone in the low and high PTH group, we measured phosphorylated β-catenin by Western blot from total bone extracts. In the CKD animals basal expression was 0.39 ± 0.18. In the CKD animals treated with antisclerostin Ab, the expression was 0.52 ± 0.28 in the high PTH group and 0.19 ± 0.17 in the low PTH group ($p = 0.3$, with differences in the two treated groups of $p = 0.008$). Phosphorylated β- catenin expression represents degradation, and therefore less degradation would indicate a positive effect of the anti-sclerostin Ab in the low PTH group, consistent with the bone volume findings.

	N, #	MAR, um/day	MS/BS, %	BFR/BS, $um^3/um^2/year$
CKD High PTH				
CTL	11	2.2 ± 1.1	31 ± 8	280 ± 156
Scl-Ab	12	2.8 ± 1.7	29 ± 8	323 ± 221
Zol	9	2.0 ± 1.0	21 ± 10	166 ± 117
CKD Low PTH				
CTL	10	1.2 ± 0.3	11 ± 5	49 ± 18
Scl-Ab	12	1.2 ± 0.6	28 ± 17	154 ± 154
Zol	9	0.4 ± 0.2	5 ± 4	8 ± 7
Normal animals				
CTL	8	1.2 ± 0.3	21 ± 7	94 ± 42
Scl-Ab	8	1.4 ± 0.3	24 ± 9	133 ± 66

Table 12. Bone histomorphometry results.

CTL= control or no treatment; Scl-Ab = treatment with anti-sclerostin Ab; Zol = treatment with zoledronic acid; MAR = mineral apposition rate; MS/BS = mineralizing surface per bone surface; BFR/BS = bone formation rate per bone surface. Data presented as mean and standard deviation. The CKD animals were compared by two-way ANOVA evaluating the effect of PTH and drug treatment. After log transformation, there were significant PTH (all < 0.001) and overall drug treatment ($p < 0.02$ for all) effects for MAR, MS/BS and BFR/BS, and a significant PTH*drug treatment interaction for MS/BS% ($p = 0.006$) and BFR/BS ($p = 0.009$) . Between group analyses revealed that Animals with higher

PTH had values compared to low PTH ($p < 0.002$ for all three measurements). The MAR and BFR/BS were both different in ZOL compared to anti-sclerostin Ab and control (both $p < 0.02$) but the anti-sclerostin Ab was not different from control. All three treatments were different from each other for the MS/BS% (all $p < 0.03$). The Normal animals with and without treatment with anti-sclerostin Ab were compared by t-test but there was no significant difference for any parameter.

Pharmacokinetic results

Three of 8 CKD rats treated with anti-sclerostin AB developed auto-antibodies to the drug. The animals that developed auto-antibodies did not have appreciably lower BV/TV than those without auto-antibodies and therefore are included in all of the analyses. The pharmacokinetic curves are shown in **Figure 25**. Thus, auto-antibodies to antihuman sclerostin antibody were formed, similar to previously reported in studies using humanized anti-OPG antibody[252-253].

Discussion

In the present study we demonstrated that treating rats by inhibiting the activity of sclerostin in advanced CKD with a relatively normal PTH improved tibial trabecular bone volume and cortical bone geometry. In contrast, in animals with high PTH no benefit was observed. In the high PTH animals, the magnitude of hyperparathyroidism was severe, leading to profound cortical porosity but relatively normal tibial trabecular bone volume; neither antisclerostin antibody nor zoledronic acid improved the porosity. The phosphorylated β-catenin was not changed over baseline in the CKD animals treated with anti-sclerostin Ab with a high PTH but were appropriately decreased in the low PTH group, consistent with the lack of benefit in the high PTH group. As expected, dynamic histomorphometry (**Table 12**) demonstrated differences between low and high PTH for MAR, MS/BS and BFR. There was also a significant interaction between PTH group and treatment in the MS/BS and BFR/BS but not MAR. The MS/BS was decreased in the ZOL and increased in the anti-sclerostin Ab treated

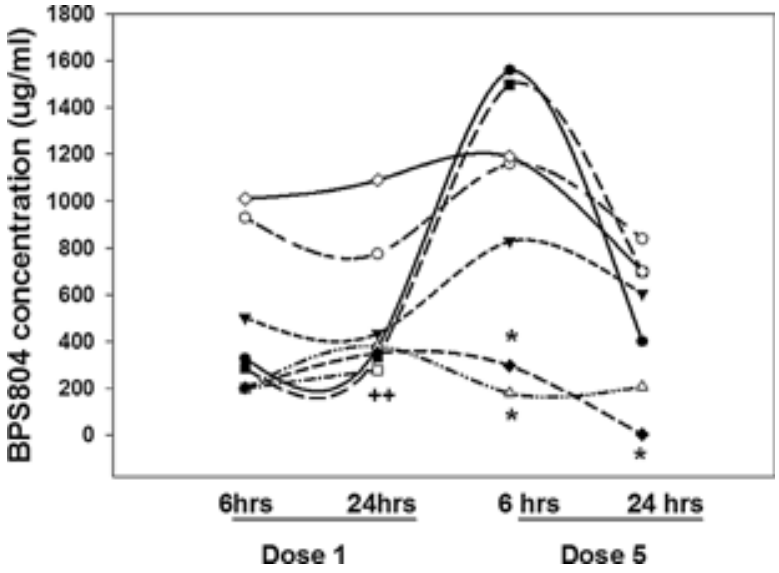

Figure 25. Pharmacokinetic results. Eight animals had blood drawn for measurement of the anti-sclerostin antibody 6 and 24 hours after the first and fifth dose. The *y*-axis represents the measured level of the anti-sclerostin antibody in the blood of each animal. Each symbol represents a different animal. *The presence of autoantibodies in serum at that time point. For the animal denoted by the open square (++), levels were undetectable at dose 5 and autoantibodies were present. BPS804 = anti-sclerostin antibody.

animals in the Low PTH but not the High PTH groups. The BFR/BS was suppressed by ZOL in the Low PTH but not the High PTH groups. Biomechanical testing demonstrated that neither anti-sclerostin antibody nor zoledronic acid were effective in improving the biomechanical properties of the bone, regardless of PTH level. These results demonstrate that cortical bone abnormalities prevail in CKD animals with elevated PTH, similar to what is observed in patients with CKD[57]. However, even in the setting of low PTH, the improvement in bone volume did not translate to improved biomechanics, suggesting other factors alter bone quality in CKD. The efficacy of anti-sclerostin Ab to improve bone volume, geometry, and biomechanics in normal rats confirms that the observed lack of efficacy in the CKD animals was due to the disease state, and not because of auto-antibody development in rats. These results suggest that abnormal Wnt signaling, especially in the high PTH group, may negate any effect of blockade of the sclerostin-mediated pathway. Alternatively, or additively, other factors in CKD may lead to such altered bone quality that anabolic changes due to the anti-sclerostin antibody are overshadowed.

Wnt signaling is mediated through the LRP5/6 pathway that is inhibited by the circulating factors sclerostin and dkk-1. PTH binds to its receptor PTH1R and activates β- catenin signaling via multiple mechanisms: 1) binding to LRP6 to activate LRP5/LRP6 signaling even in the absence of Wnt, 2) cAMP signaling to directly activate β-catenin, and 3) indirectly via osteoclast activation which then increase β-catenin activity in osteoblasts (Reviewed in [241]). Thus, PTH can activate β-catenin through non Wnt-mediated pathways. Mice expressing a

constitutively active PTH1R in osteocytes leads to cAMP signaling which increases β-catenin and osteoblast mediated bone modeling in periosteal bone[254-255]. Deletion of LRP6 in osteoblasts blunts the anabolic activity of intermittent PTH administration[256] whereas deletion of LRP5 does not[257]. Mice expressing a constitutively active PTH1R or animals receiving continuous infusion of PTH 1-84 (analogous to the secondary hyperparathyroidism in the animals in the present study) also have Wnt-dependent remodeling with increased osteoclast bone resorption via RANKL/OPG leading to osteoblast activation and β-catenin activation[255,258]. PTH suppresses expression of dkk-1 in osteoblasts, but even if dkk-1 is overexpressed, PTH can still activate the Wnt pathway via stabilization of phosphorylation of β-catenin[249]. In the present study we found increased phosphorylated (degraded) β-catenin in the high PTH animals compared to the low PTH animals treated with anti-sclerostin Ab suggesting that the elevated PTH itself does not increase β-catenin directly but more likely interferes with the LRP5/6 receptor. It is important to point out that our high PTH animals had very severe hyperparathyroidism and other studies are needed to determine if more moderate hyperparathyroidism would show beneficial bone effects of anti-sclerostin antibody.

The importance of Wnt signaling in renal osteodystrophy was first shown by Sabbagh and others[92] who characterized progressive secondary hyperparathyroidism with osteitis fibrosa in the *jck* mouse model of cystic kidney disease. They found an initial increase in immunoexpression of sclerostin and phosphorylated β-catenin in earlier CKD, but as the disease progressed and

secondary hyperparathyroidism and hyperphosphatemia developed there was a relative decline in the number of osteocytes expressing sclerostin. They also found no further increase in the phosphorylated β-catenin expression with rising PTH consistent with our results of a lower phosphorylated β-catenin in animals with high PTH compared to low PTH. They hypothesized this was due to progressive rises in PTH or in serum frizzled related protein 4 (sFRP4), another inhibitor of sclerostin[92]. We did not measure sFRP4 in our animals but this remains a possibility. In a diabetic/atherosclerotic mouse model of early stage 2 CKD, serum levels of sclerostin and Dkk1 were increased. The administration of Dkk1 monoclonal antibody to these mice led to a decrease in PTH levels, an increase in circulating sclerostin levels, and an increase in the low bone formation rate, osteoblast and osteoclast number[259]. The PTH levels, while initially increased in these animals were lower at the end of the study and equivalent in both the vehicle and anti-dkk treated animals[259]. Those results with the anti-dkk-1 antibody parallel the efficacy observed in our low PTH group with anti-sclerostin antibody treatment. Taken together the data suggest that PTH plays a major role in β-catenin signaling in renal osteodystrophy.

Circulating sclerostin levels are increased in patients with progressive decline in kidney function, beginning as early as stage 3 CKD[260]. In contrast to other circulating biomarkers, these increases do not appear related to reduced renal excretion[261]. However, in patients with primary hyperparathyroidism, sclerostin levels are lower than euparathyroid controls[262]. In patients on hemodialysis, elevated sclerostin levels, but not serum Dkk-1 levels, were

associated with increased bone mineral density at both trabecular and cortical sites by DXA and improved trabecular architecture by microCT in dialysis patients[94]. By multivariate analyses in a cohort of 60 dialysis patients, elevated sclerostin levels were only correlated with osteoblast number on bone biopsy. However, sclerostin levels had positive predictive value of 0.93 for high bone formation rate compared to only 0.57 for intact PTH; for low bone formation rates, PTH was superior[91]. Dkk-1 levels were not significantly correlated with any histomorphometric analyses. We also found elevated Dkk1 levels in our naturally occurring CKD animal model. We also saw a slight increase in the dkk-1 levels in animals treated with anti-sclerostin Ab in the high PTH group only, perhaps another explanation for a lack of efficacy of the anti-sclerostin Ab in the high PTH group.

In the present study, the sclerostin levels were greater in the high PTH animals compared to the low PTH animals. In contrast to other studies[91], we found a positive correlation between PTH and blood sclerostin levels. Given that PTH is known to suppress SOST, we then evaluated the levels of SOST expression in total bone extracts. There was no difference in basal expression of SOST in the CKD compared to normal animals, but there was a trend towards an increase in the CKD animals with low PTH (treated with calcium), and a further increase in the treatment with anti-sclerostin Ab. We hypothesize that treatment with the Ab reduces sclerostin levels leading to upregulation of SOST. Unfortunately we could not confirm this as the assay cross reacted with the Ab. The increase in SOST with the anti-sclerostin Ab was much greater in the

animals with low PTH. This may suggest that PTH inhibits SOST as has been shown[93], and/or that the elevated calcium or FGF23 in these animals increases SOST. Another potential reason why we saw a positive relationship of sclerostin with PTH may be due to the elevated phosphorus in these same animals. In a study of dialysis patients, elevated sclerostin levels were associated with lower GFR, male sex and high phosphorus levels[260]. In a rat model of CKD induced by nephrectomy, parathyroidectomy and a high phosphorus diet vs parathyroidectomy and a normal phosphorus diet led to higher circulating sclerostin levels, lower bone volume, and increased bone expression of SOST, Dkk-1, and Gsk3b suggesting that phosphorus has a PTH independent effect to suppress Wnt signaling[263]. Treating normophosphatemic stage 3 to 4 CKD patients with the non-calcium containing phosphate binder sevelamer led to a reduction in sclerostin levels, however, calcium binders had no effect on sclerostin levels despite effectively lowering phosphorus[264]. In the present study we utilized calcium in the drinking water to suppress PTH, which also acts like a phosphate binder to lower phosphorus levels. Thus it is possible that the elevated sclerostin levels in the high PTH group are due to hyperphosphatemia, and/or that the calcium administration used to lower PTH decreases sclerostin levels[91]. Clearly more work is needed to understand the regulation of SOST, especially in the setting of CKD.

Calcium (or lower PTH) also increases FGF23 levels in our animals as we have previously reported[119]. In the present study, anti-sclerostin Ab had no effect on FGF23 levels although there was a trend towards lowering of FGF23 levels in

the low PTH group. However, the variability of FGF23 in this naturally occurring animal model of CKD was such that this did not reach significance. However, treatment with anti-dkk-1 Ab in mice with early stage of CKD did not alter FGF23 levels[259]. PTH also stimulates FGF23 via cAMP and Wnt signaling[240] and thus we would have expected lower, not higher FGF23 levels in our low PTH animals. In addition, the low PTH group had elevated FGF23 that was unaffected by anti-sclerostin Ab. This implies that the calcium treatment used to lower PTH likely has a direct effect on FGF23 synthesis. Calcium treatment also led to more animals with arterial calcification, an observation that was moderated by both zoledronic acid and anti-sclerostin antibody treatment. Similarly, Fang et al found that anti-dkk-1 therapy in CKD animals reduced arterial calcification[259]. Whether sclerostin plays a pathogenic role in arterial calcification or the expression is simply a marker of osteo-chondrogenic transformation remains to be seen.

In summary, our study is the first to test the efficacy of anti-sclerostin Ab in the setting of renal osteodystrophy. In our rat model of slowly progressive CKD, the antibody enhanced trabecular bone volume and mineralization surface, but only in the setting of low PTH and this did not translate to improved biomechanical properties. In the animals with severe secondary hyperparathyroidism, the antibody was not efficacious, most likely due to PTH interference of Wnt signaling by alteration of the LRP5/6 receptor, or through effects of changes in phosphorus or FGF23.

CHAPTER 7

COMPROMISED VERTEBRAL STRUCTURAL AND MECHANICAL PROPERTIES ASSOCIATED WITH PROGRESSIVE KIDNEY DISEASE AND THE EFFECTS OF TRADITIONAL PHARMACOLOGICAL INTERVENTIONS

Material in this chapter has been accepted for publication:

Bone [doi:10.1016/j.bone.2015.04.021]

Rationale

The previous studies indicated that anti-sclerostin antibody and bisphosphonates were incapable of slowing the progression of bone disease in the presence of high levels of PTH. These assessments focused on long bones. Vertebral bone, a common site of fracture in patients with CKD, was not examined. Given the differences between sites composed of predominantly cortical bone and those primarily composed of cancellous bone, understanding whether there are different factors at play in CKD is an important component for addressing fracture risk at different skeletal sites. This study was employed to examine the disease effects of CKD on vertebral bone as well as to understand if there are differential treatment effects at this site.

Introduction

Patients with chronic kidney disease—mineral and bone disorder (CKD-MBD) have a significantly higher fracture risk than the general population[14,141,143]. This population also displays differences in fracture rates between long bones and vertebrae[141], suggesting that these two skeletal sites may be differentially affected by the disease. A study of Japanese men on dialysis who underwent screening lumbar spine imaging studies demonstrated that 20.9% of prevalent dialysis patients had evidence of spine fractures[265]. High resolution CT data have revealed significant increases in cortical porosity in the distal limbs with variable responses in trabecular bone[57]. Because vertebral elements are primarily composed of trabecular bone, the influence of secondary hyperparathyroidism on

these sites could be potentially different than in long bone cortices[266]. Furthermore, the thin cortical shell of the vertebrae bears nearly 50% of the load[267]; thus, cortical bone changes at this site would also have dramatic effects on mechanical properties and fracture risk.

Several animal models of CKD have revealed significant detriments in the biomechanical properties of long bones[110,150,268]. For example, rodent models indicate that animals with CKD exhibit lower strength and stiffness compared to their normal counterparts[108,119,127].

While much of the decline in mechanical integrity can be attributed to structural changes resulting from high parathyroid hormone (PTH) and high turnover rates, recent studies indicate that bone quality also plays a role[150]. Unfortunately, vertebral bone in CKD models has yet to be examined at any of these levels. The goal of this study was to assess the effects of progressive CKD on vertebral bone structure and mechanics and to determine the effects of treatment with either anti-remodeling medications (bisphosphonates) or anabolic treatments (anti-sclerostin antibody). We hypothesized that a significant phenotype would exist in the vertebrae of CKD animals and that treatment would restore structural mechanical properties but not the material-level mechanical properties.

Methods

Animal model

Cy/+ rats exhibit the progressive onset of polycystic kidney disease due to transmission of an autosomal dominant missense mutation in the geneAnks6, which codes for the protein SamCystin[53,161-162]. Anks6 has been shown to be important in childhood recessive cystic kidney disease although heterozygote parents have no manifestations[56,269-270]. The course of kidney disease progression in the Cy/+ rats parallels the course of human CKD-Mineral Bone Disorder (CKD-MBD)[53]. A colony of these animals is maintained at the Indiana University School of Medicine. All procedures were reviewed and approved by the Indiana University School of Medicine Institutional Animal Care and Use Committee.

Experimental design

The animals described in this work were part of a large experiment that included numerous treatment and control groups. Male Cy/+ rats began the study at 25 weeks of age at which time animals were fed a casein-based diet (Purina AIN-76A, Purina Animal Nutrition, Shreveport, LA, USA; 0.53% Ca and 0.56% Pi) in order to accentuate the disease. Subsets of Cy/+ animals were divided into the following groups (**Figure 26**):

Controls (CKD): These animals were left untreated. Based on the previously described phenotype these animals have high PTH and high bone turnover[108,178].

	CKD disease phenotype	Anti-resorptive effects	Anabolic effects
Groups	Normal littermates (NL) CKD (high PTH & high turnover)	NL CKD (high PTH + high turnover) CKD+Calcium (low PTH & low turnover) CKD + Zoledronic acid (high PTH & low turnover)	NL CKD (high PTH + high turnover) CKD+Calcium (low PTH & low turnover) CKD + SCL-AB (high PTH & high turnover) CKD + Calcium + SCL-AB (low PTH & high turnover)
Outcomes	Dynamic histomorphometry MicroCT Mechanical properties	MicroCT Mechanical properties	Micro CT Mechanical Properties
	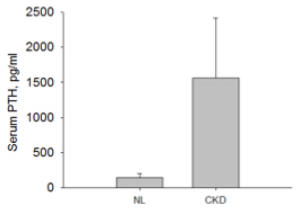	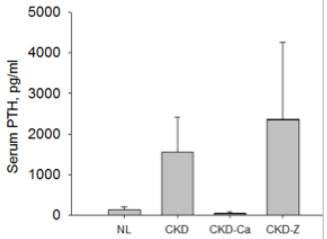	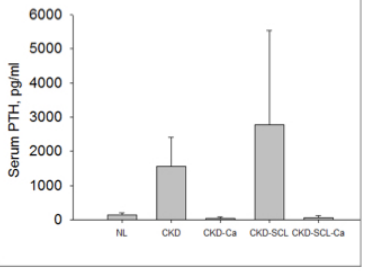

Figure 26. Overview of experimental groups, outcome measures, and serum PTH levels for the planned comparisons. PTH values from previously published manuscript[178].

Calcium (CKD-Ca): These animals were treated with calcium-supplemented water (3%) starting at 30 weeks of age. Based on the previously described phenotype these animals have low PTH and low bone turnover[108,178].

Zoledronic acid (CKD-Z): These animals were treated with zoledronic acid (20 µg/kg/BW as a single subcutaneous injection at 30 weeks of age). Based on the previously described phenotype these animals have high PTH and low bone turnover[108,178]. Zoledronic acid was chosen as a representative bisphosphonate to study in CKD as it has an infrequent dosing schedule (1x per year in post-menopausal osteoporosis treatment) and has high affinity for the bone matrix making it likely to impart persistent treatment effects.

Anti-sclerostin antibody (CKD-SCL): These animals were treated with anti-sclerostin antibody (Scl-Ab; 100 mg/kg/week starting at 30 weeks of age). Scl-AB was provided by Novartis Institutes for BioMedical Research, Novartis Pharma AG. Based on the previously described phenotype these animals have high PTH and high bone turnover[108,178]. Anti-sclerostin antibody was chosen as it has emerged as a promising potential anabolic drug treatment.

Anti-sclerostin antibody plus calcium (CKD-SCL-Ca): These animals were treated with anti-sclerostin antibody and calcium (3% in water). Based on the previously described phenotype these animals have low PTH and high bone turnover[108,178].

Normal (NL): A group of non-diseased male littermates were untreated. All animals were sacrificed at 35 weeks of age. For all experiments, serum biochemistries and long bone phenotypes have been previously reported in

various publications, yet are reported in the results when deemed necessary[108,119,178].

Dynamic Histomorphometry

In order to describe the basal remodeling phenotype of the vertebra in NL and CKD animals, the third lumbar vertebra of animals from a separate experiment[119] was processed for undecalcified histomorphometry. The vertebral arch was removed, and the body was embedded in PMMA for sectioning. Thin sections (~4 μm) were cut and left unstained for analysis. Briefly, a 2 mm^2 region of interest in the caudal region of the vertebra cranial to the growth plate was used for the analysis. Primary measurements were obtained and used for the derived parameters mineralizing surface/bone surface (MS/BS), mineral apposition rate (MAR), and bone formation rate/bone surface (BFR) as previously described[108] using standard nomenclature[211].

Computed tomography

Morphological parameters of the fourth lumbar vertebrae from all experiments were assessed using high-resolution micro-CT (Skyscan 1172). Bones were wrapped in parafilm to prevent drying during the scanning. Scans were obtained using an x-ray source, set at 60kV with a 12-μm pixel size. Images were reconstructed and analyzed using standard Skyscan software (NRecon and CTAn, respectively). Trabecular regions of interest were manually drawn to isolate it from the cortical bone between the cranial and caudal growth plates. Bone volume/tissue volume (BV/TV), trabecular number (Tb.N), and trabecular thickness (Tb.Th) were computed according to previously published

recommendations[186]. A single slice at 75% of the total vertebral length (from cranial to caudal) was used for the assessment of cortical thickness as this represents a region devoid of zygapophyseal attachment. Bone area was assessed at 25%, 50%, and 75% of the total height for normalization of mechanical properties.

Mechanics

Structural mechanical properties and apparent material properties were assessed by uniaxial compression testing of the L4 vertebra from all 3 experiments. At harvest, the vertebrae were wrapped in saline-soaked gauze and frozen at -20°. Bone height was assessed from microCT images. Prior to mechanical testing, the vertebral arch and the endplates were removed using an Isomet saw in order to create parallel surfaces (beneath the growth plates) for compression testing. Samples were loaded in displacement control at 0.5 mm/min. Load and displacement data were collected at 10 Hz and converted to stress and strain data from the initial sample height and the average bone area of 3 slices (25%, 50%, and 75% slices of the initial height of the sample). Load-displacement data were used to compute ultimate load, stiffness, and energy to failure (with failure defined as the initial decrease in load after the ultimate load), while apparent material properties were derived from the stress-strain data and used to calculate ultimate stress, elastic modulus, and toughness to the point of the ultimate stress[156].

Statistics

Statistics were carried out on select groups in order to answer a priori questions related to 1) basal phenotype of the CKD model, 2) the effects of anti-remodeling treatment with and without altered PTH levels, and 3) the effects of anabolic treatment with and without altered PTH levels (**Figure 26**). Comparisons were made using Student's t-tests or one-way ANOVA followed by Fisher protected least significant difference post hoc tests. P-values were set at ≤ 0.05. Data are reported as means and standard deviations.

Results

CKD with high PTH leads to high remodeling rate, bone loss, and compromised structural and material mechanical properties.

Select biochemistries and animal body weights are presented in **Table 13**. PTH levels in the CKD animals were over 10-fold higher than normal animals (**Figure 26)**. Histological assessment of vertebral trabecular bone revealed that mineral apposition rate was more than doubled (NL = 1.21.; CKD = 2.98), mineralizing surface/bone surface was 2.5x higher (NL = 10.5; CKD = 24.5) and bone formation was 6-fold higher in CKD animals compared to normal (**Figure 27a**).

Thus, the untreated CKD model is one of high PTH and high remodeling (**Figure 27f-g**).

	Final body weight, g	Serum calcium, mg/dL	Serum phosphorus, mg/dL	BUN, mg/dL
NL	554 ± 41	10.3 ± 0.5	4.9 ± 0.9	22 ± 5
CKD	541 ± 36	9.0 ± 2.0	8.4 ± 1.9	49.2 ± 8.2
P value	NS	NS	< 0.001	< 0.001
CKD – Calcium	499 ± 47 [ab]	11.9 ± 1.5 [b]	7.0 ± 1.2 [ab]	61.2 ± 10.5 [ab]
CKD – Zoledronic acid	531 ± 41	8.7 ± 1.9	7.6 ± 1.9 [a]	56.2 ± 16.5 [ab]
ANOVA P value	0.04	< 0.001	< 0.001	< 0.001
CKD-Scl AB	505 ± 57	9.9 ± 2.0 [a]	9.4 ± 3.9	64.4 ± 11.6 [ab]
CKD-Scl AB + Ca	515 ± 44	11.1 ± 2.7 [a]	7.9 ± 2.1	58.4 ± 13.7 [ab]
ANOVA P value	NS	0.018	0.002	< 0.001

Data as mean ± SD. Statistical comparisons were conducted as t-test (between NL and CKD), or ANOVA (between NL, CKD, CKD+Calcium, and CKD+Zoledronic Acid; and then between NL, CKD, CKD+Calcium, CKD+Scl AB, and CKD+Scl AB+Calcium). Statistically different ($p < 0.05$) values between CKD and NL are given in the t-test p values while differences in the ANOVA are noted relative to NL (a) and CKD (b).

Table 13. Descriptive characteristics of animal groups.

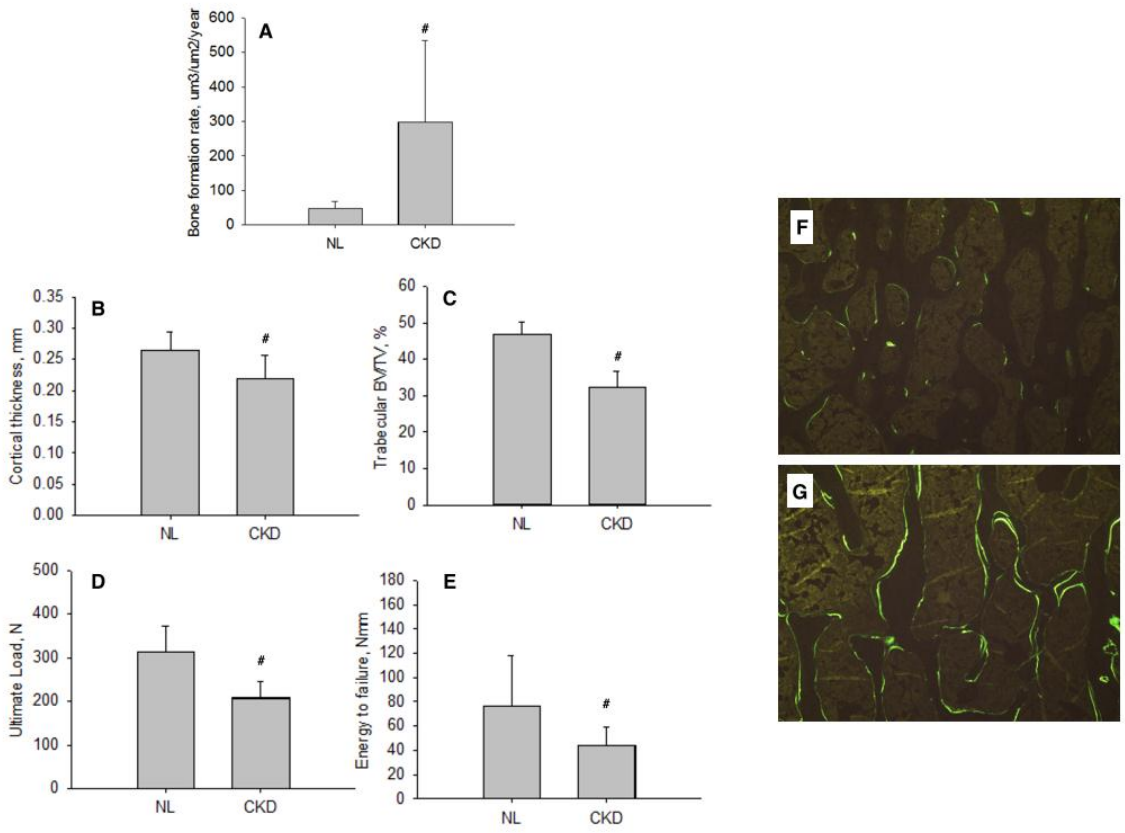

Figure 27. Vertebral phenotype of animals with high-PTH CKD compared to normal littermates (NL). (A) Trabecular bone formation rate, (B) cortical thickness, (C) trabecular BV/TV, (D) ultimate load, and (E) energy to failure. Representative fluorochrome labeling images (taken from animal with remodeling values closest to group mean) from vertebral bone of NL (F) and CKD (G) animal. # $p < 0.05$ versus NL.

Vertebral microCT analyses showed that cortical thickness (-17%) and trabecular BV/TV (-30%) were both significantly lower in CKD compared to normal (**Figure 27b-c)**. Ultimate force (-34%), stiffness (-21%), and energy to failure (-42%) were all significantly lower in CKD compared to NL **(Figure 27d-e** and **Table 14)**. Calculation of material properties revealed significant lower ultimate stress (-24%) and toughness (-34%), but not modulus, in CKD animals (**Table 14)**.

Low turnover with suppression of PTH normalizes vertebral bone morphology and mechanical properties.

CKD animals treated with calcium (CKD-Ca), which reduced PTH and suppressed tibial bone remodeling [20], had similar vertebral cortical thickness but significantly higher trabecular BV/TV (+15%), compared to normal, non-diseased animals (**Figure 28a-b**). Cortical thickness and BV/TV in CKD-Ca were both significantly higher than CKD animals. Ultimate load and energy to failure of CKD-Ca vertebrae were equivalent to NL (and higher than CKD) with the exception of stiffness, which was not significantly different among groups (**Figure 28c-d)**. Ultimate stress, modulus, and toughness of CKD-Ca were all equal or higher than NL animals (**Table 14)** and all higher than CKD.

In animals treated with zoledronic acid (CKD-Z), which suppresses bone remodeling without lowering PTH[178], the results were in stark contrast to CKD-Ca. Cortical thickness (-16%) and trabecular BV/TV (-18%) were both significantly lower than NL and CKD-Ca (**Figure 28a-b)**. Ultimate force

	Stiffness, N/mm	Ultimate stress, Pa	Modulus, Pa	Toughness, Pa
NL	1044 ± 250	30.8 ± 3.9	803 ± 208	0.95 ± 0.41
CKD	829 ± 332	23.5 ± 4.2	728 ± 290	0.63 ± 0.17
P value	0.035	0.002	NS	0.04
CKD – Calcium	804 ± 244	37.8 ± 9.9 [ab]	724 ± 211 [b]	1.37 ± 0.39 [ab]
CKD – Zoledronic acid	646 ± 345	23.4 ± 5.2 [a]	557 ± 279 [a]	0.86 ± 0.28
ANOVA P value	0.078	0.001	0.001	0.001
CKD-Scl AB	477 ± 237 [ab]	22.9 ± 5.9 [ab]	426 ± 200 [ab]	1.00 ± 0.54 [b]
CKD-Scl AB + Calcium	1072 ± 503	34.1 ± 8.5 [b]	709 ± 282	1.23 ± 0.30 [b]
ANOVA P value	0.002	0.001	0.016	0.006

Data as mean ± SD. Statistical comparisons were conducted as t-test (between NL and CKD), or ANOVA (between NL, CKD, CKD+Calcium, and CKD+Zoledronic Acid; and then between NL, CKD, CKD+Calcium, CKD+Scl AB, and CKD+Scl AB+Calcium). Statistically different ($p < 0.05$) values between CKD and NL are given in the t-test p values while differences in the ANOVA are noted relative to NL (a) and CKD (b).

Table 14. Mechanical phenotype of high PTH, high turnover CKD animals.

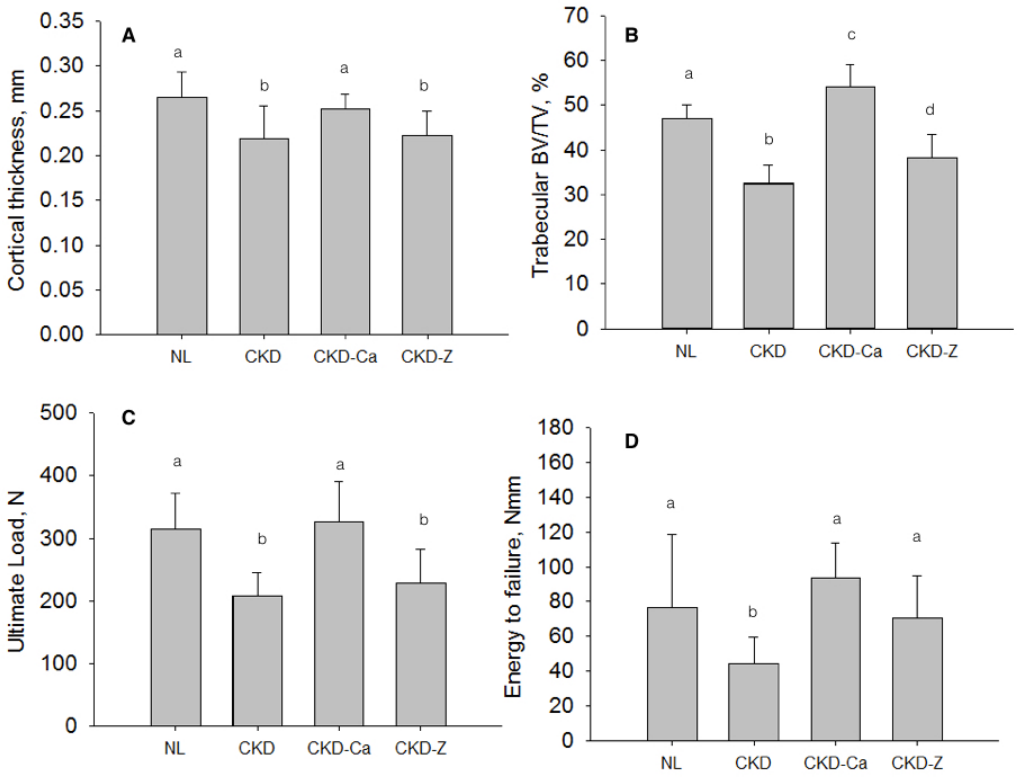

Figure 28. Influence of reducing remodeling rate, with and without lowering PTH, on the vertebral phenotype of animals with CKD. (A) cortical thickness, (B) trabecular BV/TV, (C) ultimate load, and (D) energy to failure. Groups with different letters are significantly different ($p < 0.05$). For all parameters, the overall ANOVA p value was < 0.05. NL – normal littermates; CKD – animals with chronic kidney disease with high PTH levels; CKD-Ca – animals with chronic kidney disease treated with calcium to lower remodeling and PTH; CKD-Z – animals with chronic kidney disease treated with zoledronic acid to lower remodeling.

(-28%) was significantly lower in CKD-Z compared to NL, while stiffness and energy to failure were not different (**Figure 28c-d** and **Table 14)**. Ultimate stress and modulus were lower than NL, while all three material properties were significantly lower than CKD-Ca (**Table 14)**.

High turnover with suppression of PTH, but not without, enhances vertebral morphology and vertebral mechanical properties.

CKD animals with high PTH treated with anti-sclerostin antibody, previously shown to not alter PTH or bone remodeling relative to untreated CKD [20], had significantly lower cortical thickness (-11%), trabecular bone volume (-27%), and ultimate load (-32%), and stiffness (-54%) compared to NL (**Figure 29a-c)**. Ultimate stress and modulus were both significantly lower than NL (**Table 14)**. Overall, the vertebral phenotype of the CKD-Scl animals closely resembled the CKD animals with the exception of stiffness/modulus (which were lower) and energy to failure/toughness (which were higher).

When anti-sclerostin antibody was combined with calcium (CKD-SCL-Ca), effectively reducing PTH and normalizing remodeling to NL levels [20], the results were dramatically different than anti-sclerostin alone. Cortical thickness was equivalent to NL animals while BV/TV (+15%) was significantly higher than NL, equivalent to CKD-Ca (**Figure 29a-b** and **Table 14)**. Ultimate load (+25%) was significantly higher than all other treatments while energy to failure (+51%) was significantly higher than all treatments except CKD-Ca (**Figure 29c-d** and **Table 14)** while material properties were all comparable to NL animals, higher than most other groups (**Table 14)**.

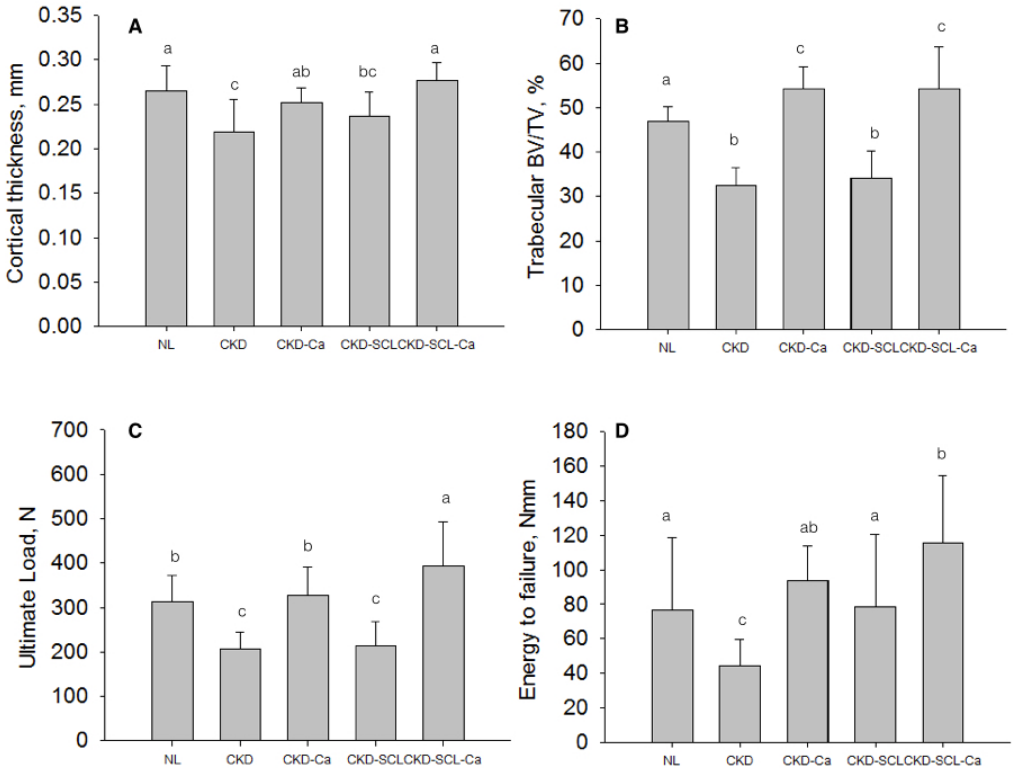

Figure 29. Influence of anti-sclerostin antibody treatment, with and without lowering PTH, on the vertebral phenotype of animals with CKD. (A) cortical thickness, (B) trabecular BV/TV, (C) ultimate load, and (D) energy to failure. Groups with different letters are significantly different ($p < 0.05$). For all parameters, the overall ANOVA p value was < 0.05. NL – normal littermates; CKD – animals with chronic kidney disease with high PTH levels; CKD-Ca – animals with chronic kidney disease treated with calcium to lower remodeling and PTH; CKD-SCL – animals with chronic kidney disease treated with anti-sclerostin antibody; CKD-SCL-Ca – animals with chronic kidney disease treated with anti-sclerostin antibody and calcium (to lower PTH).

Discussion

The goal of this study was to assess the vertebral phenotype of CKD given the high clinical risk of vertebral fracture in this patient population[80,265] and the paucity of preclinical data on spine changes with CKD. In this progressive CKD animal model we found that 1) elevations in endogenous PTH were associated with high turnover bone disease, compromised cortical and trabecular bone mass, and reduced mechanical properties (both structural and material) of the vertebra and 2) treatment of the vertebral phenotype with either anti-resorptive or anabolic therapies was only effective, from a mechanical standpoint, if serum PTH was reduced.

CKD patients have a higher risk of fracture compared to non-CKD patients[17]. Changes to long bones have been the central focus of most clinical work due to the advances in high-resolution peripheral imaging which has yielded rich information regarding changes to cortical/trabecular bone. Most notably these studies have shown that changes to the cortical bone are dramatic[57] and more severe than are typically observed with post-menopausal osteoporosis (which affects trabecular bone to a greater degree, at least initially). The risk of vertebral fracture is also increased in CKD patients[80,265,27-272], yet little information exists regarding changes to bone mass/architecture at this site. The distribution of cortical and trabecular bone in the vertebra differs significantly from long bones and although cortical bone still contributes to the mechanical integrity of the spine[267], it is possible that the intricacies of bone loss may differ from long bones. The paucity of clinical studies focused on the spine is understandable due

to imaging limitations. However for reasons that are unclear this extends to preclinical studies where few studies have examined vertebral bone[268].

The current study showed dramatic loss of trabecular bone mass and thinning of the cortical shell in the vertebra of CKD animals with high PTH, irrespective of whether they were untreated, treated with bisphosphonate, or treated with anti-sclerostin antibody. These results contrast with the long bone phenotype of these same animals where cortical porosity was higher than normal but trabecular BV/TV was positively affected in high PTH animals treated with these agents[178] (**Figure 30**). In high-PTH CKD animals, both vertebra and proximal tibia trabecular bone had high bone formation rate, suggesting that simply having high remodeling does not explain the divergent trabecular BV/TV. In conditions where PTH is normalized, using calcium supplementation, both trabecular and cortical bone area normalized (or enhanced) compared to non-CKD animals. While additional work will be necessary to elucidate why long bones and vertebra differentially respond in the setting of CKD, it raises concern about the clinical use of iliac crest bone biopsies as an assessment of trabecular bone, especially in assessing bone volume[147,273-276]. It may be that iliac crest biopsy changes are more reflective of long bone trabecular responses than they are of the vertebra. This is supported by a previous study in renal transplant patients that showed no change in iliac crest biopsy cancellous BV/TV after 6 months while spine, but not radius, BMD changed significantly during this same time frame[277].

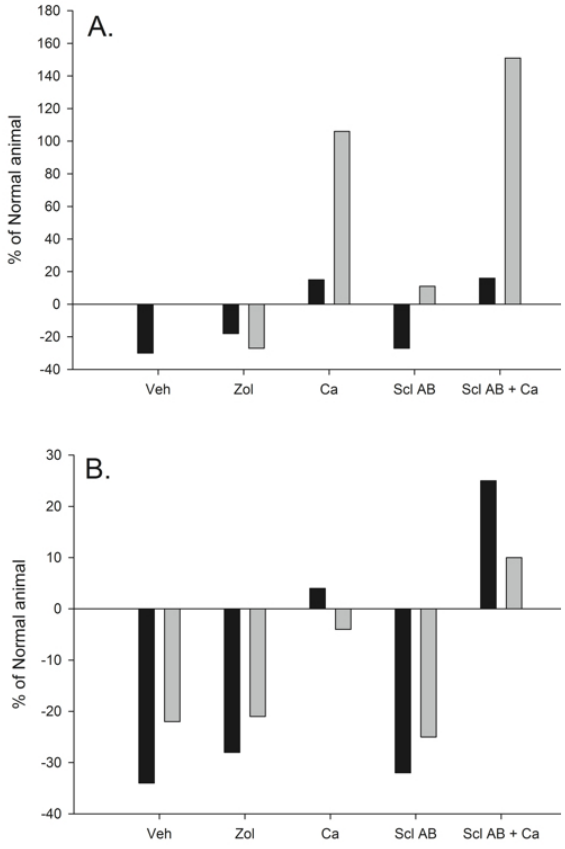

Figure 30. Summary of vertebral and long bone response to disease and treatment response. (A) Trabecular bone volume of the vertebra (black bars) and proximal tibia (gray bars). (B) Ultimate load of the vertebra (trabecular and cortical bone together; black bars) and the femoral diaphysis (purely cortical bone; gray bars). Long bone data were pulled from previous publications in this same animal model. Data presented as percent of normal animals.

The structural mechanical phenotype of the vertebrae closely follows that of the long bones in these same animals, where compromised ultimate load, stiffness, and energy to fracture existed in animals with high PTH, even if treated with the potent anti-remodeling agent zoledronic acid or the potent anabolic anti-sclerostin antibody[178]. Treatment with calcium, to lower PTH, normalized vertebra ultimate load and energy to failure, both parameters that have functional significance for fracture resistance[174]. In animals where reduced PTH was combined with the anabolic intervention of anti-sclerostin antibody, both ultimate load and energy to failure exceeded values from normal animals (**Figure 29)**. Enhanced vertebral mechanical properties have similarly been observed in ovariectomized animals treated with anti-sclerostin antibody[278]. Yet the response in these CKD animals differs from the long bone, where calcium plus anti-sclerostin antibody normalized, but did not significantly increase, ultimate load relative to NL animals[178] (**Figure 30**). These data illustrate the importance of normalizing PTH in treating the vertebral mechanical phenotype of CKD and highlight that anabolic therapy can be more effective at sites that have large proportions of both cortical and trabecular bone (such as the spine and femoral neck).

Structural mechanical properties are determined by bone mass, geometry/architecture, and the mechanical properties of the material (sometimes referred to as bone quality)[46]. Compromised bone mass and architecture are widely appreciated in CKD while the changes in bone quality have only recently begun to be explored[48,139]. We have shown, using both calculations of material

properties from whole bone tests[108,119,178] as well as by more direct measures[150] that long bones of CKD animals have reduced properties at the material level. This is associated with changes to both collagen and matrix hydration[179] although a cause-effect relationship has not been elucidated. The current work shows that high turnover, high PTH CKD disease compromises the mechanical properties of the material – as both ultimate stress and toughness, are significantly lower than NL. This means that not only does the vertebra have lower bone mass but the bone mass that exists has compromised material properties relative to normal. Controlling PTH levels normalizes the material properties – contributing to the normalization of whole bone mechanical properties while treatments that did not affect PTH (zoledronic acid and anti-sclerostin antibody alone) had mixed effects on material properties.

The current experiment utilized zoledronate as a representative bisphosphonate to study in the setting of CKD. It is well accepted that each bisphosphonate has different biophysical properties of mineral binding strength and affinity to hydroxyapatite[279]. These properties affect many of the physical and physiological actions of the drugs including drug localization, speed of onset, degree of remodeling suppression, and speed of withdrawal[280]. It is unclear whether a different bisphosphonate would be more beneficial in the setting of CKD. Zoledronate has long lasting effects on remodeling suppression, more than 5 years following a single dose[281-282] meaning that it would be difficult to washout the effect if needed. Lower affinity bisphosphonates, such as risedronate, have been shown to washout more rapidly than alendronate (a high affinity agent)[283]

suggesting that it may be more appropriate in the setting of CKD if concerns exist about treatment washout duration. More work with bisphosphonates are necessary to understand the details of their effects on bone, as well as the safety on the kidney, in the setting of CKD. It is possible that the there is diversity in the renal safety among the bisphosphonates but additional work is needed in this area[284]. In addition, despite efficacy of calcium in lowering PTH and improving serum calcium, in our previous publications we have observed increased arterial calcification suggesting that both efficacy and safety should be considered with any interventions.

In conclusion, the present study provides a clear picture of how progressive CKD, with and without interventions, affects vertebral bone properties. Since CKD-associated bone disease and fracture risk is significant at this site, it is important to recognize that response to treatment differs from long bones. Despite these differences, what is clear from this study is that reducing PTH is fundamental in normalizing mechanical properties. As such, any anti-resorptive or anabolic bone therapies utilized in CKD should be examined in combination with therapies that suppress PTH (such as calcitriol and 1,25 vitamin D analogs and calcimimetics).

CHAPTER 8

RALOXIFENE IMPROVES SKELETAL PROPERTIES IN AN ANIMAL MODEL OF CHRONIC KIDNEY DISEASE

Material in this chapter has been submitted for publication:

Kidney International

Rationale

Prior studies examining anti-sclerostin antibody and bisphosphonates in CKD showed incomplete restoration of mechanical properties. Based on the previous indications that bone quality is compromised in CKD, the application of a treatment that modifies bone quality is particularly appealing in the setting of a disease where most other osteoporosis medications are either ineffective or avoided over concerns of adverse events. Previous data have shown that raloxifene positively affects bone quality, which is why this study tested its efficacy in the setting of CKD.

Introduction

Chronic kidney disease—mineral and bone disorder (CKD-MBD) is characterized by hyperphosphatemia, secondary hyperparathyroidism, and an increased risk of fractures[8-9,60]. This metabolic complexity has made treating skeletal manifestations difficult. Currently, calcitriol and its analogues are used to control elevations in parathyroid hormone (PTH) in patients with advanced CKD[62]. They are known to have positive effects on bone mineral density (BMD) in non-CKD patients[69], and similar increases have been reported in CKD patients[285-288]. Improvements in histological parameters have also been observed[196-197,289-291], but studies examining the fracture efficacy of calcitriol in patients with CKD have not been conducted[64]. While low BMD can predict fractures in some stages of CKD[43], clinical studies have not established a consistent relationship between BMD and fracture risk, especially in dialysis

patients[35-36]. Even with recent indications that BMD is a useful surrogate for fracture risk in late stage CKD patients[45], low BMD only explains about 70% of fractures[34]. One potential reason for this low sensitivity is that bone quality (the inherent physical and chemical constitution of bone) is adversely affected in CKD[50-51,150].

For patients with early stage CKD (estimated glomerular filtration rate greater than 30 mL/min) and normal PTH levels, most guidelines adopt treatment recommendations for adults with osteoporosis[60-61]. The majority of patients with osteoporosis are treated with anti-resorptive agents that reduce osteoclast-mediated bone loss[76]. Unfortunately, the complex metabolic background of CKD and a lack of clinical data in patients with advanced disease have limited the use of these agents. For example, bisphosphonates are not recommended due to concerns over their renal clearance and their potent suppression of bone remodeling to very low levels[60]. As there are minimal data on other osteoporosis treatments in the setting of CKD, there is a significant gap in the current understanding of how to treat skeletal disease in these patients[61].

Raloxifene is a selective estrogen receptor modulator with mild anti-resorptive properties. Clinical trials have shown that it effectively reduces fracture risk in patients with osteoporosis despite modest improvements in BMD[95-96]. Preclinical studies indicate that raloxifene improves mechanical properties through its effects on bone quality[97-99]. Specifically, raloxifene positively affects bone toughness (the ability of bone to tolerate damage without fracturing). This improvement occurs in the absence of significant changes in bone mass[97-98] and

appears to be partly due to changes in bone matrix hydration[101-102]. Furthermore, secondary analyses of a human clinical trial revealed beneficial renal outcomes in patients using raloxifene[103]. Preclinical experiments[104-105] and a small clinical study in dialysis patients[106] have supported these findings. Taken together, these data suggest that raloxifene could have beneficial effects on several consequences of CKD. The goal of the current work was to test the hypothesis that raloxifene would improve skeletal properties in an animal model of progressive CKD.

Methods

Animal Model

Cy/+ rats are characterized by autosomal dominant polycystic kidney disease (PKD)[53]. These animals have a mutation (R823W) in *Anks6*, a gene that codes for the protein SamCystin. The function of this protein is unknown[54], but unlike most other PKD-related proteins, SamCystin does not localize to the primary cilia of kidney cells[55]. This gene has recently been related to nephronophthisis in humans[56]. In this rat model, the mutation leads to a slow and gradual onset of CKD[53]. It parallels the human condition through the gradual development of abnormal mineral homeostasis and vascular calcification. Blood urea nitrogen (BUN) and creatinine are elevated by 20 weeks of age and indicate a 50% reduction in kidney function. At 30 weeks, kidney function is about 20% of that observed in normal animals, leading to progressive hyperphoshpatemia, hyperparathyroidism, and skeletal abnormalities.

Experimental Design

Male Cy/+ rats were phenotyped for the presence of cystic disease by abdominal palpation and serum levels of BUN at 10 and 15 weeks of age. Animals with BUN between 30 and 50 mg/dL (with increasing BUN values from 10 to 15 weeks) were defined as having CKD. Normal littermates (n=8), defined by BUN values less than 30 mg/dL with no increase between 10 and 15 weeks and an absence of observable cystic kidney disease at sacrifice, served as controls[161-162]. At 24 weeks, animals were placed on a casein diet (Purina AIN-76A; 0.7% Pi, 0.6% Ca) to increase phosphorus availability. This diet has been shown to produce a more consistent kidney disease phenotype[53].

Starting at 25 weeks of age, Cy/+ rats were treated with vehicle (n=9) or raloxifene (n=10) (1 mg/kg daily; subcutaneous) for 5 weeks. This treatment duration was chosen as it approximates an average bone remodeling cycle in skeletally mature rats (roughly six months in humans) and has been shown to be sufficient to detect treatment-induced skeletal changes in this model[108,119]. Raloxifene doses were based upon previous studies in ovariectomized female rats[99]. All rats were injected with calcein (10 mg/kg; subcutaneous) 14 and 4 days prior to sacrifice to label surfaces with actively forming bone.

At 30 weeks of age, animals were anesthetized with isoflurane and underwent cardiac puncture for blood draw followed by exsanguination and bilateral pneumothorax to ensure death. The lumbar spine, tibiae, and femora were removed and stored at -20^{O}C for analysis. All procedures were approved by

and carried out according to the rules and regulations of the Indiana University School of Medicine's Institutional Animal Care and Use Committee.

Biochemistry

Blood plasma at 30 weeks was analyzed for BUN, calcium, and phosphorus using colorimetric assays (Point Scientific, Canton, MI, or Sigma kits). Intact PTH was determined by ELISA (Alpco, Salem, NH). FGF23 was assessed with a two-site assay (Immunotopics, San Clemente, CA)[38,53,112].

Micro-Computed Tomography (microCT)

Using microCT (Skyscan 1172), trabecular bone volume (BV/TV, %) and architecture (number, spacing, and thickness) were determined from the metaphysis of the proximal tibia and the entire L4 vertebra. Cortical bone geometry (area, thickness, bending moments of inertia, and porosity) was determined from the femoral midshaft. Cortical thickness was assessed at 75% of the height of the vertebra (from cranial to caudal) because this represents a region free of zygapophyseal attachment. All bones were wrapped in parafilm to prevent drying and scanned at a resolution of 12 μm in accordance with standard guidelines[186].

Histomorphometry

Static and dynamic histomorphometric measures were obtained from the proximal metaphysis of the left tibia and the caudal metaphysis of the L3 vertebra. Histological processing followed previously used protocols[187-189]. Tissues were embedded in methyl methacrylate for undecalcified sections. Mid-transverse sections (4 μm) of cancellous bone from the proximal tibia and the

caudal portion of the L3 vertebra were cut and left unstained for dynamic histomorphometry or stained with tartrate-resistant acid phosphatase (TRAP) for osteoclast measurements (tibia only). For tibial and vertebral cancellous bone, a region of interest (encompassing 7-8 mm^2 and 1.5-2.0 mm^2, respectively) approximately 0.8 mm from the growth plate was analyzed. The unstained sections were assessed for total bone surface, single-labeled surface, and double-labeled surface to calculate mineral apposition rate (MAR), percent mineralizing surface (MS/BS), and bone formation rate (BFR/BS). TRAP-stained sections were assessed for bone surface, osteoclast number, and osteoclast surface to calculate the number of osteoclasts per unit bone surface (N.Oc/BS) and percent osteoclast surface (Oc.S/BS). All histomorphometric nomenclature follows standard usage[190].

Whole Bone Mechanics

Structural mechanical properties of the left femur were determined by four-point bending. The anterior surface was placed on two lower supports located ±9 mm from the mid-diaphysis (18 mm span length) with an upper span length of 6 mm. Specimens were loaded to failure at a rate of 2 mm/min, producing a force-displacement curve for each sample. Structural mechanical properties (ultimate force, stiffness, energy to fracture, total displacement) were obtained directly from these curves, while apparent material properties (ultimate stress, elastic modulus, toughness) were derived from the force-displacement curves, cross-sectional moments of inertia (I_{ml}), and the distances from the centroid to the tensile surface using standard beam-bending equations for four-point bending[47].

Structural mechanical properties of the L4 vertebra were determined by uniaxial compression. Vertebra height was assessed from microCT images. Prior to mechanical testing, the vertebral arch and endplates were removed using an Isomet saw to create parallel surfaces (inside the growth plates) for compression testing. Specimens were loaded at a rate of 0.5 mm/min, producing a force-displacement curve for each sample. Structural mechanical properties were obtained directly from these curves, while apparent material properties were derived from the force-displacement curves, pre-test sample heights, and the average bone area of five microCT slices (10%, 30%, 50%, 70%, and 90% slices of the pre-test sample height) using standard equations for uniaxial compression[191-192].

Tissue Composition

The anteromedial portion of the right tibial mid-diaphysis was polished with a 0.05 μm alumina suspension in order to create a flat region for spectroscopy and subsequent indentation testing. Raman spectroscopy was performed using a LabRAM HR 800 Raman Spectrometer (HORIBA JobinYvon, Edison, NJ) connected to a BX41 microscope (Olympus, Tokyo, Japan). A 660 nm laser was focused on the bone surface using a 50X objective to a spot size of ~10 μm. Three locations were imaged ~3 mm apart on the polished surface with five 20 second acquisitions at each location as previously published[115]. A five-point linear baseline correction was applied in LabSpec 5 (HORIBA JobinYvon). Using OriginPro 8.6 (OriginLab, Northampton, MA), a single Gaussian peak was fit to the PO_4^{3-}-ν1 peak, and the areas under the PO_4^{3-}-ν1 (930-980 cm^{-1}), CO_3^{2-}-ν1

(1056-1091 cm^{-1}), and Amide I (1551-1720 cm^{-1}) bands were calculated at each location. Type B carbonate substitution was found by the band area ratio of CO_3^{2-} $\nu1/PO_4^{3-}\nu1$. The degree of matrix mineralization was determined by the band area ratio of $PO_4^{3-}\nu1$/Amide I. Mineral maturity (crystallinity) was determined by the inverse of the full width at half maximum (FWHM) of the $PO_4^{3-}\nu1$ peak.

AFM Indentation

Using the polished tibial surface described above, indentations were performed using a BioScope Catalyst atomic force microscope (Bruker, Santa Barbara, CA), operating in peak force tapping mode using previously published methods[116]. Samples were partially submerged in ultrapure water with the surface remaining uncovered for optical imaging of the surface in order to determine indentation locations but then fully submerged during testing. Indentations were performed using a tungsten carbide-coated AFM probe (Nanotec; nominal tip radius of 60 nm) with a nominal spring constant of 650 N/m. Three locations (co-localized with Raman measurements) per sample were indented, and at each location (20 μm×20 μm grid), 100 indentations were performed. Samples were loaded to 3.25 μN with force-separation curves acquired from each indentation. Within each location, indentations were spaced about 2 μm apart in order to avoid interactions from neighboring indentations. In total, 300 indentations were performed for each sample. The indentation elastic modulus was calculated from 20% to 80% of the withdrawal curve using the Sneddon model of contact between a rigid cone and an elastic half space because the indentation depth is greater than the radius of curvature of the

probe[116]. Only those indentations whose retraction curve produced an r^2 value of 0.90 or higher were included in the analysis (n=6-95 per location). The indentation elastic modulus was determined from the following equation:

$$F = \frac{2}{\pi} \cdot \frac{E_s}{1 - \nu_s} \cdot \tan \alpha \cdot \delta^2$$

where F is the indentation force, E_S is the indentation elastic modulus of the sample, ν_S is the Poisson's ratio of the sample (assumed to be 0.35), □ is the opening angle (assumed to be 20^O), and δ is the indentation depth. All of the individual indentations were averaged to produce a single value for each location, and each of these locations was averaged to produce a single value for each sample.

Nanoindentation

After AFM indentation, nanoindentation was performed on the same tibial samples using a Hysitron TI950 TriboIndenter. As above, samples were partially submerged in ultrapure water with the surface remaining uncovered for optical imaging of the surface in order to determine indentation locations but then fully submerged during testing. Three locations (co-localized with AFM indentations) per sample were indented. Pre-saved test locations were imaged using the nanoindenter for *in situ* scanning probe imaging. Within this imaged region, 6 indentations were performed on a 10 μm x 20 μm grid. Indentations were spaced 10 μm apart in order to avoid interactions from neighboring indentations. A previously calibrated fluid cell Berkovich diamond probe was used for the indentations. Machine calibrations were performed at the beginning of each day of testing. Tests were conducted in load control, and the loading profile consisted

of a 10s loading period, a 10s hold at 3000 μN, and a 10 s unloading period. From the resulting load-displacement profiles, the indentation elastic modulus and hardness were calculated according to the following equations:

$$E_r = \frac{\sqrt{\pi}}{2\sqrt{A(h_c)}} \cdot S$$

$$H = \frac{P_{max}}{A(h_c)}$$

where E_r is the reduced indentation elastic modulus of the sample, A is contact area, h_c is the contact displacement, S is the stiffness of the sample determined from 40-95% of the unloading slope, H is the hardness of the sample, and P_{max} is the peak force. All of the individual indentations (n=6 per location) were averaged to produce a single value for each location, and each of these locations was averaged to produce a single value for each sample.

Reference Point Indentation

After nanoindentation, reference point indentation (Biodent Hfc, Active Life Scientific, Santa Barbara, CA) was performed on the same tibial samples. Three locations (co-localized with nanoindentation) per sample were indented. The reference probe, which housed a BP3 test probe, was lowered vertically, normal to the surface, until it rested on the surface of the bone. In order to stabilize the unit, a reference force of ~13 N was applied before each measurement was initiated. Each test included a series of 10 cycles (load, hold, and unload) at 2 Hz with a peak force of 10 N. Bones were maintained submerged in ultrapure water throughout the duration of the test. Raw data from the RPI analysis software (version 2.0) were imported into a customized MATLAB code (Mathworks)

designed to provide cycle-by-cycle data for each test[114], from which first cycle unloading slope, indentation distance increase, first cycle energy dissipation, creep indentation distance, first cycle indentation distance, total indentation distance, and total energy dissipation were calculated for each test. Each location was averaged to produce a single value for each variable.

Collagen Morphology

Following indentation testing, the polished tibial surface was partially decalcified by soaking the bones in 0.5 M EDTA for 25 minutes followed by five minutes of sonication in a water bath. This process was repeated five times for each sample. For imaging, RTESPA probes were used (Bruker; nominal radius of 8 nm; spring constant = 40 N/m). For measurements of collagen morphology, the scan size was set at 3.5 μm with 512×512 pixels and a scan rate of 0.5 lines/s. Two locations between indentation sites were imaged per sample (one location was dropped from a raloxifene sample due to poor image quality), and 12 fibrils were measured at each location. All 24 fibrils were averaged to produce a single value for each animal (one normal sample had only 18 fibrils and two CKD samples had14 and 20 fibrils due to poor image quality). Using SPIP 5.1.10 (Image Metrology, Hørsholm, Denmark), D-periodic spacing was calculated using 2D Fast Fourier Transformations as previously described[115].

Collagen Cross-Linking

After four-point bending, proximal segments of the left femoral cortex (~3 mm in length) were fully demineralized in 20% EDTA (0.68 M, pH 7.4). Approximately 10 mg of demineralized bone were hydrolyzed in 6N HCl (~10 μL

per 1 mg) at 110°C for 20-24 hours. After evaporating the acid using a SpeedVAC centrifuge with a cold trap, each hydrolysate was resuspended in ultrapure water, split into two equal portions, and dried. Half of the residue was resuspended in ultrapure water with an internal standard (5×10^{-6} g/L pyridoxine). The solution was filtered and diluted with 0.05% heptafluorobutyric acid in 10% acetonitrile, and 50 µL of each hydrolysate were assayed by a high performance liquid chromatography (HPLC) system (Beckman-Coulter System Gold 168) with a silica-based column (Waters Spherisorb) as previously published[150]. Standards with varying concentrations of pyridinoline (PYD; Quidel), deoxypyridinoline (DPD; Quidel), pentosidine (PE; International Maillard Reaction Society), and a constant amount of pyridoxine were also assayed. Using a Waters 2475 fluorescence detector (excitation/emission of 295/400 nm for PYD and DPD and 328/378 nm for PE), chromatograms were recorded to determine the amount of each crosslink. These amounts were then normalized by collagen content, which was determined from the other half of each hydrolysate by another HPLC assay. With α-amino-butyric acid (α-ABA) included as an internal standard, the amino acids were subjected to derivatization with phenyl isothiocyanate (PITC). Along with varying concentrations of derivatized hydroxyproline (Sigma) and a constant amount of α-ABA as standards, the derivatized samples were resuspended in a buffer solution of 5% acetonitrile in 5 mM disodium phosphate. Upon injecting 50 µL of this sample, chromatograms were generated with a UV detector (Beckman-Coulter System Gold 168). The calculated mass of hydroxyproline was then multiplied by 7.5 (assuming 13–14% of type I collagen by mass) and divided by

the molecular weight of collagen (30,000 Da), thereby giving crosslink concentration as mol/mol of collagen.

^{1}H Nuclear Magnetic Resonance Spectroscopy

A ~5-mm cross-section of the left femoral mid-shaft was placed into a low proton, loop-gap-style radio-frequency (RF) coil along with a reference microsphere of water (T_2 ~ 2 s). As previously published[102], the nuclear magnetic resonance spectroscopy (NMR) analysis was performed in a 4.7-T horizontal-bore magnet (Varian Medical Systems, Santa Clara, CA) using 90°/180° RF pulses of ~9/18-μs duration and collecting Carr-Purcell-Meiboom-Gill (CPMG) measurements with 10,000 echoes at 100 μs spacing in order to separate proton signals within the bone. To generate the spectrum of transverse relaxation time constants (T_2), the echo magnitudes were fitted with multiple exponential decay functions. Upon normalizing the integrated areas of bound water (T_2 = 1200–800 μs) and pore water (T_2 = 800 μs –600 ms) to the area of the reference (T_2 = 600 ms–10 s), the volume of bound water and the volume of pore water were divided by the specimen volume (calculated using Archimedes' principle) to give bound water (bw) and pore water (pw) volume fractions.

Statistics

Comparisons among groups were assessed by one-way ANOVA with Fisher's LSD post-hoc tests. *A priori* α-levels were set at 0.05 to determine significance. Data are presented as mean ± standard deviation.

Results

Mineral Metabolism

Animals with CKD had higher serum levels of BUN compared to normal littermates (+231%), consistent with previous data indicating the presence of late stage kidney disease, estimated to be 20-25% of normal kidney function (**Table 15**). Serum calcium was normal, while phosphorus (+48%), FGF23 (+266%), and PTH levels (+1106%) were all significantly higher than their normal counterparts. Raloxifene-treated animals were nearly indistinguishable from their untreated CKD counterparts, having BUN, phosphorus, and FGF23 levels that differed from normal but not vehicle-treated CKD animals. PTH levels in raloxifene animals were significantly lower than untreated CKD animals (-42%) but still higher than normal controls (+591%).

MicroCT

Vehicle-treated CKD animals had lower trabecular bone volume (with lower trabecular number and higher trabecular spacing) relative to normal animals at the proximal tibia. Raloxifene normalized proximal tibia trabecular bone volume (due to higher trabecular number and lower spacing than CKD animals) (**Figure 31** and **Table 16**). A similar pattern of trabecular bone morphology was present in the vertebra, with CKD animals having lower trabecular bone volume (due to lower trabecular number and higher spacing) that was partially restored with raloxifene (**Figure 31** and **Table 16**).

Cortical bone of the femoral midshaft was also negatively affected by CKD. CKD animals had lower cortical area, cortical thickness, and cross-

Biochemistry	Normal	CKD (Vehicle)	CKD (Raloxifene)
BUN (mg/dL)	14.62 ± 1.95	48.32 ± 8.20 *	44.12 ± 5.12 *
Calcium (mg/dL)	9.979 ± 0.987	11.610 ± 2.323	10.061 ± 2.421
Phosphorus (mg/dL)	4.527 ± 0.579	6.682 ± 2.408 *	9.700 ± 3.591 *
PTH (pg/mL)	181.97 ± 105.05	2194.39 ± 1811.01 *	1257.46 ± 1456.22 *#
FGF23 (pg/mL)	698.36 ± 93.03	2556.83 ± 1401.96	6184.88 ± 3403.39

* vs. Normal
# vs. CKD (Vehicle)

Table 15. Biochemistry

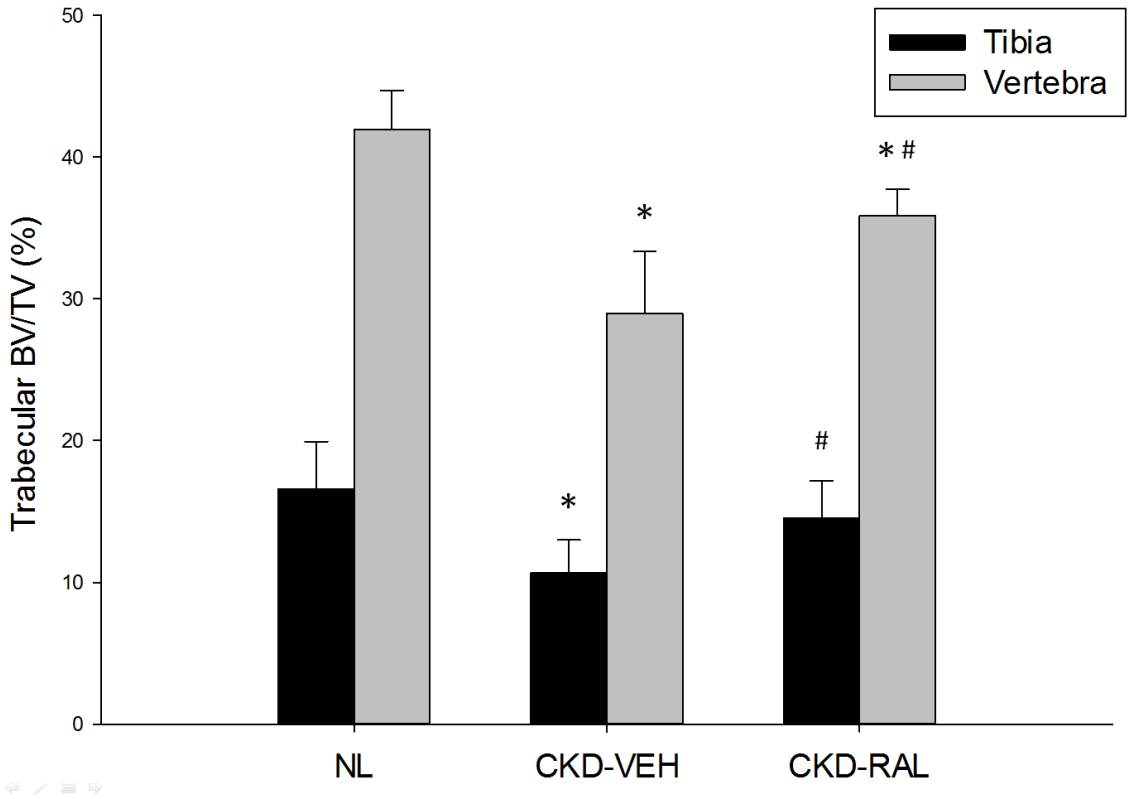

Figure 31. Cancellous bone structure in the proximal tibia and lumbar vertebra as determined by microCT. *, $p<0.05$ compared to NL; #, $p<0.05$ compared to CKD-VEH

Proximal Tibia	Normal	CKD (Vehicle)	CKD (Raloxifene)
BV/TV (%)	17.04 ± 3.34	11.26 ± 1.51 *	14.9 ± 2.70 #
Tb.Th (mm)	0.106 ± 0.010	0.108 ± 0.004	0.103 ± 0.007
Tb.N (1/mm)	1.611 ± 0.253	1.052 ± 0.150 *	1.451 ± 0.211 #
Tb.Sp (mm)	0.369 ± 0.044	0.604 ± 0.114 *	0.420 ± 0.055 #
Femoral Diaphysis			
Ct.Th (mm)	0.876 ± 0.037	0.748 ± 0.056 *	0.783 ± 0.039 *
Ct.Ar (mm^2)	8.767 ± 0.631	7.324 ± 0.358 *	7.611 ± 0.397 *
I_{ap} (mm^4)	15.00 ± 2.59	12.40 ± 0.58 *	12.30 ± 1.35 *
I_{ml} (mm^4)	10.23 ± 1.56	7.50 ± 0.59 *	7.86 ± 0.73 *
Ct.Po (%)	0.690 ± 0.324	0.948 ± 0.401	0.467 ± 0.274 #
Lumbar Vertebra			
BV/TV (%)	41.88 ± 2.92	30.01 ± 3.98 *	36.27 ± 1.76 *#
Tb.Th (mm)	0.119 ± 0.004	0.110 ± 0.007 *	0.108 ± 0.005 *
Tb.N (1/mm)	3.581 ± 0.258	2.726 ± 0.324 *	3.401 ± 0.129 #
Tb.Sp (mm)	0.213 ± 0.021	0.280 ± 0.031 *	0.235 ± 0.014 * #
Ct.Th (mm)	0.236 ± 0.033	0.170 ± 0.012 *	0.184 ± 0.025 *

* vs. Normal
# vs. CKD (Vehicle)

Table 16. MicroCT

sectional moments of inertia compared to normal controls (**Table 16**). There was no difference in cortical porosity between normal and untreated CKD animals. Raloxifene treatment led to less porosity than CKD animals but did not correct CKD-induced changes in cortical area, thickness, or moments of inertia. CKD animals had thinner vertebral cortices than their normal counterparts, and this was not corrected by raloxifene (**Table 16**).

Histology

Vehicle-treated CKD animals had higher trabecular bone formation rates in the tibia (+137%) and vertebra (+306%) compared to normal animals (**Figure 32**). This was a result of higher mineral apposition rates as well as a higher proportion of mineralizing surfaces (**Table 17**). Animals with CKD also had higher osteoclast number and percent osteoclast surface than their normal counterparts (**Table 17**). Raloxifene treatment lowered bone formation rates to normal levels at both the tibia and the vertebra (**Figure 32**) but did not change osteoclast parameters (**Table 17**).

Whole Bone Mechanics

Animals with CKD had lower femoral cortical bone ultimate force (-25%), stiffness (-22%), and energy to fracture (-23%) compared to normal animals (**Figure 33** and **Table 18**). Estimated material properties revealed a significantly lower modulus of toughness in CKD animals (-16%) (**Figure 33**). Ultimate stress and elastic modulus were not different (**Table 18**). Animals treated with raloxifene

displayed a higher energy to fracture compared to vehicle-treated CKD animals accompanied by higher (though not normal) ultimate force. There was no effect

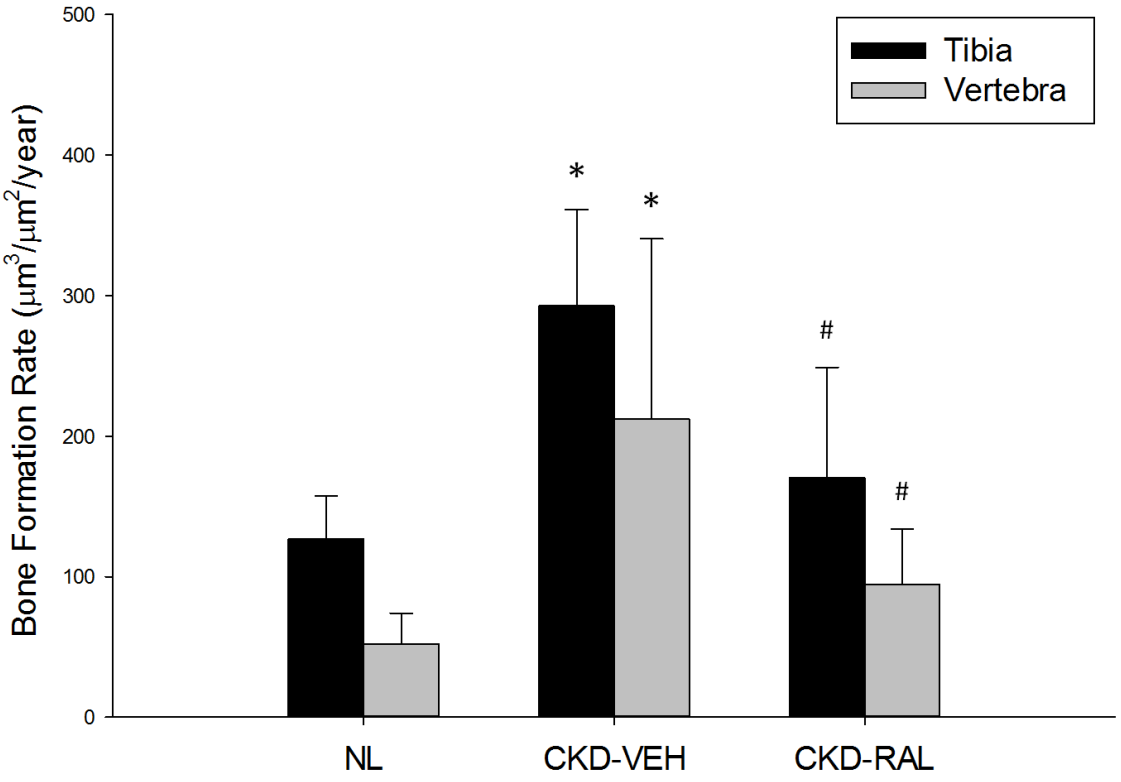

Figure 32. Bone formation rates in the proximal tibia and caudal lumbar vertebra as determined by dynamic histomorphometry. *, $p<0.05$ compared to NL; #, $p<0.05$ compared to CKD-VEH

Tibia	Normal	CKD (Vehicle)	CKD (Raloxifene)
MAR (μm/day)	1.305 ± 0.185	2.470 ± 0.569 *	1.890 ± 0.511 *
MS/BS (%)	26.56 ± 5.14	33.32 ± 4.11	23.89 ± 4.75 #
BFR ($\mu m^3/\mu m^2$/year)	126.65 ± 31.02	299.62 ± 74.35 *	170.40 ± 78.52 #
Oc.S/BS (%)	7.157 ± 1.250	15.739 ± 3.332 *	15.684 ± 6.857 *
N.Oc/BS (1/mm)	1.966 ± 0.412	4.125 ± 0.785 *	4.134 ± 1.653 *
Vertebra			
MAR (μm/day)	1.057 ± 0.339	1.983 ± 0.876 *	1.574 ± 0.400
MS/BS (%)	13.62 ± 3.98	27.81 ± 5.73 *	16.21 ± 3.73 #
BFR ($\mu m^3/\mu m^2$/year)	52.14 ± 21.76	211.94 ± 128.49 *	94.19 ± 39.80 #

* vs. Normal
# vs. CKD (Vehicle)

Table 17. Histomorphometry

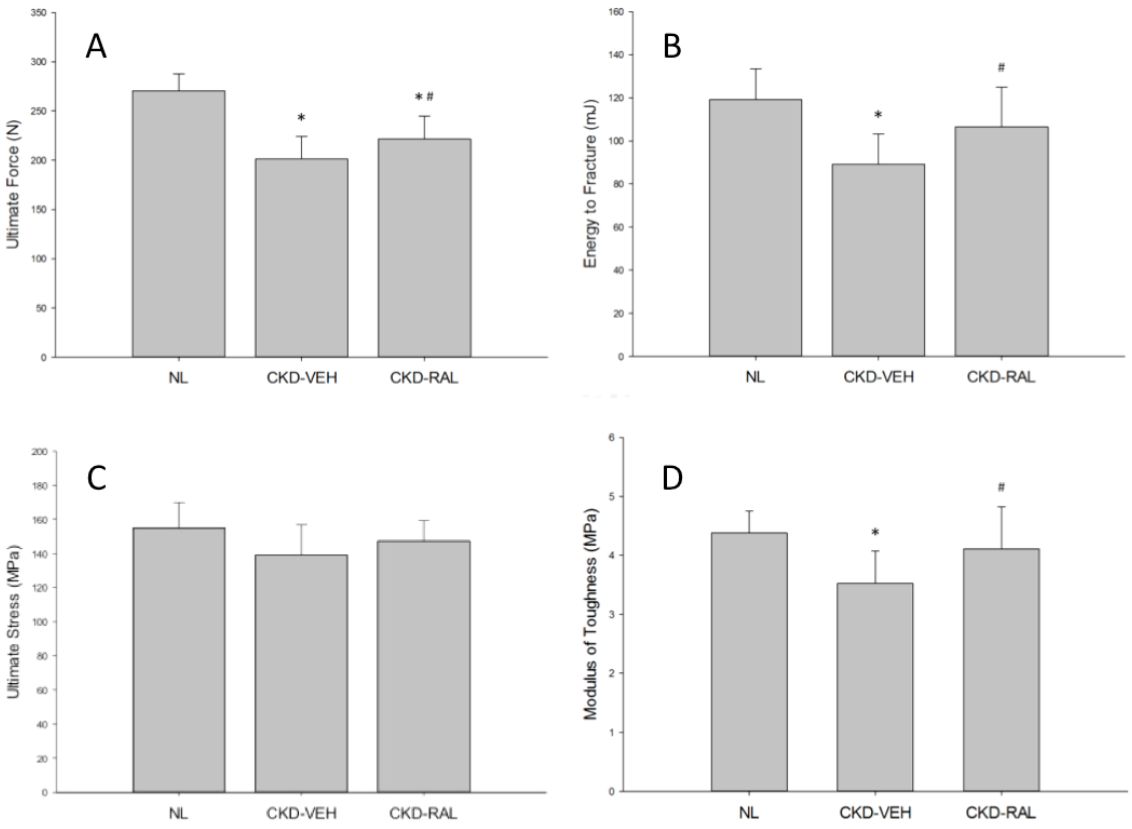

Figure 33. Whole bone mechanical and apparent material properties of the femur as determined by four-point bending: (a) ultimate load, (b) energy to fracture, (c) ultimate stress, and (d) modulus of toughness. *, $p<0.05$ compared to NL; #, $p<0.05$ compared to CKD-VEH

Femur	Normal	CKD (Vehicle)	CKD (Raloxifene)
Ultimate Force (N)	272.08 ± 17.75	204.81 ± 23.20 *	223.44 ± 23.78 * #
Stiffness (N/mm)	531.67 ± 47.41	412.96 ± 56.28 *	440.66 ± 30.52 *
Energy to Fracture (mJ)	119.16 ± 15.33	91.65 ± 14.13 *	107.24 ± 20.86 #
Pre-Yield Displacement (μm)	429.36 ± 31.14	381.76 ± 37.59 *	443.46 ± 27.98 #
Post-Yield Displacement (μm)	352.20 ± 76.44	363.39 ± 71.40	381.55 ± 96.43
Total Displacement (mm)	781.56 ± 53.46	745.15 ± 67.76	825.01 ± 95.15
Ultimate Stress (MPa)	153.81 ± 15.68	143.94 ± 17.93	146.76 ± 13.28
Elastic Modulus (MPa)	4.649 ± 0.633	5.144 ± 0.971	4.998 ± 0.466
Toughness (MPa)	4.336 ± 0.382	3.652 ± 0.545 *	4.096 ± 0.814 #
Mechanics (Vertebra)			
Ultimate Force (N)	256.89 ± 60.01	187.06 ± 48.03 *	179.57 ± 38.63 *
Stiffness (N/mm)	952.09 ± 314.20	866.74 ± 260.33	854.76 ± 277.85
Energy (mJ)	46.27 ± 10.60	28.05 ± 8.93 *	26.46 ± 7.33 *

Pre-Yield Displacement (μm)	0.408 ± 0.085	0.337 ± 0.045	0.392 ± 0.093
Post-Yield Displacement (μm)	0.036 ± 0.056	0.019 ± 0.034	0.007 ± 0.006
Total Displacement (mm)	0.445 ± 0.123	0.355 ± 0.062	0.399 ± 0.97
Ultimate Stress (MPa)	42.49 ± 10.00	38.74 ± 9.16	34.16 ± 7.89
Elastic Modulus (MPa)	954.37 ± 334.35	1174.00 ± 447.08	1124.68 ± 372.23
Toughness (MPa)	1.310 ± 0.470	0.924 ± 0.347	0.714 ± 0.135

* vs. Normal
# vs. CKD (Vehicle)

Table 18. Whole Bone Mechanics

of treatment on stiffness. There also was no effect of raloxifene treatment on ultimate stress or elastic modulus, but the modulus of toughness was restored to normal levels (**Figure 33**).

Vertebral compression tests revealed that CKD animals had lower ultimate force and energy to ultimate force but no differences in stiffness compared to normal animals (**Figure 33** and **Table 18**). There also was no effect on estimated material properties of the vertebra. Compared to animals with CKD, raloxifene had no impact on any structural or estimated material properties in the vertebra.

Bone Material Properties

CKD-vehicle animals were indistinguishable from normal animals for indentation properties determined using reference point indentation, nanoindentation, and AFM indentation (**Table 19**). Raloxifene treatment significantly increased hardness (assessed by nanoindentation) compared to both normal and CKD-vehicle animals (**Table 19**). Tissue composition (assessed by Raman spectroscopy) and collagen crosslinking (assessed by HPLC) revealed no differences among the three groups (**Table 20**). Collagen D-periodic spacing was not affected by CKD, but animals treated with raloxifene had higher D-periodicity in the collagen fibrils compared to CKD animals (**Figure 34**). NMR spectroscopic measures revealed no differences among groups for bound or free water (**Table 20**).

RPI	Normal	CKD (Vehicle)	CKD (Raloxifene)
First Cycle Indentation Distance (μm)	71.13 ± 5.47	71.78 ± 5.43	69.28 ± 2.53
First Cycle Energy Dissipation (μJ)	225.69 ± 17.71	241.51 ± 27.87	219.15 ± 7.53
First Cycle Unloading Slope (N/μm)	0.441 ± 0.069	0.466 ± 0.047	0.446 ± 0.063
First Cycle Creep Indentation Distance (μm)	4.921 ± 0.450	5.396 ± 0.749	4.916 ± 0.241
Indentation Distance Increase (μm)	9.813 ± 0.692	11.726 ± 1.968	9.856 ± 0.281
Total Indentation Distance (μm)	77.23 ± 5.50	79.41 ± 4.90	75.51 ± 2.59
Total Energy Dissipation (μJ)	561.41 ± 37.24	594.58 ± 34.84	558.21 ± 15.86
Nanoindentation			
Elastic Modulus (GPa)	11.066 ± 2.766	9.666 ± 1.021	13.200 ± 3.345
Hardness (MPa)	202.62 ± 22.86	192.68 ± 47.35	422.81 ± 291.97 #

AFM Indentation			
Elastic Modulus (GPa)	52.99 ± 25.81	43.21 ± 16.31	49.25 ± 26.20

* vs. Normal
# vs. CKD (Vehicle)

Table 19. Material Properties – Mechanics

Raman Spectroscopy	Normal	CKD (Vehicle)	CKD (Raloxifene)
Crystallinity (1/FWHM $PO_4^{3-}\nu1$)	0.0529 ± 0.0003	0.0534 ± 0.0008	0.0535 ± 0.0005
Carbonate Substitution (CO_3^{2-} $\nu1$/ $PO_4^{3-}\nu1$)	0.247 ± 0.008	0.242 ± 0.013	0.239 ± 0.015
Relative Mineralization (PO_4^{3-} $\nu1$/Amide I)	2.650 ± 0.332	2.274 ± 0.501	2.384 ± .0422
Collagen Morphology			
D-Periodicity (nm)	65.321 ± 0.946	64.466 ± 1.391	65.438 ± 1.289 #
Collagen Cross-Linking			
Pyridinoline per Collagen (mol/mol)	0.474 ± 0.485	0.223 ± 0.087	0..305 ± 0.079
Deoxypyridinoline per Collagen (mol/mol)	0.372 ± 0.388	0.203 ± 0.095	0.271 ± 0.088
Pentosidine per Collagen (mmol/mol)	815.39 ± 621.34	507.06 ± 288.11	617.48 ± 171.46

NMR Spectroscopy			
Bound Water (%)	18.60 ± 3.61	17.88 ± 4.00	17.34 ± 3.43
Pore Water (%)	3.829 ± 0.988	5.572 ± 3.567	4.158 ± 0.965

* vs. Normal
# vs. CKD (Vehicle)

Table 20. Material Properties – Composition and Morphology

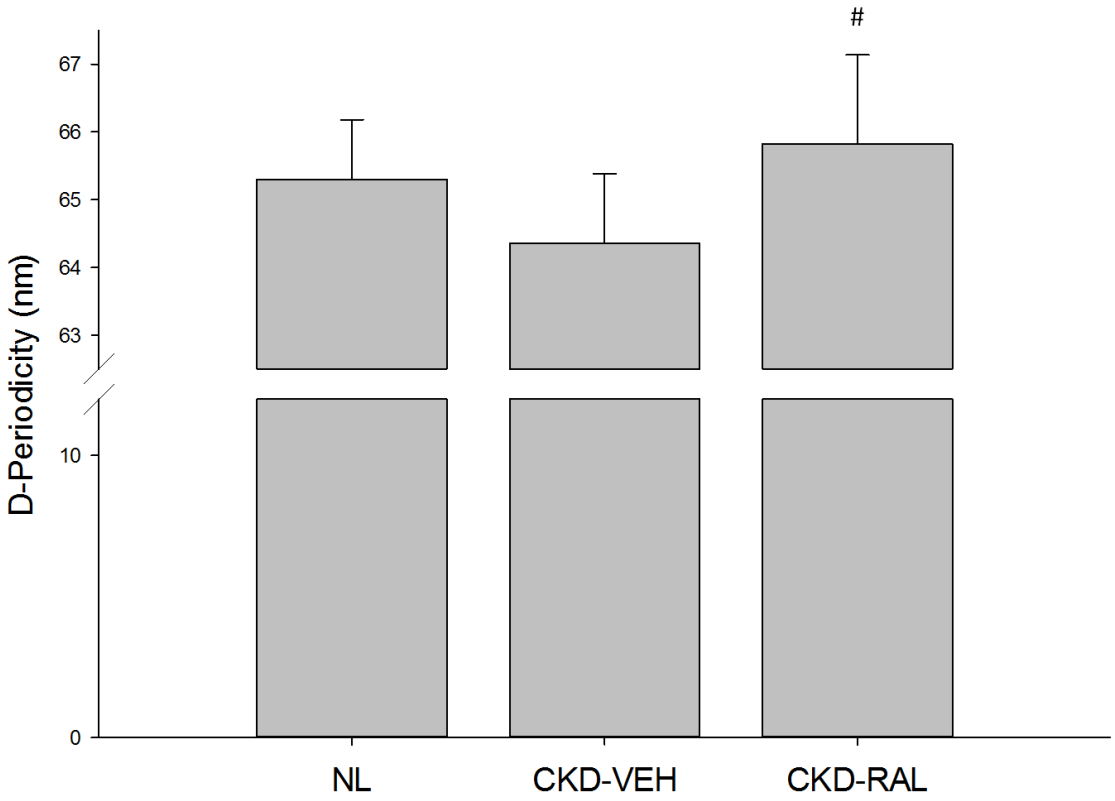

Figure 34. Collagen fibril D-periodic spacing as determined by AFM imaging. #, $p<0.05$ compared to CKD-VEH

Discussion

These data show that in the setting of progressive CKD with high bone turnover, raloxifene can suppress long bone and vertebral trabecular bone remodeling and enhance long bone mechanical properties to levels of normal controls. Nanoindentation also revealed that raloxifene substantially increased the hardness of cortical bone, while AFM imaging of collagen D-periodic spacing detected raloxifene-specific effects. These changes demonstrate that raloxifene can improve skeletal material properties (those independent of bone mass) as well as structural properties and that together these ameliorate CKD-associated deficits in whole bone mechanical properties.

Raloxifene led to an unexpected lowering of PTH in the CKD animals. Although PTH levels remained higher than normal, they were 43% lower than the untreated CKD animals. Previous studies have shown that reducing PTH levels in this animal model imparts significant skeletal benefits[108,119] (although in those studies, PTH levels were actually below normal levels). Nonetheless, because of this reduction in PTH, we cannot isolate the direct skeletal effects of raloxifene from changes associated with this reduction in PTH. Previous data have also shown that raloxifene may slow the progression of kidney failure in some settings[103-106], but few data exist on the relationship between raloxifene and PTH[292]. Based on the BUN assessment in the current study, raloxifene does not appear to have any beneficial renal effects in this model, though more extensive histopathology assessments would be necessary to make definitive conclusions.

Raloxifene effectively suppressed the high bone formation rates induced by CKD to the level of normal animals. This normalization of remodeling is in contrast to previous work in the same model using bisphosphonates and calcium, both of which suppressed remodeling in trabecular bone to below normal levels[108,119]. Due to concerns of dramatic suppression of bone remodeling in patients with CKD, the suppression observed with raloxifene may be advantageous. Unexpectedly, osteoclast number and percent osteoclast surface remained high in raloxifene-treated animals. Although raloxifene is typically associated with suppressed osteoclast formation, reduced osteoclast activity without a reduction in number has been shown to occur[293-294]. In this model of hyperparathyroidism, the high levels of PTH may overshadow raloxifene's effect on osteoclast formation with its effect on the activity of mature osteoclasts becoming more pronounced.

Though raloxifene-induced improvements were observed in trabecular bone volume, there was little effect on the CKD-induced changes to cortical bone morphology. Untreated CKD animals had compromised mechanical properties of the long bones, consistent with previous studies in this model[108,119]. Raloxifene normalized energy to fracture, restoring it to the level of normal animals. Estimated material properties indicate that raloxifene specifically improved material-level toughness. These effects were absent in the vertebra. Because vertebral compression testing ceases at the ultimate load, information regarding whole bone and material-level toughness may be limited.

To make more direct assessments of cortical bone material properties, several indentation measurements were conducted at various length scales. Of these, raloxifene had positive effects on hardness as measured by nanoindentation. Though hardness is generally believed to be a byproduct of mineralization, these data indicate that hardness is not determined by mineralization alone. In addition, these data are consistent with previous observations that raloxifene increased hardness in murine and ovine ovariectomy models[295-296]. While it is not clear how improving material-level hardness leads to increases in the modulus of toughness and energy to fracture, all of these changes have been previously observed in animals treated with raloxifene[97-98,101,295-296].

Previous studies have revealed that raloxifene improvements in material properties are associated with higher bound water in the extracellular matrix[101-102]. The current NMR data are inconsistent with these previous data because they revealed no effect on bound water in raloxifene-treated animals. The reason for this discrepancy is unclear. For example, CKD-associated changes in bone metabolism may prevent raloxifene from impacting bound water in these animals. Differences in animal models (dogs were used in previous studies) may be a factor as well[101-102]. These differences may also reflect variations in the magnetic resonance techniques across these studies[101-102].

Rather than changes in hydration, the current work showed that raloxifene increased collagen fibril spacing (D-periodicity). This effect is consistent with previous work using raloxifene[101], though the exact contribution of D-periodicity

to whole bone mechanical properties remains unclear. Previous studies have shown decreased D-periodic spacing in animals with reduced energy to fracture[297-298]. This work improves the current understanding of D-periodicity by showing that increases in D-periodicity are associated with improved bone toughness. Because of the failure to clearly understand how changes in D-periodicity are related to hardness and how these contribute to whole bone mechanical properties, subtler differences in material properties may be present. After all, several indentation tests failed to detect changes, and the examination of tissue composition and collagen cross-linking failed to provide a compelling explanation. These data indicate that raloxifene's impact on D-periodicity may be having a more prominent impact on the interaction between collagen fibrils and mineral crystals[101], an interaction not addressed in the present study.

Most clinical data examining raloxifene's use in CKD are derived from trials that inadvertently enrolled patients with mild CKD[236]. Like their osteoporosis counterparts, CKD patients treated with raloxifene had a lower rate of vertebral fractures as well as increased BMD at the hip and spine. Far fewer data exist for patients with late stage disease due to their exclusion from osteoporosis trials. One small study examined BMD in patients on dialysis and showed that raloxifene improved BMD in the spine but not in the hip[106]. Another study examined BMD at the distal radius and found that raloxifene improved BMD in patients with mild hyperparathyroidism[299]. Despite these data, there have been no assessments of fracture efficacy using raloxifene in CKD. Because the current study suggests significant mechanical benefits despite modest changes in bone

mass, the positive effects of raloxifene may be overlooked if BMD alone is used to determine efficacy.

The current results support previous recommendations[60] that clinical trials using raloxifene in patients with late stage CKD should be considered. However, they also highlight the fact that measures of bone beyond BMD may be needed to truly assess efficacy. Recent techniques assessing bone quality have been developed for and examined in humans (ultrashort echo time magnetic resonance imaging[159] and reference point indentation[121,123]). These, alongside BMD, may provide a better picture of the potential efficacy of raloxifene in patients with advanced kidney disease. Because there are concerns about the increased risk of thromboembolism (though it was not worse than the general population in the post-hoc analyses [34]), late stage predialysis patients might be the most logical population to examine first.

In summary, these analyses show that raloxifene reduced bone turnover and improved whole bone mechanical properties in the setting of CKD. Because these changes occurred mostly independently of changes in bone mass, traditional methods to evaluate efficacy in CKD bone disease may be insufficient for the evaluation of raloxifene in these patients.

CHAPTER 9

DISCUSSION

Summary

The current series of studies was conducted to better understand the effects of CKD on skeletal properties and to examine the specific structural and mechanical effects of multiple agents currently used or being considered for use in patients with CKD. Understanding the multiple factors that lead to fracture in CKD, and how these are affected (or not) by treatment, is an important step currently missing in much of the CKD literature.

Animals with progressive kidney disease were examined at two different times for the presence of abnormalities in tissue-level mechanical properties and tissue composition. Material-level mechanical effects were present by 30 weeks (both apparent material properties and directly measured properties), though the exact cause of these changes was not definitively identified. At this age, there were no disease-driven changes in bone matrix hydration, collagen cross-linking, tissue composition, or collagen morphology. Yet, AFM indentation revealed substantial heterogeneity in nanoscale mechanical properties (elastic modulus), indicative of a change in matrix mechanics. One potential explanation for the mechanical changes, despite no change in mineral, collagen, or hydration, could be that each technique on its own could not detect subtle change present at this point. At 35 weeks, changes in bone matrix hydration and collagen cross-linking were present and likely contributed significantly to the whole bone defects in mechanical properties detected in those animals. Given the lack of difference in

Raman-based mineral assessments, these data suggest negative changes in the organic matrix and hydration are driving the mechanical phenotype in CKD. This is supported by the fact that these two variables are both specifically linked to changes in bone toughness, one of the properties specifically impacted by CKD bone disease.

Patients with CKD and secondary hyperparathyroidism are currently treated with calcitriol and other active vitamin D analogues. Treatment efficacy is based primarily upon changes in serum PTH levels. Yet, there are few studies that have examined bone outcomes related to PTH suppression in CKD patients or even CKD animals. In an effort to better understand how current therapy affects CKD bone disease, animals with secondary hyperparathyroidism (PTH levels 12-fold higher than normal) were treated with a dose of calcitriol sufficient to provide 50% suppression of PTH levels (considered clinically efficacious). Though PTH was suppressed, there were no positive skeletal effects observed in animals with CKD despite a fairly comprehensive skeletal evaluation (imaging, histology, mechanics, material-level assessment of collagen and mineral). Because of the paucity of clinical data examining skeletal outcomes of calcitriol on CKD bone disease in humans, future studies (both clinical and preclinical) will need to examine various levels of PTH suppression and its impact on skeletal parameters and fracture risk to assess whether the currently recommended levels of PTH suppression actually have the intended effects on skeletal outcomes.

Suppression of PTH levels with calcium supplementation in drinking water had substantial positive skeletal effects, essentially normalizing skeletal properties. In contrast to calcitriol treatment, calcium supplementation led to PTH values below normal controls. Unfortunately, the skeletal effectiveness occurred at the cost of increased vascular calcification. These data are consistent with concerns raised about the use of calcium supplementation and calcium-based phosphate binders in late stage CKD patients. The level of PTH suppression in these studies to levels at or even below normal controls is uncommon clinically, meaning that it remains possible that some level of PTH suppression between that of calcium (below normal) and calcitriol (about 60% of CKD) could provide the optimal balance of bone efficacy without vascular complications. This balance is also important as it strikes a skeletal balance between the high bone turnover in secondary hyperparathyroidism and the concerns of low bone turnover that may result from oversuppressing PTH. In addition, the combination of calcium with zoledronic acid and anti-sclerostin antibody, agents that provide no PTH-lowering effects on their own, provided some additive structural and mechanical effects. This clearly highlights the idea that the evaluation of osteoporosis treatments in CKD needs to be done in a setting where PTH is controlled to near normal levels.

Zoledronic acid, a high affinity bisphosphonate with significant benefits in osteoporosis[78], was mostly ineffective in these CKD experiments. While it suppressed trabecular bone remodeling, cortical porosity remained high, and whole bone structural and mechanical properties were no different than untreated

CKD animals. One possible reason for this unexpected result is the dosing schedule utilized (one injection every five weeks based upon effective dosing in ovariectomized rats[293]). While this dosing schedule is effective in an osteoporosis setting it appears insufficient in the setting of CKD. Normally upon dosing, bisphosphonates cover the bone surface and inhibit osteoclasts that come into contact with the bone surface. In the setting of drastic hyperparathyroidism associated with CKD (**Figure 35**), there may be enough osteoclast production such that once several osteoclasts deplete the surface of bisphosphonates, subsequent osteoclasts begin to resorb the bone normally as though the bone were in an untreated state. Daily or weekly bisphosphonates may be a means to overcome this problem because more frequent administration would continuously cover any surfaces depleted by high levels of osteoclast activity. On the other hand, though zoledronate did result in efficient suppression of bone resorption in cancellous bone, there was no additional detriment observed in CKD animals with zoledronate beyond the significant deterioration already present.

For anabolic therapy, teriparatide (recombinant human PTH) is currently the only approved agent for patients with osteoporosis. However, the existence of high PTH in late stage CKD patients often precludes its application. Given the early increases in sclerostin that occur in CKD, though, the experimental anti-sclerostin antibody seemed like a promising approach. Unfortunately, as was the case with zoledronate, anti-sclerostin antibody was only effective in the setting of calcium-driven PTH suppression. As expected, it led to higher bone formation rates and a decline in stiffness, both of which are consistent with the formation of

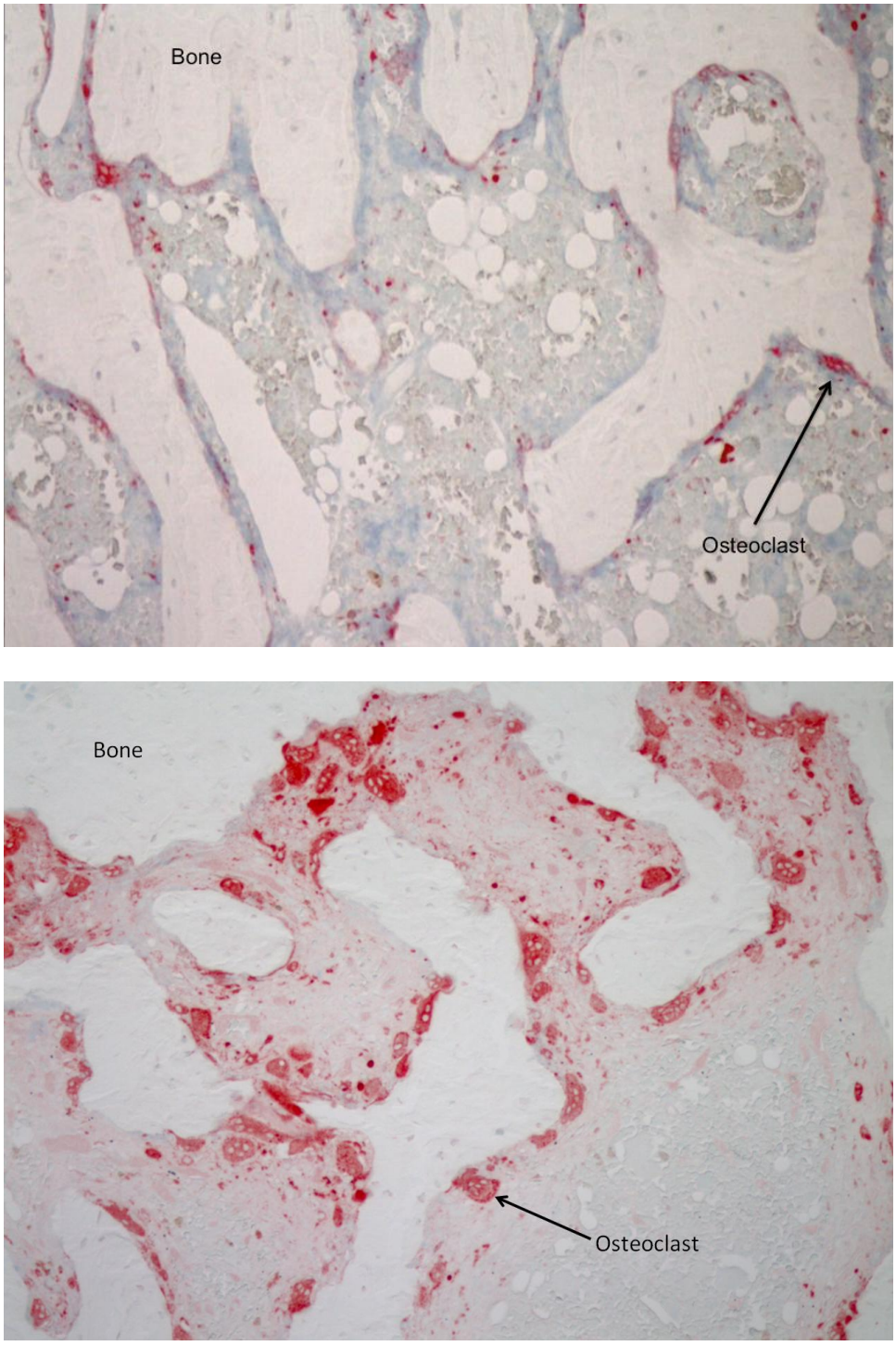

Figure 35. Differences in osteoclast surface coverage in normal animals (top) and animals with CKD (bottom).

new osteoid. On its own, there was no improvement in cortical bone mass or trabecular architecture, and mechanical properties were identical to untreated animals. This highlights the importance of bone quality, as even in the presence of adding new matrix, the biomechanical properties of the bone remain compromised. Simply adding bone in CKD patients is insufficient.

Raloxifene, on the other hand, though surrounded by a cloud of questions regarding efficacy and safety (e.g., thrombosis) had a substantial impact on bone parameters in CKD animals. It corrected cancellous bone loss in both the tibia and vertebra secondary to its normalization of bone formation rates in CKD animals. Whether these changes in bone remodeling persist to 35 weeks when more severe disease is present will need to be examined. Aside from remodeling, raloxifene also improved long bone structural and apparent material toughness. These changes were associated with microscale changes in hardness and higher D-periodicity in collagen fibrils, which may be responsible for raloxifene's positive influence on toughness. More data will need to be collected to better understand raloxifene's mechanism of action and whether or not it differs in CKD compared to the other animal models in which it has been examined.

Clinical Implications

The value of understanding the impact of bone quality on fracture risk is ultimately dictated by the ability of current clinical methods to adequately predict fracture. This is why recent studies examining BMD in CKD patients have been

so important. While BMD only predicts around 70% of fractures in these late stage patients, the actual contribution of bone quality to CKD-related fractures is still unknown.

While there have been conflicting data regarding BMD in CKD, studies over the last few years appear to indicate that BMD at all stages of CKD does indeed have a predictive impact on fracture risk[34-36,45]. The data in early stage CKD patients are hardly surprising and are consistent with recommendations that these patients should be treated as though they were osteoporosis patients. The later stage data are more intriguing as these most recent studies are the first to show a clear predictive relationship between BMD and fracture risk[34,45]. In fact, these studies indicate that the KDIGO guidelines (which do not recommend BMD estimates in these patients) may need to be adjusted.

With this predictive capacity available to clinicians, what value does bone quality have in the clinical discussion? Unfortunately, even the best predictors have only accounted for 70% of the fractures in this population. Determining the value of BMD estimates in individual patients is even more problematic. Therefore, future studies will need to examine aspects of bone quality in these patients to understand its role in fracture risk. While there are no currently approved diagnostics used in CKD, newly developed methods using UTE-MRI (to measure bone hydration) and *in vivo* mechanical testing devices (reference point indentation devices such as BioDent and OsteoProbe) may provide a means by which to assess bone quality clinically. Because RPI was able to detect differences in CKD versus normal animals in the current work (but see

Table 5), and bone matrix hydration appears to be altered in later stages of CKD, these two aspects of bone quality could provide important data in combination with BMD. MRI techniques have already been applied to late stage CKD patients[159]. In addition, recent studies using OsteoProbe in diabetic patients have shown that it can detect differences in bone quality when compared to normal patients. This is important as this population has a high risk of progressing to late stage CKD (17% of the diabetes group in this study had co-existing kidney disease). Because of these findings, CKD may be an important conduit by which to employ these methods in future clinical studies.

Despite calcitriol being the standard of care in CKD patients with secondary hyperparathyroidism, the current studies indicate that its suppression of PTH may not translate to useful skeletal outcomes in CKD patients. While some clinical studies indicate that calcitriol may suppress bone formation (in contrast to the current studies), fracture data are unavailable. On the other hand, recent studies indicate that cinacalcet not only suppresses PTH effectively[66] but also lead to a reduction in fractures[65]. Future studies should examine the level of PTH suppression necessary to reduce fractures risk and other adverse metabolic outcomes in patients with late stage CKD.

Though zoledronate and anti-sclerotin antibody were ineffective on their own (and only modestly effective when combined with calcium), significant questions about their utility in CKD still remain. Also, their utility in patients with hyperparathyroidism may be substantially different than their use in patients with controlled PTH levels. First, though, more studies need to be performed to

determine dosing regimen for these agents. The assumption that dosage approaches (amount and frequency) based on osteoporosis are appropriate has been significantly challenged by these animal studies.

In terms of safety, the current studies indicate that bisphosphonates did effectively suppress trabecular bone turnover rates to at or below the levels of normal controls. This is consistent with many of the clinical concerns about the oversuppression of bone remodeling. Because some remodeling remained intact, it is not clear if the fear of adynamic bone disease in the context of bisphosphonate therapy is warranted. However, while mechanical properties were not improved with zoledronate, no further detrimental effects were observed either, which is what might be expected if low bone turnover does have detrimental effects in these patients. Fracture studies need to be conducted before any definitive connection between low bone remodeling from bisphosphonates and fracture risk outweigh the possible benefits from inhibiting parathyroid hormone and increasing bone mass (though these changes were not observed in the current studies).

Raloxifene has had a varied history in treating osteoporosis. While patients show mild increases in BMD, the fracture efficacy (predominantly in the vertebrae) is much greater than would be predicted from BMD changes alone. In fact, this small effect on BMD has likely led to its diminished use in patients with osteoporosis. After all, small changes in BMD are difficult to interpret in the absence of considerations of bone quality, especially when one considers that bisphosphonates increase BMD by ~10%. While the minimal data available in

patients with CKD indicate similar outcomes of BMD, there has been great hesitation related to its efficacy as well as concerns over thrombosis[61]. While post-hoc analyses of early stage CKD patients receiving raloxifene did not show any differences in thrombotic events between patients with and without CKD, the introduction of catheters in dialysis patients presents great concerns. Hence, pragmatism would indicate that future studies ought to occur in late stage (stages 3 and 4) predialysis patients, particularly in the setting of hyperparathyroidism. Histomorphometry data will be important to determine if there are differences in efficacy in patients with high turnover disease and those with low turnover disease and may provide helpful information for determining whether there is a place for considering combination therapy with agents that suppress PTH. Any studies with raloxifene should include the aforementioned tools used to assess bone quality since raloxifene's primary impact appears to be on skeletal material properties.

Future Studies

The current results answer several important questions about CKD but also lead to several more questions. The studies described herein focused on CKD-induced bone quality changes of cortical bone. Bone quality in cancellous bone is currently understudied. Examining these features would address much of the data suggesting a discord between how CKD impacts cortical sites and trabecular sites determining if the differences are simply due changes in mass or in quality as well. Furthermore, differences in cortical and cancellous bone need

to be understood within the contexts of quality changes in existing bone and the disease effects that compromise the accumulation of newer bone. After all, most cortical bone is formed in these animals prior to the onset of advanced CKD. In these rodents, employing a series of dynamic labels would allow for the comparison of material properties across multiple tissue ages in cortical bone. This would provide important insight into whether CKD is predominantly impacting new bone formation or whether it is also significantly compromising bone that has already been formed.

Secondly, the use of rodent models in a disease that preferentially impacts cortical bone is limited. Studies employing larger animal models that normally undergo intracortical remodeling would be important. Unfortunately, since there are no naturally occurring large animal models of CKD, nephrectomy approaches would be necessary. While this would present many of the same difficulties discussed regarding rodent nephrectomy models, it would potentially provide a better cortical bone assessment than currently available. It would allow for the assessment of *in vivo* microdamage, intracortical remodeling, and provide more controlled assessments of bone material properties with a greater availability of skeletal tissue.

Future studies of calcitriol should focus on dosing in order to determine the necessary level of PTH suppression to impart positive skeletal effects. Also, given the relationship between serum $1,25[OH]_2D_3$ levels and bone formation[294], serum vitamin D levels should be assessed. In any such work, bone outcomes similar to those examined in the current study should be employed to provide a

comprehensive assessment of bone quality and bone quantity. A comparative study between calcium and calcitriol would be interesting given the results described in these studies. Finally, only one study has employed cinacalcet (R568) in the current animal model, and its effect on bone outcomes was modest. It too would make for an appropriate comparison in these proposed studies.

In the area of bisphosphonates, a number of studies should be pursued. These could address potential variations in bone binding affinity as well as dosing frequency. To further examine zoledronate's ineffectiveness with the single dose regimen used in the current studies, a five-week dosing regimen with radiolabeled zoledronate would provide data as to the degree of binding and retention on the bone surface. If it is the case that rampant osteoclast activity associated with secondary hyperparathyroidism actually depletes the surface of bisphosphonates, several alternative approaches could be taken to facilitate bisphosphonate use in CKD. First, a higher dosing frequency using zoledronic acid could be enacted. For example, in these studies, zoledronate was given every five weeks based on its effectiveness in other osteoporosis models. A dosing frequency of every two weeks might be a logical next step to examine its effectiveness in this model. After all, even raloxifene, which is a very mild anti-remodeling agent, appeared to have positive effects on remodeling and bone structure, potentially due to its daily administration. An alternative to weekly or bi-weekly zoledronate doses (which is not a standard clinical dosing regimen) would be daily or weekly alendronate. These types of studies are essential as the

determination of efficacy and safety necessitates an assessment in which the drug is binding to the surface and inhibiting osteoclasts as intended. If, even with the intended inhibition of osteoclasts, mechanical properties are not preserved, then this class of agents may not be sufficient for use in the setting of CKD.

Additional work is warranted for raloxifene. As animals with CKD show dramatic changes in bone properties from 30 weeks to 35 weeks, the promising results for raloxifene at 30 weeks should be further examined at 35 weeks. Such studies would be important for examining raloxifene's efficacy in more severe disease. Because of the implications of suppressing PTH, raloxifene should also be employed in combination with calcitriol or calcimimetics. More examination will also need to be given to the mechanism by raloxifene alone suppresses PTH. Because raloxifene has been shown to have positive skeletal outcomes in larger mammal models with intracortical remodeling, these studies should also be considered in large mammal CKD models.

Clinical studies should focus on assessments of raloxifene alone or in combination with other agents that suppress PTH activity. Specific outcomes should include BMD (including HR-pQCT), RPI (OsteoProbe), and UTE-MRI studies, though fracture assessment would be the ideal outcome. In addition, the acquisition of biopsy samples for histology may also provide samples for other bone quality assessments. Specifically, these studies could employ Raman spectroscopy for compositional analysis, nanoindentation, and HPLC. Because controls would be difficult to obtain, baseline measures could be used from one hip with the contralateral hip serving as the endpoint sample. These analyses

would provide almost identical outcomes to those examined in these studies, providing the strongest link to how well these studies conducted in Cy/+ rats would translate to humans with CKD.

Conclusion

Using an animal model of progressive CKD, significant defects in bone quality were detected. These data may help explain the dramatic fracture risk associated with CKD. While calcitriol is the current standard of care in secondary hyperparathyroidism, these results raise questions about how well the partial suppression of PTH actually impacts fracture risk since there was no benefit to mechanical properties. Anti-resorptives and anabolic osteoporosis therapies may still have potential, but the administration of these medications in the absence of PTH control did not normalize mechanical properties in the setting of CKD. Finally, raloxifene was shown to improve whole bone mechanical properties by virtue of its impact on the inherent material properties of CKD bone. These studies, taken as a whole, call for the assessment of bone quality in CKD patients as well as a renewed consideration of the role of raloxifene in treating patients with bone abnormalities secondary to late stage CKD.

REFERENCES

1. Go AS et al. (2004). Chronic kidney disease and the risks of death, cardiovascular events, hospitalization. New Engl J Med 351:1296-1305.
2. Coresh J et al. (2007). Prevalence of chronic kidney disease in the United States. JAMA 298:2038-2047.
3. Ortiz A et al. (2014). Epidemiology, contributors to, and clinical trials of mortality risk in chronic kidney failure. Lancet 383:1831-1843.
4. Taal MW, Brenner BM (2006). Predicting initiation and progression of chronic kidney disease: developing renal risk scores. Kidney Int 70:1694-1705.
5. Eknoyan et al. (2004). The burden of kidney disease: improving global outcomes. Kidney Int 66:1310-1314.
6. Levey AS, Coresh J (2012). Chronic kidney disease. Lancet 379:165-180.
7. Bargmann JM, Skorecki K (2012). Chronic kidney disease. In: Harrison's Principles of Internal Medicine (18th ed.), edited by Longo DL, Fauci AS, Kasper DL, Hauser SL, Jameson JL, Loscalzo J. New York: McGraw Hill.
8. Levey AS et al. (2005). Definition and classification of chronic kidney disease: a position statement from Kidney Disease Improving Global Outcomes (KDIGO). Kidney Int 67:2089-2100.
9. Levin A et al. (2007). Prevalence of abnormal serum vitamin D, PTH, calcium, and phosphorus in patients with chronic kidney disease: results of the study to evaluate early kidney disease. Kidney Int 71:31-38.
10. Atscejkumi K et al. (1999). Risk factors for vertebral fractures in renal osteodystrophy. Am J Kidney Dis 33:287-293.
11. Alem et al. (2000). Increased risk of hip fracture among patients with end-stage renal disease. Kidney Int 58:396-399.11
12. Ball AM et al. (2002). Risk of hip fracture among dialysis and renal transplant recipients. JAMA 288:3014-3018.
13. Mittalhenkle A, Gillen DL, Stehman-Breen CO (2004). Increased risk of mortality associated with hip fracture in the dialysis population. Am J Kidney Dis 44:672-679.
14. Nickolas TL, McMahon DJ, Shane E (2006). Relationship between moderate to severe kidney disease and hip fracture in the United States. J Am Soc Nephrol 17:3223-3232.
15. Fried LF et al. (2007). Association of kidney function with incident hip fracture in older adults. J Am Soc Nephrol 18:282-286.
16. Dooley AC, Weiss NS, Kestenbaum B (2008). Increased risk of hip fracture among men with CKD. Am J Kidney Dis 51:38-44.
17. Nickolas TL, Leonard MB, Shane E (2008). Chronic kidney disease and bone fracture: a growing concern. Kidney Int 74:721-731.
18. Nitsch D et al. (2009). Chronic kidney disease and hip-fracture-related mortality in older people in the UK. Nephrol Dial Transplant 24:1539-1544.
19. Kansal S, Fried L (2010). Bone disease in elderly individuals with CKD. Adv Chronic Kidney D 17:e41-e51.

20. DiMeglio LA, Imel EA (2014). Calcium and phosphate: hormonal regulation and metabolism. In: Basic and Applied Bone Biology, edited by Allen MR, Burr BD. New York: Academic Press.
21. Moe SM, Sprague SM (2011). Chronic kidney disease—mineral bone disorder. In: Brenner and Rector's The Kidney (8th ed.), edited by Taal MW, Chertow GM, Mardsen PA, Scorecki K, Yu ASL, Brenner BM. Philadelphia: Elsevier.
22. Bricker NS, Morrin PA, Kime SW Jr (1960). The pathologic physiology of chronic Bright's disease: an exposition of the "intact nephron hypothesis." Am J Med 28:77-98.
23. Bricker NS (1972). On the pathogenesis of the uremic state: an exposition of the "trade-off hypothesis." N Engl J Med 286:1093-1099.
24. Ben-Dov IZ et al. (2007). The parathyroid is a target organ for FGF23 in rats. J Clin Invest 117:4003-4008.
25. Krajisnik T et al. (2007). Fibroblast growth factor-23 regulates parathyroid hormone and 1alpha-hydroxylase expression in cultured bovine parathyroid cells. J Endocrinol 195:125-131.
26. Hruska et al. (2007). Phosphorus metabolism and management in chronic kidney disease: renal osteodystrophy, phosphate homeostasis, and vascular calcification. Semin Dialysis 20:309-315.
27. Goodman WG (2004). The consequences of uncontrolled secondary hyperparathyroidism and its treatment in chronic kidney disease. Semin Dialysis 17:209-216.
28. Bellido T et al. (2005). Chronic elevation of parathyroid hormone in mice reduces expression of sclerostin by osteocytes: a novel mechanism for hormonal control of osteoblastogenesis. Endocrinology 146:4577-4583.
29. Fraser WD (2009). Hyperparathyroidism. Lancet 374:145-158.
30. Tentori et al. (2013). High rates of death and hospitalization follow bone fracture among hemodialysis patients. Kidney Int 85:166-173.
31. Nickolas TL et al. (2010). Bone mass and microarchitecture in CKD patients with fracture. J Am Soc Nephrol 21:1371-1380.
32. Vu TDT et al. (2013). New insights into the effects of primary hyperparathyroidism on the cortical and trabecular compartments of bone. Bone 55:57-63.
33. Cejka D et al. (2011). Bone microarchitecture in hemodialysis patients assessed by HR-pQCT. Clin J Am Soc Nephrol 6:2264–71.
34. West SL et al. (2014). Bone mineral density predicts fractures in chronic kidney disease. J Bone Miner Res [10.1002/jbmr.2406].
35. Jassal SK, von Muhlen D, Barrett-Connor E (2007). Measures of renal function, BMD, bone loss, and osteoporotic fracture in older adults: the Rancho Bernardo study. J Bone Miner Res 22:203-210.
36. Iimori S et al. (2012). Diagnostic usefulness of bone mineral density and biochemical markers of bone turnover in predicting fracture in CKD stage 5D patients—a single-center cohort study. Nephrol Dial Transplant 27:345-351.

37. Klawansky S et al. (2003). Relationship between age, renal function and bone mineral density in the US population. Osteoporos Int 14:570-576.
38. Nickolas TL et al. (2011). Discriminants of prevalent fractures in chronic kidney disease. J Am Soc Nephrol 22:1560-1572.
39. Jamal SA et al. (2012): Bone mineral density by DXA and HR pQCT can discriminate fracture status in men and women with stages 3 to 5 chronic kidney disease. Osteoporos Int 23:2805-2813.
40. Jamal SA, Hayden JA, Beyene J (2007). Low bone mineral density and fractures in long-term hemodialysis patients: a meta-analysis. Am J Kidney Dis 49:674-681.
41. Yamaguchi T et al. (1996). Retrospective study on the usefulness of radius and lumbar bone density in the separation of hemodialysis patients with fractures from those without fractures. Bone 19:549–555.
42. Piraino B et al. (1988). Fractures and vertebral bone mineral density in patients with renal osteodystrophy. Clin Nephrol 30:57-62.
43. Yenchek RH et al. (2012). Bone mineral density and fracture risk in older individuals with CKD. Clin J Am Soc Nephrol 7:1130-1136.
44. Nickolas TL (2012). BMD and fracture risk in CKD: where should we go from here? Clin J Am Soc Nephrol 7:1058-1060.
45. Bucur RC et al. (2015). Low bone mineral density and fractures in stages 3–5 CKD: an updated systematic review and meta-analysis. Osteoporosis Int 26:449-458.
46. Seeman E, Delmas PD (2006). Bone quality: the material and structural basis of bone strength and fragility. N Engl J Med 354:2250-2261.
47. Turner CH, Burr DB (2002). Experimental techniques for bone mechanics. In: Bone Mechanics Handbook, edited by Cowin SC. Boca Raton: CRC Press.
48. Malluche HH, Porter DS, Pienkowski D (2013). Evaluating bone quality in patients with chronic kidney disease. Nat Rev Nephrol 9:671-680.
49. Shobeiri N, Adams MA, Holden RM (2010). Vascular calcification in animal models of CKD: a review. Am J Nephrol 31:471-481.
50. Kadokawa S et al. (2011). Assessment of trabecular bone architecture and intrinsic properties of cortical bone tissue in a mouse model of chronic kidney disease. J Hard Tissue Biol 20:79-86.
51. Iwasaki Y et al. (2013). Accumulated uremic toxins attenuate bone mechanical properties in rats with chronic kidney disease. Bone 57:477-483.
52. Nagao S et al. (2012). Animal models for human polycystic kidney disease. Exp Anim Tokyo 61:477-488.
53. Moe SM et al. (2009) A rat model of chronic kidney disease-mineral bone disorder. Kidney Int 75:176-184.
54. Nagao S et al. (2010). Polycystic kidney disease in Han:SPRD Cy rats is associated with elevated expression and mislocalization of SamCystin. Am J Physiol Renal Physiol 299:F1078-F1086.
55. Stagner EE et al. (2009). The polycystic kidney disease-related proteins Bicc1 and SamCystin interact. Biochem Bioph Res Co 383:16-21.

56. Hoff S et al. (2013). ANKS6 is a central component of a nephronophthisis module linking NEK8 to INVS and NPHP3. Nat Genet 45:951-956.
57. Nickolas TL et al. (2013). Rapid cortical bone loss in patients with chronic kidney disease. J Bone Miner Res 28:1811-1820.
58. Moe SM et al. (2010). A randomized trial of cholecalciferol versus doxercalciferol for lowering parathyroid hormone in chronic kidney disease. Clin J Am Soc Nephrol 5:299-306.
59. Charytan et al. (2005). Cinacalcet hydrochloride is an effective treatment for secondary hyperparathyroidism in patients with CKD not receiving dialysis. Am J Kidney Dis 46:58-67.
60. KDIGO (2009). Clinical practice guidelines for the management of CKD–MBD. Kidney Int 76:S1-S130.
61. Ott SM (2013). Therapy for patients with CKD and low bone mineral density. Nat Rev Nephrol 9:681-692.
62. Kandula P et al. (2011). Vitamin D supplementation in chronic kidney disease: a systematic review and meta-analysis of observational studies and randomized control trials. J Am Soc Nephrol 6:50-62.
63. Palmer SC et al. (2009). Vitamin D compounds for people with chronic kidney disease not requiring dialysis. Cochrane DB Syst Rev 4:CD008175.
64. Moorthi RN, Kandula P, Moe SM (2011). Optimal vitamin D, calcitriol, and vitamin D analog replacement in chronic kidney disease: to D or not to D? That is the question. Curr Opin Nephrol Hy 20:354-359.
65. Moe SM et al. (2014). Effects of cinacalcet on fracture events in patients receiving hemodialysis: the EVOLVE trial. J Am Soc Nephrol [doi: 10.1681/ASN.2014040414].
66. EVOLVE Trial Investigators et al. (2012). Effect of cinacalcet on cardiovascular disease in patients undergoing dialysis. N Engl J Med 367:2482-2494.
67. Moe SM, Thadhani R (2013). What have we learned about CKD-MBD from the EVOLVE and PRIMO trials? Curr Opin Nephrol Hypertens 22:651-655.
68. Sharma A et al. (2014). Cost effectiveness of paricalcitol versus cinacalcet with low-dose vitamin D for management of secondary hyperparathyroidism in haemodialysis patients in the USA. Clin Drug Investig 34:107-115.
69. Bischoff-Ferrari HA et al. (2005). Fracture prevention with vitamin D supplementation: a meta-analysis of randomized controlled trials. JAMA 293:2257-2264.
70. Peppone LJ et al. (2010). The efficacy of calcitriol therapy in the management of bone loss and fractures: a qualitative review. Osteoporos Int 21:1133-1149.
71. Faugere MC et al. (1986). Calctriol corrects bone loss induced by oophorectomy in rats. Am J Physiol 250:E35-38.

72. Tanaka Y et al. (1996). Effects of a synthetic vitamin D analog, ED-71, on bone dynamics and strength in cancellous and cortical bone in prednisolone-treated rats. J Bone Miner Res 11: 325-336.
73. Shiraishi A et al. (1999). The advantage of alfacalcidol over vitamin D in the treatment of osteoporosis. Calcif Tissue Int 65:311-316.
74. Shiraishi A et al. (2000). Alfacalcidol inhibits bone resorption and stimulates formation in an ovariectomized rat model of osteoporosis: distinct actions from estrogen. J Bone Miner Res 15:770-779.
75. Ke HZ et al. (2005). A new vitamin D analog, 2MD, restores trabecular and cortical bone mass and strength in ovariectomized rats with established osteopenia. J Bone Miner Res 20:1742-1755.
76. McClung M et al. (2013). Bisphosphonate therapy for osteoporosis: benefits, risks, and drug holiday. Am J Med 126:13-20.
77. Shane E et al. (2014), Atypical subtrochanteric and diaphyseal femoral fractures: second report of a task force of the American Society for Bone and Mineral Research. J Bone Miner Res 29:1–23.
78. Bilezikian JP (2009). Efficacy of bisphosphonates in reducing fracture risk in postmenopausal osteoporosis. Am J Med 122(5 Suppl):S14-S21.
79. Miller PD et al. (2005). Safety and efficacy of risedronate in patients with age-related reduced renal function as estimated by the Cockcroft and Gault method: a pooled analysis of nine clinical trials. J Bone Miner Res 20:2105-2115.
80. Jamal SA et al. (2007). Alendronate treatment in women with normal to severely impaired renal function: an analysis of the fracture intervention trial. J Bone Miner Res 22:503-508.
81. Andress DL (2008). Adynamic bone in patients with chronic kidney disease. Kidney Int 73:1345-1354.
82. London GM et al. (2004). Arterial calcifications and bone histomorphometry in end-stage renal disease. J Am Soc Nephrol 15:1943-1951.
83. Tomiyama C et al. (2010). Coronary calcification is associated with lower bone formation rate in CKD patients not yet in dialysis treatment. J Bone Miner Res 25:499-504.
84. Barreto DV et al. (2008). Association of changes in bone remodeling and coronary calcification in hemodialysis patients: a prospective study. Am J Kidney Dis 52:1139-1150.
85. Asci et al. (2011). The link between bone and coronary calcifications in CKD-5 patients on hemodialysis. Nephrol Dial Transplant 26:1010-1015.
86. Bover J et al. (2014). Adynamic bone disease: from bone to vessels in chronic kidney disease. Semin Nephrol 34:626-640.
87. Amerling R et al. (2010). Bisphosphonate use in chronic kidney disease: association with adynamic bone disease in a bone histology series. Blood Purif 29:293-299.
88. Neer et al. (2001). Effect of parathyroid hormone (1-34) on fractures and bone mineral density in postmenopausal women with osteoporosis. New Engl J Med 10:1434-1431.

89. Bodenner D, Redman C, Riggs A (2007). Teriparatide in the management of osteoporosis. Clin Interv Aging 2:499-507.
90. McClung MR et al. (2014). Romosozumab in postmenopausal women with low bone mineral density. New Engl J Med 370:412-420.
91. Cejka D et al. (2011). Sclerostin and Dickkopf-1 in renal osteodystrophy. Clin J Am Soc Nephrol 6:877-882.
92. Sabbagh Y et al. (2012). Repression of osteocyte Wnt/beta-catenin signaling is an early event in the progression of renal osteodystrophy. J Bone Miner Res 27:1757-1772.
93. Bellido T, Saini V, Pajevic PD (2013). Effects of PTH on osteocyte function. Bone 54:250-257.134
94. Cejka D et al. (2012). Sclerostin serum levels correlate positively with bone mineral density and microarchitecture in haemodialysis patients. Nephrol Dial Transplant 27:226-230.
95. Ettinger B et al. (1999). Reduction of Vertebral Fracture Risk in Postmenopausal Women With Osteoporosis Treated With Raloxifene: Results From a 3-Year Randomized Clinical Trial. JAMA 282:637-645.
96. Reginster JY (2011). Antifracture efficacy of currently available therapies for postmenopausal osteoporosis. Drugs 71:65-78.
97. Allen MR et al. (2007). Raloxifene enhances material-level mechanical properties of femoral cortical and trabecular bone. Endocrinology 148:3908-3913.
98. Allen MR et al. (2006). Raloxifene enhances vertebral mechanical properties independent of bone density. Bone 39:1130-1135.
99. Diab T et al. (2011). Effects of the combination treatment of raloxifene and alendronate on the biomechanical properties of vertebral bone. J Bone Miner Res 26:270-276.
100. Allen MR, Burr DB (2011). Bisphosphonate effects on bone turnover, microdamage, and mechanical properties: What we think we know and what we know that we don't know. Bone 49:56-65.
101. Gallant et al. (2014). Bone cell-independent benefits of raloxifene on the skeleton: A novel mechanism for improving bone material properties. Bone 61:191-200.
102. Allen et al. (2015). In vivo UTE-MRI Reveals Positive Effects of Raloxifene on Skeletal Bound Water in Skeletally Mature Beagle Dogs. J Bone Miner Res [10.1002/jbmr.2470].
103. Melamed ML et al. (2011). Raloxifene, a selective estrogen receptor modulator, is renoprotective: a post-hoc analysis. Kidney Int 79:241-249.
104. Dixon A et al. (2011). Renoprotective effects of a selective estrogen receptor modulator, raloxifene, in an animal model of diabetic nephropathy. Am J Nephrol 27:120-128.
105. Zhang Y et al. (2010). Raloxifene modulates estrogen-mediated β cell autoreactivity in NZB/W F1 mice. J Rheumatol 37:1646-1657.
106. Hernandez E et al. (2003). Effects of raloxifene on bone metabolism and serum lipids in postmenopausal women on chronic hemodialysis. Kidney Int 63:2269-2274.

107. Cole JH, van der Meulen MCH (2011) Whole bone mechanics and bone quality. Clin Orthop Relat Res 469: 2139–2149.
108. Allen MR et al. (2013). Skeletal effects of zoledronic acid in an animal model of chronic kidney disease. Osteoporos Int 24:1471-1481.
109. Iwamoto J et al. (2012) Vitamin K2 improves renal function and increases femoral bone strength in rats with renal insufficiency. Calcif Tissue Int 90:50-59.
110. Iwasaki Y et al. (2011) Changes in chemical composition of cortical bone associated with bone fragility in rat model with chronic kidney disease. Bone 48:1260-1267.
111. Jokihaara J et al. (2006). Paracalcitol [19-Nor-1,25-$(OH)_2D_2$] in the treatment of experimental renal bone disease. J Bone Miner Res 21:745-751.
112. Moe SM et al. (2011). The pathophysiology of early-stage chronic kidney disease-mineral bone disorder (CKD-MBD) and response to phosphate binders in the rat. J Bone Miner Res 26:2672-2681.
113. Gattone VH II et al. (2004). Development of multiorgan pathology in the wpk rat model of polycystic kidney disease. Anat Rec 277A:384-395.
114. Aref M et al. (2013). In vivo reference point indentation reveals positive effects of raloxifene on mechanical properties following 6 months of treatment in skeletally mature beagle dogs. Bone 56:449-53.
115. Hammond MA et al. (2014). Nanoscale changes in collagen are reflected in physical and mechanical properties of bone at the microscale in diabetic rats. Bone 60:26-32.
116. Wallace JM (2012). Applications of atomic force microscopy for the assessment of nanoscale morphological and mechanical properties of bone. Bone 50:420-427
117. Buckley A, Hill KE, Davidson JM (1988). Collagen metabolism. In: Colowick SP, Kaplan NO, Di Sabato G, editors. Methods in Enzymology: Immunochemical Techniques, Part M: Chemotaxis and inflammation. London: Academic Press, pp. 674-693.
118. Saito M et al. (1997). Single-column high- performance liquid chromatographic-fluorescence detection of immature, mature, and senescent cross-links of collagen. Anal Biochem 253:26-32.
119. Moe SM et al. (2014). A comparison of calcium to zoledronic Acid for improvement of cortical bone in an animal model of CKD. J Bone Miner Res 29:902-910.
120. Gallant MA et al. (2013). Reference-point indentation correlates with bone toughness assessed using whole-bone traditional mechanical testing. Bone 53:301-305.
121. Diez-Perez A et al. (2010). Microindentation for in vivo measurement of bone tissue mechanical properties in humans. J Bone Miner Res 25:1877-1885.
122. Güerri-Fernández RC et al. (2013). Microindentation for in vivo measurement of bone tissue material properties in atypical femoral fracture patients and controls. J Bone Miner Res 28:162-168.

123. Farr JN et al. (2014). In vivo assessment of bone quality in postmenopausal women with type 2 diabetes. J Bone Miner Res 29:787-795.
124. Tai K et al. (2007). Nanoscale heterogeneity promotes energy dissipation in bone. Nat Mater 6:454-462.
125. Phelps JB et al. (2000). Microstructural heterogeneity and the fracture toughness of bone. J Biomed Mater Res 51:735-741.
126. Currey J (2005). Structural heterogeneity in bone: good or bad? J Musculoskelet Neuronal Interact 5:317.
127. Aoki C et al. (2013). Advanced glycation end products suppress lysyl oxidase and induce bone collagen degradation in a rat model of renal osteodystrophy. Lab Invest 93:1170-1183.
128. Galli F (2007). Protein damage and inflammation in uraemia and dialysis patients. Nephrol Dial Transplant 22(Suppl 5):20–36.
129. Miyata T et al. (1996). Accumulation of albumin-linked and free-form pentosidine in the circulation of uremic patients with end-stage renal failure: renal implications in the pathophysiology of pentosidine. J Am Soc Nephrol 7:1198-1206.
130. Sakata N et al. (2003). Modification of elastin by pentosidine is associated with the calcification of aortic media in patients with end-stage renal disease. Nephrol Dial Transplant 18:1601-1609.
131. Zoccali C et al. (2001). Pentosidine, carotid atherosclerosis and alterations in left ventricular geometry in hemodialysis patients. J Nephrol 14:293-298.
132. Arsov S et al. (2014). Advanced glycation end-products and skin autofluorescence in end-stage renal disease: a review. Clin Chem Lab Med 52:11-20.
133. Mitome J et al. (2011). Nonenzymatic cross-linking pentosidine increase in bone collagen and are associated with disorders of bone mineralization in dialysis patients. Calcif Tissue Int 88:521-529.
134. Glenn JV et al. (2007). Confocal Raman microscopy can quantify advanced glycation end product (AGE) modifications in Bruch's membrane leading to accurate, nondestructive prediction of ocular aging. FASEB J 21:3542-3552.
135. Nyman JS et al. (2006). Age-related effect on the concentration of collagen crosslinks in human osteonal and interstitial bone tissue. Bone 39:1210-1217.
136. Odetti P et al. (2005). Advanced glycation end products and bone loss during aging. Ann NY Acad Sci 1043:710-717.
137. Saito M, et al. (2006). Role of enzymatic and glycation induced cross-links as a determinant of bone quality in spontaneously diabetic WBN/Kob rats. Osteoporosis Int 17:1514-1523.
138. Silva MJ et al. (2009) Type 1 diabetes in young rats leads to progressive trabecular bone loss, cessation of cortical bone growth, and diminished whole bone strength and fatigue life. J Bone Miner Res 24:1618-1627.

139. Malluche HH et al. (2012). Differences in bone quality in low- and high-turnover renal osteodystrophy. J Am Soc Nephrol 23:525-532.
140. Moe S et al. (2006). Definition, evaluation, and classification of renal osteodystrophy: a position statement from Kidney Disease: Improving Global Outcomes (KDIGO). Kidney Int 69:1945-1953.
141. Ensrud KE et al. (2007). Renal function and risk of hip and vertebral fractures in older women. Arch Intern Med 167:133-139.
142. Anderson S et al. (2009). Prediction, progression, and outcomes of chronic kidney disease in older adults. J Am Soc Nephrol 20:1199-1209.
143. Jamal SA, West SL, Miller PD (2011). Fracture risk assessment in patients with chronic kidney disease. Osteoporos Int 23:1191-1198.
144. Fusaro M, Gallieni M, Jamal SA (2013). Fractures in chronic kidney disease: neglected, common, and associated with sickness and death. 85:20-22.
145. Negrea LA (2012). Biochemical abnormalities in chronic kidney disease–mineral bone disease. Clinic Rev Bone Miner Metab 10:149-162.
146. Kiattisunthorn K, Moe SM (2011). Chronic kidney disease-mineral bone disorder: definitions and rationale for a systemic disorder. Clinic Rev Bone Miner Metab 10:119-127.
147. Ott SM (2009). Bone histomorphometry in renal osteodystrophy. Semin Nephrol 29:122-132.
148. Terpstra AM et al. (2012). Bone density and cortical structure after pediatric renal transplantation. J Am Soc Nephrol 23:715-726.
149. Miller MA et al. (1998). Disparate effects of mild, moderate, and severe secondary hyperparathyroidism on cancellous and cortical bone in rats with chronic renal insufficiency. Bone 23:257-266.
150. Newman CL et al. (2014). Cortical bone mechanical properties are altered in an animal model of progressive chronic kidney disease. PLoS One 9:e9926.
151. Viguet-Carrin S, Garnero P, Delmas PD (2005). The role of collagen in bone strength. Osteoporos Int 17:319-336.
152. Vashishth D et al. (2001). Influence of nonenzymatic glycation on biomechanical properties of cortical bone. Bone 28:195-201.
153. Wang X et al. (2001) The role of collagen in determining bone mechanical properties. J Orthop Res 19:1021-1026.
154. Currey JD (2003). Role of collagen and other organics in the mechanical properties of bone. Osteoporos Int 14(Suppl 5):S29–S36.
155. Oxlund H et al. (1995). Reduced concentrations of collagen cross-links are associated with reduced strength of bone. Bone 17:S365–S371.
156. Turner CH, Burr DB (1993). Basic biomechanical measurements of bone: a tutorial. Bone 14:595-608.
157. Dempster WT, Liddicoat RT (1952). Compact bone as a non-isotropic material. Am J Anat 91:331-362.
158. Nyman JS et al. (2013). Partial removal of pore and loosely bound water by low-energy drying decreases cortical bone toughness in young and old donors. J Mech Behav Biomed Mater 22:136-145.

159. Techawiboonwong A et al. (2008). Cortical bone water: in vivo quantification with ultrashort echo-time MR imaging. Radiology 248:824-833.
160. Anumula S et al. (2010). Ultra-short echo-time MRI detects changes in bone mineralization and water content in OVX rat bone in response to alendronate treatment. Bone 46:1391-1399.
161. Cowley BD et al. (1996). Modification of disease progression in rats with inherited polycystic kidney disease. Am J Kidney Dis 27:865-879.
162. Cowley BD et al. (1993). Autosomal-dominant polycystic kidney disease in the rat. Kidney Int 43:522-534.
163. Horch RA et al. (2010). RF coil considerations for short-T2 MRI. Magn Reson Med 64:1652-1657.
164. Horch RA et al. (2010). Characterization of ^{1}H NMR signal in human cortical bone for magnetic resonance imaging. Magn Reson Med 64:680-687.
165. Horch RA et al. (2011). Non-invasive predictors of human cortical bone mechanical properties: T(2)-discriminated H NMR compared with high resolution X-ray. PLoS One 6:e16359.
166. Leonard MB (2009). A structural approach to skeletal fragility in chronic kidney disease. Semin Nephrol 29:133-143.
167. Manhard MK et al. (2014). Validation of quantitative bound- and pore-water imaging in cortical bone. Magn Reson Med 71:2166-2171.
168. Di Donato A et al. (1997). Lysyl oxidase expression and collagen cross-linking during chronic adriamycin nephropathy. Nephron 76:192-200.
169. Ureña P et al. (1995). Serum pyridinoline as a specific marker of collagen breakdown and bone metabolism in hemodialysis patients. J Bone Miner Res 10:932-939.
170. Suliman ME et al. (2003). Plasma pentosidine is associated with inflammation and malnutrition in end-stage renal disease patients starting on dialysis therapy. J Am Soc Nephrol 14:1614-1622.
171. Mallipattu SK, Uribarri J (2014). Advanced glycation end product accumulation. Curr Opin Nephrol Hypertens 6:547-554.
172. Miyata T et al. (1998). Renal catabolism of advanced glycation end products: the fate of pentosidine. Kidney Int 53:416-422.
173. Tang SY et al. (2009). Changes in non-enzymatic glycation and its association with altered mechanical properties following 1-year treatment with risedronate or alendronate. Osteoporos Int 20:887-894.
174. Burr D (2011). Why bones bend but don’t break. 11:270–285.
175. Bae WC et al. (2012). Quantitative ultrashort echo time (UTE) MRI of human cortical bone: correlation with porosity and biomechanical properties. J Bone Miner Res 27:848-857.
176. Coburn JW et al. (2004). Doxercalciferol safely suppresses PTH levels in patients with secondary hyperparathyroidism associated with chronic kidney disease stages 3 and 4. Am J Kidney Dis 43:877-890.
177. Coyne D et al. (2006). Paricalcitol capsule for the treatment of secondary hyperparathyroidism in stages 3 and 4 CKD. Am J Kidney Dis 47:263-276.

178. Moe SM et al. (2015). Anti-sclerostin antibody treatment in a rat model of progressive renal osteodystrophy. J Bone Miner Res 30:539-549.
179. Allen MR et al. (2015). Changes in skeletal collagen cross-links and matrix hydration in high- and low-turnover chronic kidney disease. Osteoporosis Int 26:977-985.
180. Goodman WG et al. (2000). Coronary-artery calcification in young adults with end-stage renal disease who are undergoing dialysis. N Engl J Med 342:1478-1483.
181. Brock GA et al. (2007). Mortality effect of coronary calcification and phosphate binder choice in incident hemodialysis patients. Kidney Int 71:438-441.
182. Russo D et al. (2007). The progression of coronary artery calcification in predialysis patients on calcium carbonate or sevelamer. Kidney Int 72:1255-1261.
183. Elder GJ (2011). Calcium supplementation: lessons from the general population for chronic kidney disease and back. Curr Opin Nephrol Hyperten 20:369-375.
184. West SL, Swan VJ, Jamal SA (2010). Effects of calcium on cardiovascular events in patients with kidney disease and in a healthy population. Clin J Am Soc Nephrol 5(Suppl 1):S41-S47.
185. Spence LA, Weaver CM (2013). Calcium intake, vascular calcification, and vascular disease. Nutr Rev 71:15-22.
186. Bouxsein ML et al. (2010). Guidelines for assessment of bone microstructure in rodents using micro-computed tomography. J Bone Miner Res 25:1468-1486.
187. Allen MR et al. (2006). Antiremodeling agents influence osteoblast activity differently in modeling and remodeling sites of canine rib. Calcif Tissue Int 79:255-261.
188. Allen MR et al. (2010). Morphological assessment of basic multicellular unit resorption parameters in dogs shows additional mechanisms of bisphosphonate effects on bone. Calcif Tissue Int 86:67-71.
189. Allen MR, Kubek DJ, Burr DB (2010). Cancer treatment dosing regimens of zoledronic acid result in near-complete suppression of mandible intracortical bone remodeling in beagle dogs. J Bone Miner Res 25:98-105.
190. Dempster DW et al. (2013). Standardized nomenclature, symbols, and units for bone histomorphometry: A 2012 update of the report of the ASBMR Histomorphometry Nomenclature Committee. J Bone Miner Res 28:2-17.
191. Hogan H, Ruhmann S, Sampson H (2000). The mechanical properties of cancellous bone in the proximal tibia of ovariectomized rats. J Bone Miner Res 15:284-292.
192. Bloomfield S et al. (2002). Site- and compartment-specific changes in bone with hindlimb unloading in mature adult rats. Bone 31:149-157.

193. Dogan E et al. (2008). Effect of depot oral cholecalciferol treatment on secondary hyperparathyroidism in stage 3 and stage 4 chronic kidney diseases patients. Renal Failure 30:407-410.
194. Chandra P et al. (2008). Cholecalciferol (vitamin D_3) therapy and vitamin D insufficiency in patients with chronic kidney disease: a randomized controlled pilot study. Endocr Pract 14:10-17.
195. Wesseling-Perry et al. (2011). Calcitriol and doxercalciferol are equivalent in controlling bone turnover, suppressing parathyroid hormone, and increasing fibroblast growth factor-23 in secondary hyperparathyroidism. Kidney Int 79:112-119.
196. Hamdy NAT et al. (1995). Effect of alfacalcidol on natural course of renal bone disease in mild to moderate renal failure. BMJ 310:358-363.
197. Baker LR et al. (1989). Early therapy of renal bone disease with calcitriol: a prospective double-blind study. Kidney Int Suppl 27:S140-S142.
198. Finch JL et al. (2010). Effect of paricalcitol and cinacalcet on serum phosphate, FGF-23, and bone in rats with chronic kidney disease. Am J Physiol Renal 298:F1315-F1322.
199. Naves Diaz M et al. (2007). Effects of estradiol, calcitriol and both treatments combined on bone histomorphometry in rats with chronic kidney disease and ovariectomy. Bone 41:614-619.
200. Jablonski G et al. (1995). Vitamin D_3 analogs and salmon calcitonin partially reverse the development of renal osteodystrophy in rats. Calcif Tissue Int 57:385-391.
201. Imel EA, DiMeglio LA (2010). Treatment of x-linked hypophosphatemia with calcitriol and phosphate increases circulating fibroblast growth factor 23 concentrations. J Clin Endocrinol Metab 95:1846-1850.
202. Liu S et al. (2006). Fibroblast growth factor 23 is a counter-regulatory phosphaturic hormone for vitamin D. J Am Soc Nephrol 17:1305-1315.
203. Kazema JJ et al. (2005). Pretreatment serum FGF-23 levels predict the efficacy of calcitriol therapy in dialysis patients with secondary hyperparathyroidism. Kidney Int 67:1120-1125.
204. Nishi H et al. (2005). Intravenous calcitriol therapy increases serum concentrations of fibroblast growth factor-23 in dialysis patients with secondary hyperparathyroidism. Nephron Clin Pract 101:c94-c99.
205. Wetmore JB et al. (2010). Effects of cinacalcet and concurrent low-dose vitamin D on FGF23 levels in ESRD. Clin J Am Soc Nephrol 5:110-116.
206. Kim HJ et al. (2013). Cinacalcet lowering of serum fibroblast growth factor-23 concentration may be independent from serum Ca, P, PTH and dose of active vitamin D in peritoneal dialysis patients: a randomized controlled study. BMC Nephrol 14:112.
207. Lindberg JS, Moe SM (1999). Osteoporosis in end-state renal disease. Semin Nephrol 19:115–22.
208. Moe SM et al. (2009). R-568 reduces ectopic calcification in a rat model of chronic kidney disease-mineral bone disorder (CKD-MBD). Nephrol Dial Transplant 24:2371-2377.

209. Allen MR, Burr DB (2009). The pathogenesis of bisphosphonate-related osteonecrosis of the jaw: so many hypotheses, so few data. J Oral Maxillofac Surg 67(5 Suppl):61–70.
210. Patntirapong S et al. (2012). Zoledronic acid suppresses mineralization through direct cytotoxicity and osteoblast differentiation inhibition. J Oral Pathol Med 41:713-720.
211. Parfitt AM et al. (1987). Bone histomorphometry: standardization of nomenclature, symbols, and units: report of the ASBMR histomorphometry nomenclature committee. J Bone Miner Res 2:595–610.
212. Barreto DV et al. (2008). Phosphate binder impact on bone remodeling and coronary calcification—results from the BRiC study. Nephron Clin Pract 110:c273-283.
213. Black DM et al. (2007). Once-yearly zoledronic acid for treatment of postmenopausal osteoporosis. N Engl J Med 356:1809-1822.
214. Brown JE et al. (2007). Prolonged efficacy of a single dose of the bisphosphonate zoledronic acid. Clin Cancer Res 13:5406-5410.
215. Calis KA, Pucino F (2007). Zoledronic acid and secondary prevention of fractures. N Engl J Med 357:1861-1862.
216. Bischoff-Ferrari HA et al. (2007). Calcium intake and hip fracture risk in men and women: a meta-analysis of prospective cohort studies and randomized controlled trials. Am J Clin Nutr 86:1780-1790.
217. Bolland MJ et al. (2010). Effect of calcium supplements on risk of myocardial infarction and cardiovascular events: meta-analysis. BMJ 341:c3691.
218. Parfitt AM (1997). The hyperparathyroidism of chronic renal failure: a disorder of growth. Kidney Int 52:3-9.
219. Parfitt AM (2002). Misconceptions (2): turnover is always higher in cancellous than in cortical bone. Bone 30:807-809.
220. Sprague SM, Moe SM (2013). The case for routine parathyroid hormone monitoring. Clin J Am Soc Nephrol 8:313-318.
221. Tamura K et al. (2007). Prevention of aortic calcification by etidronate in the renal failure rat model. Eur J Pharmacol 558:159-166.
222. Price PA, Faus SA, Williamson MK (2001). Bisphosphonates alendronate and ibandronate inhibit artery calcification at doses comparable to those that inhibit bone resorption. Arterioscler Thromb Vasc Biol 21:817-824.
223. Lomashvili KA et al. (2009). Effect of bisphosphonates on vascular calcification and bone metabolism in experimental renal failure. Kidney Int 75:617-625.
224. Touchberry CD et al. (2013). FGF23 is a novel regulator of intracellular calcium and cardiac contractility in addition to cardiac hypertrophy. Am J Physiol Endocrinol Metab 304:E863-E873.
225. Moe SM (2006). Vascular calcification and renal osteodystrophy relationship in chronic kidney disease. Eur J Clin Invest 36(Suppl 2):51–62.
226. Kurz P et al. (1994). Evidence for abnormal calcium homeostasis in patients with adynamic bone disease. Kidney Int 46:855-861.

227. Hill KM et al. (2013). Oral calcium carbonate affects calcium but not phosphorus balance in stage 3–4 chronic kidney disease. Kidney Int 83:959-966.
228. Rodriguez-Ortiz ME et al. (2012). Calcium deficiency reduces circulating levels of FGF23. J Am Soc Nephrol 23:1190-1197.
229. Lim K et al. (2012). Vascular Klotho deficiency potentiates the development of human artery calcification and mediates resistance to fibroblast growth factor 23. Circulation 125:2243-2255.
230. Faul C et al. (2011). FGF23 induces left ventricular hypertrophy. J Clin Invest 121:4393-4408.
231. Nitta K et al. (2004). Effects of cyclic intermittent etidronate therapy on coronary artery calcification in patients receiving long-term hemodialysis. Am J Kidney Dis 44:680-688.
232. Hashiba H et al. (2004). Inhibitory effects of etidronate on the progression of vascular calcification in hemodialysis patients. Ther Apher Dial 8:241-247.
233. Quinn SJ et al. (2013). Interactions between calcium and phosphorus in the regulation of the production of fibroblast growth factor 23 in vivo. Am J Physiol Endocrinol Metab 304:E310-E320.
234. Toussaint ND et al. (2010). Effect of alendronate on vascular calcification in CKD stages 3 and 4: a pilot randomized controlled trial. Am J Kidney Dis 56:57–68.
235. Moe SM et al. (2007). Chronic kidney disease-mineral-bone disorder: a new paradigm. Adv Chronic Kidney Dis 14:3-12.
236. Ishani A et al. (2008). The effect of raloxifene treatment in postmenopausal women with CKD. J Am Soc Nephrol 19:1430-1438.
237. Jamal SA et al. (2011). Effects of denosumab on fracture and bone mineral density by level of kidney function. J Bone Miner Res 26:1829-35.
238. Sprague SM, Moe SM (2013). Rebuttal: PTH--a particularly tricky hormone: why measure it at all in kidney patients? Clin J Am Soc Nephrol 8:321.
239. Lavi-Moshayoff V et al. (2010). PTH increases FGF23 gene expression and mediates the high-FGF23 levels of experimental kidney failure: a bone parathyroid feedback loop. Am J Physiol Renal Physiol 299:F882-F889.
240. Rhee Y et al. (2011). Parathyroid hormone receptor signaling in osteocytes increases the expression of fibroblast growth factor-23 in vitro and in vivo. Bone 49:636-643.
241. Baron R, Kneissel M (2013). WNT signaling in bone homeostasis and disease: from human mutations to treatments. Nat Med 19:179-192.
242. Marenzana M et al. (2013) Effect of sclerostin-neutralising antibody on periarticular and systemic bone in a murine model of rheumatoid arthritis: a microCT study. Arthritis Res Ther 15:R125.
243. McGee-Lawrence ME et al. (2013). Sclerostin deficient mice rapidly heal bone defects by activating beta-catenin and increasing intramembranous ossification. Biochem Biophys Res Commun 441:886-890.

244. Taut AD et al. (2013). Sclerostin antibody stimulates bone regeneration after experimental periodontitis. J Bone Miner Res 28:2347-2356.
245. Virk MS et al. (2013). Systemic administration of sclerostin antibody enhances bone repair in a critical-sized femoral defect in a rat model. J Bone Joint Surg Am 95:694-701.
246. Williams BO (2014). Insights into the mechanisms of sclerostin action in regulating bone mass accrual. J Bone Miner Res 29:24-28.
247. McColm J et al. (2013). Single- and multiple-dose randomized studies of blosozumab, a monoclonal antibody against sclerostin, in healthy postmenopausal women. J Bone Miner Res 29:935-943.
248. Allen MR et al. (2013). Adverse mandibular bone effects associated with kidney disease are only partially corrected with bisphosphonate and/or calcium treatment. Am J Nephrol 38:458-464.
249. Guo J et al. (2010). Suppression of Wnt signaling by Dkk1 attenuates PTH-mediated stromal cell response and new bone formation. Cell Metab 11:161-71.
250. Hirano T et al. (2000). Does suppression of bone turnover impair mechanical properties by allowing microdamage accumulation? Bone 27:13-20.
251. Chen NX et al. (2013). Transglutaminase 2 accelerates vascular calcification in chronic kidney disease. Am J Nephrol 37:191-198.
252. Ominsky MS et al. (2008). RANKL inhibition with osteoprotegerin increases bone strength by improving cortical and trabecular bone architecture in ovariectomized rats. J Bone Miner Res 23:672-682.
253. Kostenuik PJ et a. (2001). OPG and PTH-(1-34) have additive effects on bone density and mechanical strength in osteopenic ovariectomized rats. Endocrinology 142:4295-4304.
254. O'Brien CA et al. (2008). Control of bone mass and remodeling by PTH receptor signaling in osteocytes. PLoS One 3:e2942.
255. Rhee Y et al. (2013). Resorption controls bone anabolism driven by parathyroid hormone (PTH) receptor signaling in osteocytes. J Biol Chem 288:29809-29820.
256. Li C et al. (2013). Disruption of LRP6 in osteoblasts blunts the bone anabolic activity of PTH. J Bone Miner Res 28:2094-2108.
257. Sawakami K et al. (2006). The Wnt co-receptor LRP5 is essential for skeletal mechanotransduction but not for the anabolic bone response to parathyroid hormone treatment. J Biol Chem 281:23698-23711.
258. Jilka RL et al. (2010). Continuous elevation of PTH increases the number of osteoblasts via both osteoclast-dependent and -independent mechanisms. J Bone Miner Res 25:2427-2437.
259. Fang Y et al. (2014). CKD-Induced Wingless/Integration1 Inhibitors and Phosphorus Cause the CKD-Mineral and Bone Disorder. J Am Soc Nephrol 25:1760-1773.
260. Pelletier S et al. (2013). The relation between renal function and serum sclerostin in adult patients with CKD. Clin J Am Soc Nephrol 8:819-823.

261. Cejka D et al. (2014). Renal elimination of sclerostin increases with declining kidney function. J Clin Endocrinol Metab 99:248-255.
262. van Lierop AH et al. (2010). Patients with primary hyperparathyroidism have lower circulating sclerostin levels than euparathyroid controls. Eur J Endocrinol 163:833-837.
263. Ferreira JC et al. (2013). Effects of dietary phosphate on adynamic bone disease in rats with chronic kidney disease--role of sclerostin? PLoS One 8:e79721.
264. Oliveira RB et al. (2010). Early control of PTH and FGF23 in normophosphatemic CKD patients: a new target in CKD-MBD therapy? Clin J Am Soc Nephrol 5:286-291.
265. Atsumi K et al. (1999). Risk factors for vertebral fractures in renal osteodystrophy. Am J Kidney Dis 33:287-293.
266. Parfitt AM (1998). A structural approach to renal bone disease. J Bone Miner Res 13:1213-1220.
267. Eswaran SK et al. (2006). Cortical and trabecular load sharing in the human vertebral body. J Bone Miner Res 21:307-314.
268. Shipov A et al. (2014). The effect of naturally occurring chronic kidney disease on the micro-structural and mechanical properties of bone. PLoS ONE 9:e110057.
269. Taskiran EZ, Korkmaz E, Gucer S (2014). Mutations in ANKS6 cause a nephronophthisis-like phenotype with ESRD. J Am Soc Nephrol [doi: 10.1681/ASN.2013060646].
270. Brown JH et al. (2005). Missense mutation in sterile alpha motif of novel protein SamCystin is associated with polycystic kidney disease in (cy/+) rat. J Am Soc Nephrol 16:3517-3526.
271. Dukas L, Schacht E, Stähelin HB (2005). In elderly men and women treated for osteoporosis a low creatinine clearance of <65 ml/min is a risk factor for falls and fractures. Osteoporos Int 16:1683-1690.
272. Danese MD et al. (2006). PTH and the risks for hip, vertebral, and pelvic fractures among patients on dialysis. Am J Kidney Dis 47:149-156.
273. Christov M, Pereira R, Wesseling-Perry K (2013). Bone biopsy in renal osteodystrophy: continued insights into a complex disease. Curr Opin Nephrol Hy 22:210-215.
274. Malluche HH, Monier-Faugere MC (1994). The role of bone biopsy in the management of patients with renal osteodystrophy. J Am Soc Nephrol 4:1631-1642.
275. Spasovski GB (2004). Bone biopsy as a diagnostic tool in the assessment of renal osteodystrophy. Int J Artif Organs 27:918-923.
276. Barreto FC et al. (2006). Osteoporosis in hemodialysis patients revisited by bone histomorphometry: a new insight into an old problem. Kidney Int 69:1852-1857.
277. Julian BA et al. (1991). Rapid loss of vertebral mineral density after renal transplantation. N Engl J Med 325:544-550.

278. Li X et al. (2009). Sclerostin antibody treatment increases bone formation, bone mass, and bone strength in a rat model of postmenopausal osteoporosis. J Bone Miner Res 24:578-588.
279. Nancollas GH et al. (2006). Novel insights into actions of bisphosphonates on bone: differences in interactions with hydroxyapatite. Bone 38:617-627.
280. Allen MR, Burr DB (2011). Bisphosphonate effects on bone turnover, microdamage, and mechanical properties: what we think we know and what we know that we don't know. Bone 49:56-65.
281. Grey A et al. (2012). Five years of anti-resorptive activity after a single dose of zoledronate: results from a randomized double-blind placebo-controlled trial. Bone 6:1389-1393.
282. Reid IR et al. (2011). A single infusion of zoledronic acid produces sustained remissions in Paget's disease: data to 6.5 years. J Bone Miner Res 26:2261-2270.
283. Fuchs RK, Phipps RJ, Burr DB (2008). Recovery of trabecular and cortical bone turnover after discontinuation of risedronate and alendronate therapy in ovariectomized rats. J Bone Miner Res 23:1689-1697.
284. Pfister T, Atzpodien E, Bauss F (2003). The renal effects of minimally nephrotoxic doses of ibandronate and zoledronate following single and intermittent intravenous administration in rats. Toxicology 191:159-167.
285. Rix M, Eskildsen P, Olgaard K (2004). Effect of 18 months of treatment with alfacalcidol on bone in patients with mild to moderate chronic renal failure. Nephrol Dial Transplant 19:870-876.
286. Ruedin P et al. (1994). Effects of oral calcitriol on bone mineral density in patients with end-stage renal failure. Kidney Int 45:245-252.
287. Tsukamoto et al. (1993). Long-term effect of oral calcitriol pulse therapy on bone in hemodialysis patients. Bone 14:421-425.
288. Przedlacki J, Manelius J, Huttunen K (1995). Bone mineral density evaluated by dual-energy x-ray absorptiometry after one-year treatment with calcitriol started in the predialysis phase of chronic renal failure. Nephron 69:433-437.
289. Costa AFP et al. (2003). Effects of calcitriol on parathyroid function and on bone remodeling in secondary hyperparathyroidism. Nephrol Dial Transplant 18:743-749.
290. Goodman WG et al. (1994). Development of adynamic bone in patients with secondary hyperparathyroidism after intermittent calcitriol therapy. Kidney Int 46:1160-1166.
291. Coen G et al. (1995). Metabolic acidosis and osteodystrophic bone disease in predialysis chronic renal failure: effect of calcitriol treatment. Miner Electrol Metab 21:375-382.
292. Zanchetta JR, Bogado CE (2001). Raloxifene reverses bone loss in postmenopausal women with mild asymptomatic primary hyperparathyroidism. J Bone Miner Res 16:189-190.
293. Taranta A et al. (2002). The selective estrogen receptor modulator raloxifene regulates osteoclast and osteoblast activity in vitro. Bone 30:368-376.

294. Prestwood KM et al. (2000). A comparison of the effects of raloxifene and estrogen on bone in postmenopausal women. J Clin Endocr Metab 85:2197-2202.
295. Brennan TC, Rizzoli R, Ammann P (2009). Selective modification of bone quality by PTH, pamidronate, or raloxifene. J Bone Miner Res 24:800-808.
296. Burket JC et al. (2013). Variations in nanomechanical properties and tissue composition within trabeculae from an ovine model of osteoporosis and treatment. Bone 52:326-336.
297. Wallace JM et al. (2010). Distribution of type I collagen morphologies in bone: relation to estrogen depletion. Bone 46:1349-1354.
298. Bart ZR, Hammond MA, Wallace JM (2014). Multi-scale analysis of bone chemistry, morphology and mechanics in the oim model of osteogenesis imperfecta. Connect Tissue Res 55:4-8.
299. Tanaka M et al. (2011). Effects of raloxifene on bone mineral metabolism in postmenopausal Japanese women on hemodialysis. Ther Apher Dial 15(Suppl. 1):62-66.
300. Gasser JA et al. (2008). Long-term protective effects of zoledronic acid on cancellous and cortical bone in the ovariectomized rat. J Bone Miner Res 23:544-551.
301. Coen G et al. (2005). 25-hydroxyvitamin D levels and bone histomorphometry in hemodialysis renal osteodystrophy. Kidney Int 68:1840-1848.

CURRICULUM VITAE

Christopher L. Newman

Education

2010 - Present	Doctor of Medicine Indiana University School of Medicine
2012 - 2015	Doctor of Philosophy Major: Anatomy and Cell Biology Indiana University
2007 - 2010	Master of Science Major: Human Biology University of Indianapolis
2003 - 2007	Bachelor of Arts Major: Anthropology (with Honors) and Zoology Miami University

Research Interests

How do mechanical forces impact the skeleton? What are the cellular and molecular mechanisms by which bones respond to these forces? What processes account for the ability of bone to repair damaged skeletal matrix? What disease processes result from the failure of these mechanisms? How can this breakdown be inhibited or reversed in patients with such diseases?

Teaching Experience

2013 - 2014	Member of the *Human Structure* Course Development Team for Curricular Reform. Indiana University School of Medicine.
Summer 2010	Adjunct Professor. Cultural Anthropology (Anthropology 154). Ivy Tech Community College (Indianapolis).
Spring 2010	Adjunct Professor. Introduction to Archaeology (Anthropology 254). Ivy Tech Community College (Indianapolis).
Spring 2010	Adjunct Professor. Principles of Human Physiology (Biology 104). University of Indianapolis (Indianapolis).

Spring 2010	Teaching Assistant. Advanced Dental Science (Anthropology 525). University of Indianapolis (Indianapolis).
Fall 2009	Adjunct Professor. Principles of Human Anatomy (Biology 103). University of Indianapolis (Indianapolis).
Spring 2009	Teaching Assistant. Functional Anatomy (Biology 305). University of Indianapolis (Indianapolis).
Fall 2008	Teaching Assistant. Gross Anatomy (Biology 504/610). University of Indianapolis (Indianapolis).
Fall 2006	Teaching Assistant. Foundations of Biological Anthropology (Anthropology 255). Miami University (Oxford, OH).
Fall 2006	Teaching Assistant. Introduction to Archaeological Theory and Methods (Anthropology 212). Miami University (Oxford, OH).

Academic Positions

2009 - 2010	University of Indianapolis Indiana Prehistory Laboratory Coordinator • Planned, coordinated, and conducted various graduate and undergraduate research projects ranging from osteological analysis and dental anthropology research to archaeological artifact analysis, performed basic laboratory maintenance, and maintained the laboratory artifact catalog.
2008 - 2009	University of Indianapolis Gross Anatomy Laboratory Coordinator • Arranged the transfer of cadavers to and from the Indiana Anatomical Education Program at the Indiana University School of Medicine, performed basic laboratory maintenance, and coordinated research conducted in the lab.

Past Research Experience

2011	Indiana University School of Medicine Student Research Program in Academic Medicine (Matthew R. Allen Lab) • Developed protocols for contrast-enhanced micro-computed tomography in order to three-dimensionally examine how the process of targeted bone remodeling changes with age.

2009 – 2010	University of Indianapolis Genetics Laboratory Assistant • Participated in research employing DNA extraction techniques, the extraction of genetic material from skeletal remains, and the analysis and interpretation of ancient and modern human genetic markers.
2007 – 2010	University of Indianapolis Indiana Prehistory Laboratory Assistant • Participated in bioarchaeological research covering various aspects of dental anthropology (dental texture analysis and molding and casting teeth for topographical analysis) and bone biology (osteological analysis of skeletal remains and histological techniques and analysis).
2007 – 2010	University of Indianapolis Archeology and Forensics Laboratory Assistant • Participated in the curation and analysis of forensic cases and historic archaeological populations as well as the recovery of human remains from forensic and archaeological contexts.

Field Experience

2010	Forensic Archaeology Workshop, Indianapolis. • Participated in a short course conducted by the Archaeology and Forensics Laboratory at the University of Indianapolis that introduced the methods and techniques used by forensic archaeologists in association with ongoing law enforcement homicide investigations.
2007	Field Bioarchaeologist. The Wright Cemetery Excavation, Indianapolis. • Participated in the excavation and repatriation of a 19th century cemetery in Indianapolis as part of a coordinated effort between the University of Indianapolis, a regional cultural resource management organization, and the Indiana Department of Transportation.
2005	Field Archaeologist. The Brandenburg Site. Oxford, Ohio. • Conducted initial surveying of the site as well as excavation and initial curation of the artifacts recovered from the site.

Grants

Agency: National Institutes of Health (F30)
Title: Assessing and modifying bone quality in chronic kidney disease.
Duration: 09/16/2013 to 10/31/2018
Role: Principal Investigator

Agency: Clinical and Translational Sciences Institute of Indiana
Title: Assessing and modifying bone quality in chronic kidney disease.
Duration: 07/01/2013 to 09/15/2013 (discontinued due to NIH support)
Role: Principal Investigator

Professional Societies

American Association of Anatomists (2012 – Present)
International Bone and Mineral Society (2013 – 2014)
American Association of Physical Anthropologist (2008 – 2009)

Publications

Newman CL, Chen NX, Smith E, Smith M, Brown D, Moe SM, Allen MR (In Press). Compromised vertebral structural and mechanical properties associated with progressive kidney disease and the effects of traditional pharmacological interventions. Bone.

Allen MR, **Newman CL**, Chen N, Granke M, Nyman JS, Moe SM (2015). Changes in skeletal collagen crosslinks and matrix hydration in high and low turnover chronic kidney disease. Osteoporosis International 26:977-985.

Moe SM, Chen NX, **Newman CL**, Organ JM, Kneissel M, Kramer I, Gattone VH, Allen MR (2015). Anti-sclerostin antibody treatment in a rat model of progressive renal osteodystrophy. Journal of Bone and Mineral Research 30:499-509.

Allen MR, **Newman CL**, Smith E, Brown DM, Organ JM (2014). Variability of *in vivo* reference point indentation in skeletally mature inbred rats. Journal of Biomechanics 47:2504-2507.

Newman CL, Moe SM, Chen NX, Hammond MA, Wallace JM, Nyman JS, Allen MR (2014). Cortical bone material properties in an animal model of progressive chronic kidney disease. PLoS ONE 9(6): e99262. doi:10.1371/journal.pone.0099262.

Moe SM, Chen NX, **Newman CL**, Gattone VH II, Organ JM, Chen X, Allen MR (2014). A comparison of calcium to zoledronic acid for improvement of cortical bone in an animal model of CKD. Journal of Bone and Mineral Research 29:902-910.

Aref M, Gallant MA, Organ JM, Wallace JM, **Newman CL**, Burr DB, Brown DM, Allen MR (2013). *In vivo* reference point indentation reveals positive effects of raloxifene on mechanical properties following 6 months of treatment in skeletally mature beagle dogs. Bone 56:449-453.

Newman CL, Allen MR (2012). Bone remodeling. Mooren FC ed., Encyclopedia of Exercise Medicine in Health and Disease. Berlin: Springer Verlag.

Schmidt CW, Lockhart-Sharkey R, **Newman C**, Serrano A, Zolnierz M, Plunkett AP, Bader A (2010). Skeletal evidence of cultural variation: mutilation related to warfare. Auerbach BM (ed.), Human Variation in the Americas: The Integration of Archaeology and Biological Anthropology. Carbondale, IL: Center for Archaeological Investigations.

Nawrocki SP, **Newman C**, Richardson R, Madaj E, Eriksen A, Halling C (2010). Forensic Anthropology Report, Case # UI-05-09, Archaeology and Forensics Laboratory, University of Indianapolis. Submitted to the Newton County Coroner's Office, Morocco, Indiana.

Conference Presentations

Newman CL, Granke M, Nyman JS, Tian N, Hammond MA, Wallace JM, Brown DM, Gattone II VH, Chen NX, Moe SM, Allen MR (2015). Assessing and treating bone quality in chronic kidney disease (*poster*). Annual Meeting of the American Association of Anatomists, Boston.

Newman CL, Brown DM, Chen NX, Moe SM, Allen MR (2014). Raloxifene, but not calcitriol improves the structural and mechanical properties of bone in an animal model of chronic kidney disease (*podium*). Annual Meeting of the American Society of Nephrology, Philadelphia.

Newman CL, Granke M, Nyman JS, Chen NX, Moe SM, Allen MR (2014). Collagen cross-linking and bone matrix hydration in chronic kidney disease (*poster*). Annual Meeting of the American Society of Bone and Mineral Research, Houston.

Newman CL, Brown DM, Chen NX, Moe SM, Allen MR (2014). Raloxifene, but not calcitriol, improves the structural and mechanical properties of bone in an animal model of chronic kidney disease (*podium*). Annual Meeting of the American Society of Nephrology, Philadelphia.

Newman CL, Chen NX, Gattone VH, Moe SM, Hammond MA, Wallace JM, Allen MR (2013). Cortical bone material properties in an animal model of chronic kidney disease (*podium* and *poster*). Annual Sun Valley Bone Workshop, Sun Valley, Idaho.

Newman CL, Moe SM, Chen NX, Brown DM, Gattone VH, Allen MR (2013). Reducing parathyroid hormone is important for correcting cortical bone deficiencies associated with chronic kidney disease (*podium* and *poster*). Annual Meeting of the American Association of Anatomists, Boston.

Newman CL, Moe S, Chen N, Gattone V, Chen M, Brown D, Carr A, Allen MR (2012). Developing treatments for skeletal abnormalities associated with chronic kidney disease (*poster*). Annual Indiana University School of Medicine Anatomy and Cell Biology Research Forum, Indianapolis.

Newman C, Allen MR (2011). The effect of aging on targeted bone remodeling as determined by contrast-enhanced micro-computed tomography (*podium* and *poster*). Annual Indiana University School of Medicine Student Research Program in Academic Medicine Medical Student Research Poster Session, Indianapolis.

Newman C, Sharkey R, Juarez J, Koehl T, Latham K (2009). Assessing the quantity and quality of DNA isolated from cadavers (*podium*). Annual Meeting of the Midwest Bioarchaeology and Forensic Anthropology Association, Indianapolis.

Newman C, Serrano A, Schmidt CW (2009). The Woodland Ridge site: evidence of conflict in a small late prehistoric Indiana population (*podium*). Annual Meeting of the American Association of Physical Anthropology, Chicago.

Newman C (2008). The impact of subsistence changes on the femur midshaft in prehistoric Indiana (*podium*). Annual Meeting of the Midwest Bioarchaeology and Forensic Anthropology Association, Allendale, Michigan.

Newman C (2007). Methods in skeletal population analysis (*poster*). Annual Miami University Undergraduate Research Forum, Oxford, Ohio.

Invited Lectures

Newman C (2009). The application of computed tomography techniques to biological anthropology research. Three-Dimensional Imaging Workshop, Annual Meeting of the Midwest Bioarchaeology and Forensic Anthropology Association, Indianapolis.

Newman C (2007). Pedal phalanx proportions and load-bearing in the lower limbs of great apes and humans. February Meeting of the Primatology Club, Department of Anthropology, Miami University, Oxford, Ohio.

Awards

2014 Visiting Scholar Award (American Association of Anatomists)
• Conducted research training for the determination of collagen cross-linking (high performance liquid chromatography) and skeletal matrix hydration (nuclear magnetic resonance) at the Vanderbilt University Medical Center

2013 Alice L. Jee Young Investigator Award (Sun Valley Bone Workshop)
• “Cortical bone material properties in an animal model of chronic kidney disease”

2013 Langman Award (American Association of Anatomists)
• Recognizes the best oral presentation by a student at the annual meeting
• “Reducing parathyroid hormone is important for correcting cortical bone deficiencies associated with chronic kidney disease”

2005 Rebecca Jeanne Andrew Memorial Award for Primate Research
• “Pedal phalanx proportions and load-bearing in the lower limbs of great apes and humans”